JOURNAL OF THE AERONAUTICAL SCIENCES

VOLUME 7 DECEMBER, 1939 NUMBER 2

The Buckling of Spherical Shells by External Pressure*

TH. VON KÁRMÁN AND HSUE-SHEN TSIEN

California Institute of Technology

General Considerations

THE general theory of thin shells was developed by A. E. H. Love. He assumed small deflections and for that reason neglected in the energy expression all terms higher than quadratic, and thus obtained linear differential equations for the determination of the equilibrium position of a shell under given forces. The theory of buckling of thin shells is also based essentially on Love's equations. The buckling of cylindrical shells of uniform thickness under the action of a uniformly distributed axial load was calculated by R. Lorentz, R. V. Southwell, S. Timoshenko, W. Flügge, L. H. Donnell, and others. The same problem was also investigated experimentally by many authors, especially by E. E. Lundquist and L. H. Donnell. Unfortunately, a systematic discrepancy was found between the theoretically calculated and experimentally obtained buckling loads; the theoretical values are as much as 3 to 4 times higher than the experimental values. To remedy this situation W. Flügge[1] first considered the deviation of the assumed end conditions of the cylindrical shell from that realized in the laboratory. However, this effect is not sufficient to explain the discrepancy. The influence of the end conditions extends only to a distance approximately equal to $\sqrt{Rt}$, where R is the radius of the shell and t the thickness. The cylinders tested, however, usually have a length which is large compared to this value. Furthermore, Flügge's analysis would indicate a progressive increase of the wave amplitude until plastic deformation occurs, whereas the experimental evidence indicates that the failure of cylindrical shells under compression is not progressive but very rapid.

Another attempt was made by W. Flügge[1] and later by L. H. Donnell[2] to lower the theoretical buckling load by taking into account the initial deviation of the form of the shell from the exact cylindrical shape. According to their assumptions the buckling load, or rather the failing load would be determined by the plastic failure of the material. This explanation has several drawbacks: first, to obtain the low values of the buckling load found experimentally one has to assume deviations from the cylindrical shape as large as ten times the shell thickness. Such a large deviation in the shape of the specimens would be easily detected by visual observations. This is not substantiated by experience. Second, the failure of a cylindrical shell is not necessarily a plastic failure (yielding), especially when the wall of the cylinder is very thin. In many cases it has been observed that upon removing the load the buckling waves completely disappeared. Therefore, the phenomenon must be completely elastic, instead of being plastic as assumed in L. H. Donnell's analysis. Furthermore, the initial deviations from the exact cylindrical form would cause the deformation to increase gradually, which is again contrary to experimental observations.

A similar discrepancy between theory and experiment exists in the case of the buckling of spherical shells under uniform external pressure. The theoretical buckling load based upon Love's equations has been calculated by R. Zoelly, E. Schwerin, and A. Van der Neut.[3] If the buckling stress σ_{cr} is defined by

$$\sigma_{cr} = \frac{p_{cr}R}{2t} \qquad (1)$$

Received October 30, 1939.

* The theoretical investigation reported in this paper was carried out by the authors in connection with the research project "General Instability Criteria for Stiffened Metal Cylinders," sponsored by the Civil Aeronautics Authority, Airworthiness Section.

where p_{cr} is the buckling pressure, t the thickness, and R the radius of the sphere, then the theory gives

$$\sigma_{cr} = \frac{Et/R}{\sqrt{3(1-\nu^2)}} \tag{2}$$

where ν is Poisson's ratio and E is Young's modulus of elasticity. While no systematic experimental work has been done on this problem—at least to the authors' knowledge—some tests made by E. E. Sechler and W. Bollay at the California Institute of Technology indicated that the experimental buckling load is only about $^1/_4$ that of the theoretical value.

Besides these differences between the theoretically and experimentally obtained buckling loads the wave form predicted by the theory is also at variance with laboratory experience. According to theoretical calculations the same load would produce buckling either inward or outward; experiments have shown that the shell has a definite preference for buckling inward. For the case of a spherical shell it is observed that the buckling wave is restricted to a small dimple subtended by a solid angle of about 16°. The linear theory predicts a wave form extending over the whole spherical surface.

What may be the reason for these discrepancies between the prediction of the theory and the experimental evidence? It is very unlikely that there is an error in the fundamental equations of the theory of elasticity. For example, in the case of a flat plate not only the buckling load but also the behavior of the plate after buckling is predicted quite accurately by the theory. Hence, there must be an essential difference between the physical process of the buckling of a flat plate and a curved shell that is not embraced by the previous theory. The same opinion was expressed recently by H. L. Cox[4] in a lecture delivered to the Royal Aeronautical Society.

In this paper a new conception of the mechanism of the collapse of curved sheets is presented.

It is advantageous to start the investigation with the case of a spherical shell loaded by a uniform external pressure, because the geometrical symmetry of the shell will considerably simplify the calculations.

Consider a segment of an extremely thin spherical shell as shown in Fig. 1, and assume that the bending stiffness, which is proportional to t^3 can be completely neglected. Under this assumption the strain energy consists only of the energy due to extension of the shell or compression of the median surface, and it is equal to zero in the deflected position (3) provided it is zero in the undeflected position (1), Fig. 1. In other words, neglecting the bending stiffness, the shell will be in equilibrium in the reflected position (3) without the aid of any external pressure applied to the shell surface.

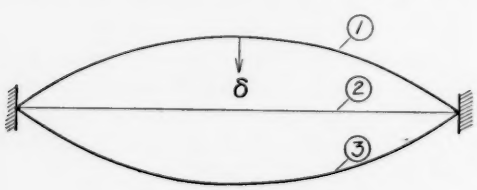

Fig. 1.

On the other hand, the intermediate positions between (1) and (3) do involve compression of the shell elements, and, therefore, the shell can be held in equilibrium in these positions only by external pressure. When the deflection δ of the shell is between the positions (2) and (3), a negative external pressure is necessary to maintain equilibrium as the compressed elements tend to force the shell to take the equilibrium position (3). The pressure-deflection curve, under the assumption of negligible bending stiffness, is, therefore, of the form shown in Fig. 2a.

The effect of the bending stiffness is to increase the positive external pressure necessary to hold the shell

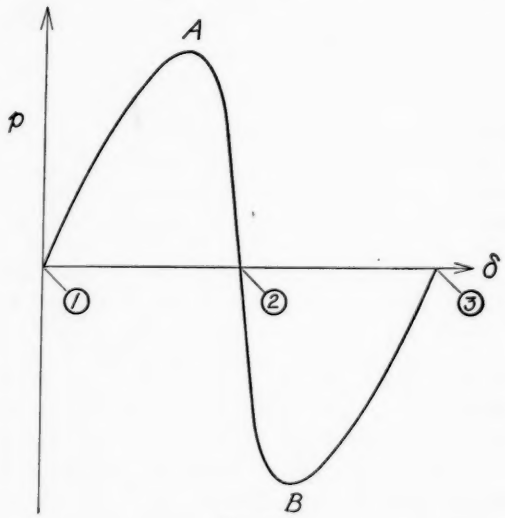

Fig. 2a.

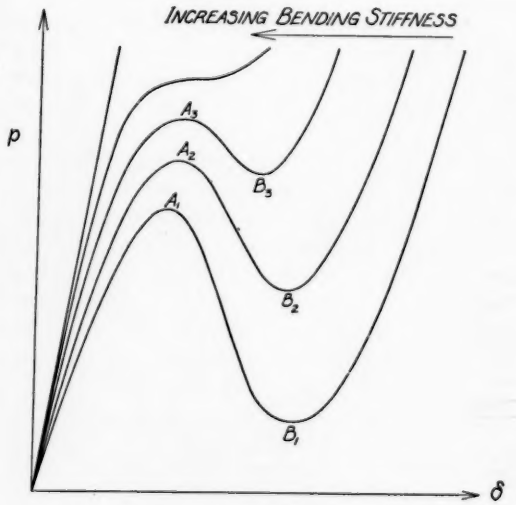

Fig. 2b.

in equilibrium. If the case of clamped edges is considered, then, for increasing values of the bending stiffness of the shell, the pressure-deflection curve will take the form shown by the curves 1, 2, etc., in Fig. 2b.

The next question concerns the load at which the shell, subjected to external pressure, will actually fail. The equilibrium positions represented by the portions A_1B_1, A_2B_2, etc. (Fig. 2b) are highly unstable; hence, if the load passes the peak A, which is determined by the stiffness of the particular shell, it immediately drops to the value represented by B. Now the ordinate of A and the form of the peak are extremely sensitive to initial imperfections of the shape of the shell, to vibrations, etc. Furthermore, the curve in Fig. 2b is based upon the assumption of a symmetrical type of deflection; the peak in the curve may be lowered by an anti-symmetric type of deflection, *i.e.*, if one part of the shell is allowed to move out while the other part moves in. The somewhat analogous problem of a curved bar loaded by a concentrated force was recently investigated by K. Marguerre[5]; he demonstrated that the process indicated in Fig. 1—the "Durchschlag,"* according to German terminology—is actually precipitated by an anti-symmetric type of deflection. It seems, therefore, probable that if no special precaution is taken to reach the peak A, the failing load observed in the laboratory corresponds to the minimum load B.

It is believed that these simple considerations throw some light on the problem of buckling of curved shells. Consider, for example, a complete spherical shell under the action of uniform external pressure. The classical theory is correct in stating that until the buckling load obtained by the classical theory is reached, any infinitesimal deviation from the spherical form involves an increase of the potential energy of the shell, and, therefore, the spherical form is stable. However, the same classical theory fails to reveal that there are configurations not far away from the spherical form which involve a lower level of the potential energy, and, therefore, the shell will actually jump over into one of these configurations. Such configurations are clearly indicated by the foregoing considerations. Assume, for example, that a segment of the shell subtended by a solid angle 2β is deflected and takes the shape corresponding to the minimum load B, whereas the rest of the shell remains spherical. If it can be shown that the load corresponding to B is lower than the classical buckling load, then the discrepancy between the failing load predicted by the classical theory and found by experiment is explained. The problem is reduced to the determination of the value of the solid angle 2β, which gives the smallest value of the minimum load p_B.

The configuration indicated above is not an exact equilibrium position of the shell, since the curvature has a discontinuity at the boundary of the deflected region; in other words, it does not take into account the reaction moment at the clamped edge. This reaction moment must be taken by the rest of the shell. In the last section of the present paper (the calculation of the failing load of a spherical shell) the work done by this reaction moment is neglected. It is difficult to estimate the effect of this omission on the value of the failing load. Therefore, a more accurate computation would be highly desirable.

The calculations in this paper refer to the case of the spherical shell. The problem of buckling of a cylindrical shell under axial compression has been attacked by the authors by similar methods, but the investigations have not as yet been completed.

The Energy Expression and the Equation of Equilibrium for a Spherical Segment under Uniform External Pressure

For the exact calculation of the load-deflection curve of a spherical segment under uniform external pressure the inclusion of non-linear terms in the equations of equilibrium is very complicated.* Therefore, the following simplifying assumptions were made:

(1) The solid angle of the segment is small.
(2) The deflection is rotationally symmetric.
(3) The deflection of any element of the shell is parallel to the axis of rotational symmetry.
(4) The effect of lateral contraction is neglected, *i.e.*, Poisson's ratio is assumed to be zero.

Assumption (3) presumably increases the failing load, since it is a characteristic of the variational method used in the following calculation that any deviation from the exact equilibrium shape increases the load. Assumption (4) probably will not change the results to any appreciable amount. This assumption was made in this paper only because it materially reduces the numerical work.

Fig. 3 indicates the notations used in the following calculations. The choice of the inclination θ of the meridian line as the dependent variable is essential for the simplicity of the equations. As can be seen from Fig. 3, due to the assumed vertical deflection of the shell, stretching or compression of the shell occurs only in the meridian direction. An element whose initial length along the meridian is equal to $dr/\cos\alpha$ has the length $dr/\cos\theta$ after deflection. The strain is, therefore,

$$\epsilon = \frac{\dfrac{dr}{\cos\theta} - \dfrac{dr}{\cos\alpha}}{dr/\cos\alpha} = \frac{\cos\alpha}{\cos\theta} - 1$$

Hence, the strain energy due to the extension of the elements of the shell is given by

* There is a need for an English expression for this process; the most descriptive the authors can think of is the popular expression "oil canning."

* The "Durchschlag" of a spherical shell with small curvature under action of a concentrated force was calculated by C. B. Biezeno.[6]

$$W_1 = \frac{Et}{2}\int_0^\beta \left(\frac{\cos\alpha}{\cos\theta} - 1\right)^2 2\pi r \frac{dr}{\cos\alpha}$$

or, with $r = R\sin\alpha$ and $dr = R\cos\alpha\, d\alpha$,

$$W_1 = \frac{ER^3}{2}\left(\frac{t}{R}\right) 2\pi \int_0^\beta \left(\frac{\cos\alpha}{\cos\theta} - 1\right)^2 \sin\alpha\, d\alpha \quad (3)$$

The two components of the curvature of the shell at an arbitrary point P are equal to $1/R$ before deflection occurs. After deflection the curvature in a meridian plane is

$$\frac{d\theta}{ds} = \frac{d\theta/d\alpha}{ds/d\alpha} = \frac{d\theta/d\alpha}{R\cos\alpha/\cos\theta}$$

Hence, the change in curvature of a meridian section is

$$\frac{d\theta/d\alpha}{R\cos\alpha/\cos\theta} - \frac{1}{R} = \frac{1}{R}\left[\frac{\cos\theta}{\cos\alpha}\frac{d\theta}{d\alpha} - 1\right]$$

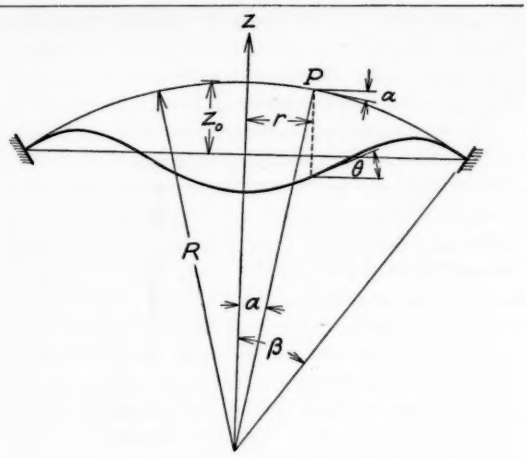

FIG. 3.

Similarly, the change in curvature of a section orthogonal to a meridian plane is $\frac{1}{R}\left[\frac{\sin\theta}{\sin\alpha} - 1\right]$
The strain energy due to bending is, therefore,

$$W_2 = \frac{Et^3}{24}\int_0^\beta 2\pi R^2 \sin\alpha\, d\alpha \frac{1}{R^2}\left[\left(\frac{\cos\theta}{\cos\alpha}\frac{d\theta}{d\alpha} - 1\right)^2 + \left(\frac{\sin\theta}{\sin\alpha} - 1\right)^2\right] =$$

$$\frac{ER^3}{2}\left(\frac{t}{R}\right)^3 \frac{2\pi}{12}\int_0^\beta \sin\alpha\left[\left(\frac{\cos\theta}{\cos\alpha}\frac{d\theta}{d\alpha} - 1\right)^2 + \left(\frac{\sin\theta}{\sin\alpha} - 1\right)^2\right] d\alpha \quad (4)$$

The potential energy corresponding to the work done by the external pressure is equal to the pressure p times the volume included between the initial and the deflected surface of the shell. The volume enclosed between the deflected surface and the plane of its circular edge is equal to

$$\int_0^\beta 2\pi r z\, dr = \left[2\pi\frac{r^2}{2}z\right]_0^\beta - \int_0^\beta \pi r^2 \frac{dz}{dr}\, dr = \pi\int_0^\beta R^2\sin^2\alpha\tan\theta\, R\cos\alpha\, d\alpha = R^3\pi\int_0^\beta \sin^2\alpha\tan\theta\cos\alpha\, d\alpha$$

The volume enclosed by the initial surface and the plane is equal to $R^3\pi\int_0^\beta \sin^3\alpha\, d\alpha$. Hence, the potential energy is given by

$$W_3 = R^3\pi\int_0^\beta \sin^2\alpha(\tan\theta - \tan\alpha)\cos\alpha\, d\alpha \quad (5)$$

The total energy, W, of the system is the sum of the strain energy and the potential energy due to external pressure Thus, from Eqs. (3), (4), and (5),

$$\frac{W}{R^3\pi} = E\left(\frac{t}{R}\right)\int_0^\beta \left(\frac{\cos\alpha}{\cos\theta} - 1\right)^2 \sin\alpha\, d\alpha + \frac{E\left(\frac{t}{R}\right)^3}{12}\int_0^\beta \left[\left(\frac{\cos\theta}{\cos\alpha}\frac{d\theta}{d\alpha} - 1\right)^2 + \left(\frac{\sin\theta}{\sin\alpha} - 1\right)^2\right]\sin\alpha\, d\alpha +$$

$$p\int_0^\beta \sin^2\alpha\cos\alpha(\tan\theta - \tan\alpha)d\alpha \quad (6)$$

At the equilibrium position, the total energy must be a minimum, therefore, the equation of equilibrium can be obtained by finding the relation between θ and α which will make the integral (6) a minimum. Using the rules of the calculus of variations, the following equation is obtained:

$$2E\left(\frac{t}{R}\right)\left[\frac{\sin\alpha\cos\alpha}{\cos\theta}\tan\theta\left(\frac{\cos\alpha}{\cos\theta} - 1\right)\right] + \frac{E\left(\frac{t}{R}\right)^3}{6}\left[\cos\theta\left(\frac{\sin\theta}{\sin\alpha} + \tan^2\alpha\right) - \frac{\cos^2\theta}{\cos\alpha}(2\tan^2\alpha + 1)\frac{d\theta}{d\alpha} + \right.$$

$$\left.\frac{\sin\theta\cos\theta\tan\alpha}{\cos\alpha}\left(\frac{d\theta}{d\alpha}\right)^2 - \frac{\cos^2\theta\tan\alpha}{\cos\alpha}\frac{d^2\theta}{d\alpha^2}\right] + p\sin^2\alpha\cos\alpha\sec^2\theta = 0 \quad (7)$$

The boundary conditions for this equation are:

$$\theta = 0 \text{ at } \alpha = 0;\ \theta = \beta \text{ at } \alpha = \beta \tag{8}$$

Eqs. (6) and (7) are unwieldy. However, a great simplification results if β, the solid angle of the shell segment, is small. Then by expanding the sine and cosine functions into power series and neglecting terms of higher than the third order in α, θ, and the derivatives of θ, Eqs. (6) and (7) reduce to

$$\frac{W}{R^2\pi} = \frac{E\left(\frac{t}{R}\right)}{4}\int_0^\beta (\theta^2 - \alpha^2)^2\alpha\, d\alpha + \frac{E\left(\frac{t}{R}\right)^3}{12}\int_0^\beta \left[\left(\frac{d\theta}{d\alpha} - 1\right)^2 + \left(\frac{\theta}{\alpha} - 1\right)^2\right]\alpha\, d\alpha + p\int_0^\beta \alpha^2(\theta - \alpha)d\alpha \tag{9}$$

and

$$\alpha\frac{d^2\theta}{d\alpha^2} + \frac{d\theta}{d\alpha} - \frac{\theta}{\alpha} = \frac{6}{(t/R)^2}\alpha\theta(\theta^2 - \alpha^2) + \frac{6p}{E(t/R)^3}\alpha^2 \tag{10}$$

These are the simplified energy expression and the equation of equilibrium, respectively. It can be seen that the terms on the left side of Eq. (10) are linear in θ and in its derivatives. They appear also in the usual theory. The first term on the right side brings in the influence of finite deflection.

In order to calculate the maximum deflection δ at the center, first the ordinate z_0 (Fig. 3) at the center has to be computed. By means of the boundary condition $z = 0$ at $\alpha = \beta$, the following relation is obtained:

$$z_0 + \int_0^\beta (dz/dr)dr = 0$$

or

$$z_0 = R\int_0^\beta \tan\theta\cos\alpha\, d\alpha \tag{11}$$

Before deformation the ordinate at the center is equal to $R(1 - \cos\beta)$. Therefore, the deflection δ at the center is given by:

$$\delta = R\int_0^\beta (\tan\alpha - \tan\theta)\cos\alpha\, d\alpha \tag{12}$$

If β is again assumed to be small, Eq. (12) is simplified to

$$\delta = R\int_0^\beta (\alpha - \theta)d\alpha \tag{13}$$

Approximate Solution by the Rayleigh-Ritz Method

To calculate the load-deflection curve, one can either solve the differential equation (10) or minimize the integral (9) directly by means of the Rayleigh-Ritz method. Due to the non-linear character of the Eq. (10), it is difficult, if not impossible, to solve it analytically. Therefore, in this paper the Rayleigh-Ritz method is used. To apply this method it is first necessary to find a plausible form of deflection satisfying the boundary conditions.

Due to the assumed symmetrical deflection it is evident that θ must be an odd function of α. The simplest form for a function $\theta(\alpha)$ which satisfies the boundary conditions is

$$\theta = \alpha[1 - K(1 - \alpha^2/\beta^2)] \tag{14}$$

where K is an undetermined parameter. Substituting the expression (14) in Eq. (13), the following relation between the parameter K and the deflection δ is obtained:

$$K = 4\delta/R\beta^2 \tag{15}$$

If Eq. (14) is introduced into the energy expression, Eq. (9), and the integrations are carried out, the total energy is obtained in the form

$$\frac{W}{R^2\pi} = \frac{Et}{60R}\beta^6\left(K^2 - \frac{K^3}{2} + \frac{K^4}{14}\right) + \frac{Et^3}{18R^3}\beta^2K^2 - \frac{p\beta^4}{12}K \tag{16}$$

The equilibrium condition between the pressure p and the deflection is obtained by putting $\partial W/\partial K = 0$,

$$\frac{1}{R^2\pi}\frac{\partial W}{\partial K} = \frac{Et}{60R}\beta^6\left(2K - \frac{3K^2}{2} + \frac{2K^3}{7}\right) + \frac{Et^3}{9R^3}\beta^2K - \frac{p\beta^4}{12} = 0 \tag{17}$$

Writing $\sigma = pR/2t$, where σ is the uniform compression stress produced by the pressure p under the assumption of small deflections, the following relation is obtained from Eq. (14):

$$\frac{\sigma}{E} = \frac{\beta^2}{5}\left(K - \frac{3}{4}K^2 + \frac{1}{7}K^3\right) + \frac{2}{3}\left(\frac{t}{R}\right)^2\frac{K}{\beta^2} \tag{18}$$

Introducing the deflection δ by using Eq. (15), Eq. (18) can be written

$$\frac{\sigma}{E} = \frac{4}{5}\left(\frac{\delta}{R} - 3\frac{\delta^2}{R^2\beta^2} + \frac{16}{7}\frac{\delta^3}{R^3\beta^4}\right) + \frac{8}{3}\frac{t^2\delta}{R^3\beta^4} \tag{19}$$

If σ/E is plotted as a function of δ/R, it is found that the load-deflection curve has the shape indicated in Fig. 2 when

$$\frac{t}{R} < \frac{1}{4}\sqrt{\frac{3}{2}}\,\beta^2 \tag{20}$$

If t/R is larger than the value on the right side of Eq. (20), the load increases with the deflection without having a maximum and a minimum; for $t/R = \frac{1}{4}\sqrt{\frac{3}{2}}\,\beta^2$ the curve for load *vs.* deflection has an inflection point with a horizontal tangent.

To find the smallest of the minimum values of the functions $\sigma/E = f(\delta/R)$, first vary β, and determine $(\sigma/E)_{min.}$ for given values of δ/R. By differentiation of Eq. (19) with respect to β^2, the value of β^2 which makes σ/E a minimum is obtained in the form:

$$\beta^2 = \frac{32}{21}\frac{\delta}{R} + \frac{20}{9}\frac{t^2}{\delta R} \tag{21}$$

Substituting this value of β^2 into Eq. (19), the following relation is obtained:

$$\frac{\sigma}{E} = \frac{4}{5}\frac{\delta}{R}\frac{1 + \frac{3}{280}\left(\frac{\delta}{t}\right)^2}{1 + \frac{24}{35}\left(\frac{\delta}{t}\right)^2} \tag{22}$$

or

$$\frac{\sigma R}{Et} = \frac{4}{5}\frac{\delta}{t}\frac{1 + \frac{3}{280}\left(\frac{\delta}{t}\right)^2}{1 + \frac{24}{35}\left(\frac{\delta}{t}\right)^2} \tag{23}$$

Therefore, $\sigma R/Et$ is a function of δ/t only. The function defined by Eq. (23) is represented in Fig. 4 by the curve labeled "envelope." The physical meaning of this curve is as follows: For values of $\sigma R/Et$ and δ/t corresponding to points that lie below the curve, no equilibrium position is possible, for any value of the solid angle of the segment 2β. This is particularly clear when Eq. (19) is rewritten in the following form:

$$\frac{\sigma R}{Et} = \frac{4}{105}\left(\frac{\delta}{t}\right)\left[21 - 63\left(\frac{\delta}{t}\right)\frac{t/R}{\beta^2} + \left(48\,\frac{\delta^2}{t^2} + 70\right)\frac{(t/R)^2}{\beta^4}\right]$$

Using $\beta^2/(t/R)$ as a parameter a family of curves expressing the relation between $\sigma R/Et$ and δ/t can be plotted (Fig. 4). Then the relation given by Eq. (23) represents the envelope of this family of curves. Hence, the maximum of the envelope curve $\sigma = 0.4908Et/R$ gives the smallest value for any peak through which the load has to pass before the shell collapses, provided the shell is of exact spherical shape and its deformation occurs with exact axial symmetry. It is noteworthy that the maximum corresponds to a deflection-thickness ratio as small as $\delta/t = 1.248$. The minimum value of the load which is able to keep the shell in a deflected shape corresponds to $\delta/t = 9.349$, and is given by $\sigma R/Et = 0.2377$ or

$$\sigma = 0.2377E\left(\frac{t}{R}\right) \tag{24}$$

Application to the Buckling Problem. Comparison with the Experiment

The results of the last section indicate that equilibrium positions involving finite deflections exist at much smaller loads than the buckling load given by the classical linear theory. To apply the method to the problem of buckling of a spherical shell under external pressure the energy expression, Eq. (9), must be modified to include the strain produced by uniform compression of the spherical shell before buckling. The total energy can be written as

$$\frac{W}{R^2\pi} = \frac{Et}{R}\int_0^\beta\left[\frac{1}{2}(\theta^2 - \alpha^2) - \frac{pR}{2Et}\right]^2\alpha\,d\alpha + \frac{Et^3}{12R^3}\int_0^\beta\left[\left(\frac{d\theta}{d\alpha} - 1\right)^2 + \left(\frac{\theta}{\alpha} - 1\right)^2\right]\alpha\,d\alpha + p\int_0^\beta\alpha^2(\theta - \alpha)\,d\alpha \tag{25}$$

Using again Eq. (14) for θ, the equilibrium condition $\partial W/\partial K = 0$ leads in this case to

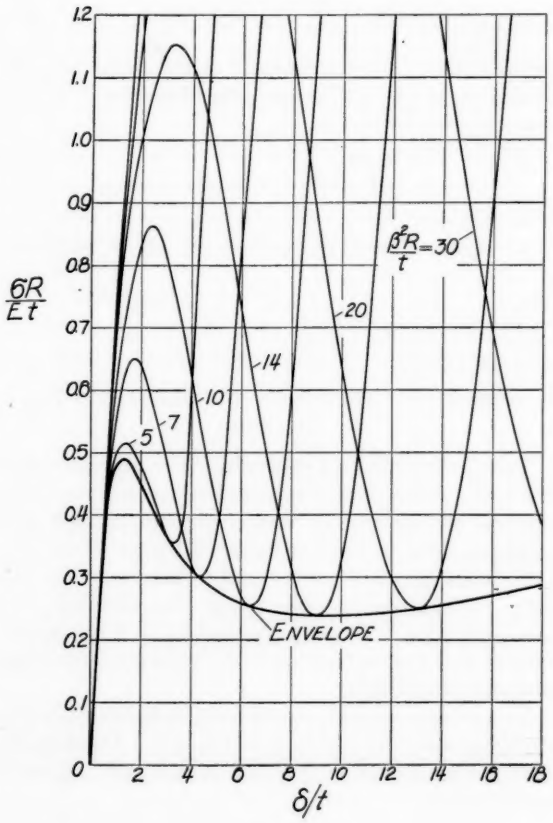

Fig. 4.

$$\frac{\sigma}{E} = \frac{1}{70}\beta^2[28 - 21K + 4K^2] + \frac{4}{3}\left(\frac{t}{R}\right)^2 \frac{1}{\beta^2} \quad (26)$$

Substituting K from Eq. (15), Eq. (26) becomes

$$\frac{\sigma}{E} = \frac{2}{5}\beta^2 - \frac{6}{5}\frac{\delta}{R} + \left[\frac{32}{35}\frac{\delta^2}{R^2} + \frac{4}{3}\frac{t^2}{R^2}\right]\frac{1}{\beta^2} \quad (27)$$

Now determine the minimum of σ/E for a given value of δ/R by varying β^2, thus

$$\beta^2 = \sqrt{\frac{16}{7}\left(\frac{\delta}{R}\right)^2 + \frac{10}{3}\left(\frac{t}{R}\right)^2}$$

and

$$\frac{\sigma R}{Et} = \frac{4}{5}\left\{\sqrt{\frac{16}{7}\left(\frac{\delta}{t}\right)^2 + \frac{10}{3}} - \frac{3}{2}\left(\frac{\delta}{t}\right)\right\} \quad (28)$$

This relation is plotted in Fig. 5. For $\delta/t = 0$,

$$\sigma = 1.4606Et/R \quad (29)$$

Of course this value of the buckling stress is much higher than the value given by the linear theory. This is expected because the assumed buckling form is far away from that resulting from the linear theory, *i.e.*, it is a very "unfavorable" shape for infinitesimal deflections. The minimum of $\sigma R/Et$ is equal to 0.18258, *i.e.*, the minimum load necessary to keep the shell in the buckled shape corresponds to:

$$\sigma_{min.} = 0.18258Et/R \quad (30)$$

This shows that the assumed shape is "favorable" for finite deflections.

The value of β corresponding to $\sigma_{min.}$ is

$$\beta = 3.8218\sqrt{t/R} \quad (31)$$

The value of β corresponding to the value given by Eq. (29) is equal to $\beta = 1.8257\sqrt{t/R}$. The deflection corresponding to $\sigma_{min.}$ is equal to about ten times the thickness t of the shell.

E. E. Sechler and W. Bollay found, by subjecting a thin-walled copper hemisphere of 18 in. radius to external fluid pressure, a buckling stress of

$$\sigma = 2480 \text{ lbs. per sq.in.}$$

With $E = 14.5 \times 10^6$ lbs. per sq.in., $t = 0.020$ in., *i.e.*, $R/t = 900$, this value corresponds to

$$\sigma = 0.154Et/R \quad (32)$$

The experimental result compares quite favorably with the theoretical value given by Eq. (30). The experimental values obtained for β and δ were: $\beta = 8°$ and $\delta \cong 0.25$ in., *i.e.*, $\delta/t \cong 12.5$. The present theory gives: $\beta = 7.4°$ (cf. Eq. (31)) and $\delta/t \cong 10$. The theory, therefore, reproduces to a fair approximation the physical process. The linear theory gives (cf. Eq. (2)) $\sigma = 0.606Et/R$; the value of β (corresponding to the first nodal line) would be, according to the linear theory, 3.3°, and δ/t is undetermined.

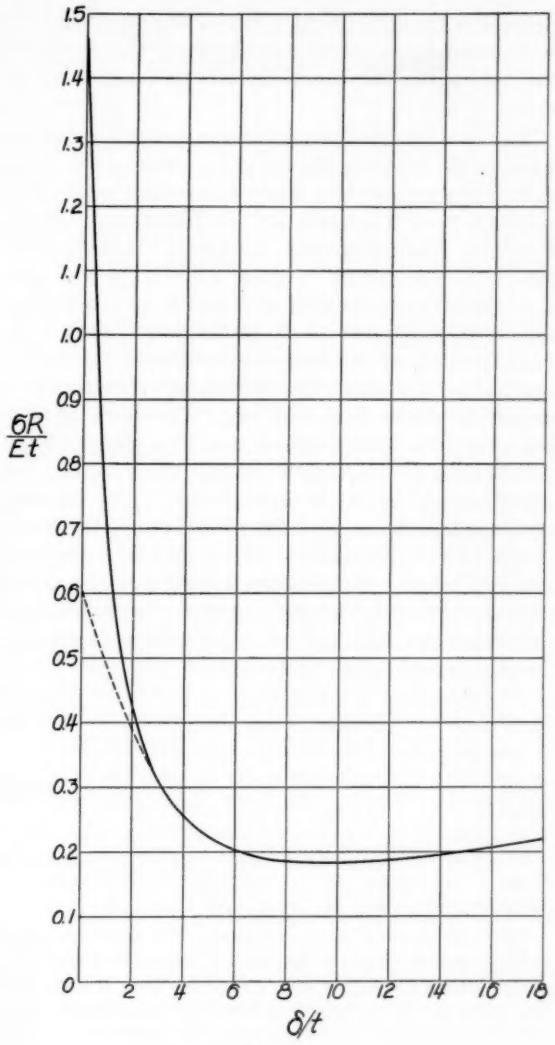

FIG. 5.

It appears that in the case of curved shells it is necessary to introduce an "upper" buckling load given by the classical linear theory and a "lower" buckling load which is equal to the minimum load necessary to keep the shell in a buckled shape with finite deformations. In Fig. 5 the probable shape of the curve for load *vs.* deflection connecting both values is indicated by a dotted line. The essential feature of the present theory is that it determines a lower buckling load independently of the initial imperfectness of the specimen or the load arrangement, whereas all previous attempts to take into account finite deformations led to failing loads which depend on arbitrary assumptions concerning the magnitude of such imperfections or lack of symmetry. It seems that the upper buckling load can be approached experimentally only if extreme precaution is taken both in the manufacture of the specimen and in performing the test. With the amount of imperfections and toler-

ances in engineering practice, the buckling load obtained will invariably be very near the lower buckling load, and, of course, this lower value is to be specified for design.

The new theory also reveals the essential difference between the buckling of a flat and a curved plate. The finite deformations of a buckled flat plate were calculated by several authors, *e.g.*, S. Timoshenko,[7] H. L. Cox,[8] M. Yamamoto and K. Kondo,[9] and K. Marguerre.[10] The results of these authors do not agree completely due to the different simplifying assumptions introduced. However, all investigators agree that after buckling of the plate an increase in the load is necessary to increase the deflections. The load falls only if the elastic limit is passed. The senior author[11] has shown for the analogous case of a straight beam that, due to the decrease of the load after buckling, the experimental scatter is much larger if the buckling occurs in the plastic range than if it occurs in the elastic range. The rapid decrease of the load after buckling revealed in this paper for curved shells is a pure elastic phenomenon, and, therefore, changes the entire theoretical and practical aspects of the buckling problem as far as curved shells are concerned.

References

[1] Flügge, W., *Die Stabilität der Kreiszylinderschale*, Ingenieur-Archiv, Vol. 3, pages 463–506, 1932.

[2] Donnell, L. H., *A New Theory for the Buckling of Thin Cylinders Under Axial Compression and Bending*, Transactions A.S.M.E., Vol. 56, pages 795–806, 1934.

[3] A brief account of the classical theory of buckling of spherical shell under uniform external pressure, including references, is given in S. Timoshenko's *Theory of Elastic Stability*, pages 491–497; McGraw-Hill, New York, 1936.

[4] Cox, H. L., *Stress Analysis of Thin Metal Construction*, Preprint of Royal Aeronautical Society, 1939.

[5] Marguerre, K., *Die Durchschlagskraft eines schwach gekrümmten Balkens*, Sitzungsberichte der Berliner Mathematischen Gesellschaft, Vol. 37, pages 22–40, 1938.

[6] Biezeno, C. B., *Über die Bestimmung der Durchschlagkraft einer schwach gekrümmten kreisförmigen Platte*, Z.A.M.M., Vol. 15, pages 13–30, 1938.

[7] Timoshenko, S., *Theory of Elastic Stability*, pages 390–393; McGraw-Hill, New York, 1936.

[8] Cox, H. L., *The Buckling of Thin Plates in Compression*, British A.R.C. Reports and Memoranda, No. 1554, 1933.

[9] Yamamoto, M., and Kondo, K., *Buckling and Failure of Thin Rectangular Plates in Compression*, Rep. of Aero. Res. Inst., Tokyo, No. 119, 1935.

[10] Marguerre, K., *Die mittragende Breite der gedrückten Platte*, Luftfahrtforschung, Vol. 14, pages 121–128, 1937.

[11] von Kármán, Th., *Untersuchungen über Knickfestigkeit*, Forschungsarbeiten, No. 81, Berlin, 1910.

Book Review

Principles and Practice of Aviation Medicine, by Captain Harry G. Armstrong, M.D.; The Williams and Wilkins Company, Baltimore, 1939; 496 pages, $6.50.

This book has been prepared primarily as a text for students and as a reference work for those actively engaged in the practice of aviation medicine. The intimate relationship between certain basic principles of aviation medicine and success in design, operation, and piloting of airplanes makes it highly desirable that those in the aviation industry have available a reference work of general information in this field. In the absence of a medical manual prepared specifically for their needs, aeronautical engineers will find much in the book which they can use in their work.

The book starts with a short historical account, beginning with the first fliers, describing medical services to fliers during the World War, and leading up to the recent establishment of Medical Service Centers by the Civil Aeronautics Authority.

There follows a chapter on "The Flight Surgeon" describing his qualifications and duties.

Chapters III through IX deal with pilot selection. The first two, on evolution of an introduction to pilot selection, lead up to chapters on eye, cardiovascular, ear, nose and throat, general physical, and neurophysic examinations. These go into some detail and are of interest mainly to the physician.

Chapter X on "Care of the Flier" is of general interest and gives in lay terms the various tests and the part played by both the physician and by the individual in keeping pilots and flying personnel fit.

Following chapters deal with the physiological effects of noxious fluids and gases, wind, ventilation, cold, heat, light, and vibration, effect of flight on the ear, and aerial equilibrium and orientation.

Airsickness, one of the most important unsolved problems, is given careful consideration. Several hypotheses are presented which seem to offer likely explanations of its occurrence. Suggestions regarding the kinds of food that should be served in flight are given. It is encouraging to learn that medical records do not show any permanent ill effects or deaths from airsickness.

Anoxia, acute and chronic altitude sickness, oxygen supply, mechanical effects of low pressures, and aeroembolism are taken up in detail in the next six chapters. This section, dealing with the effects of flight at high altitude, is especially interesting and timely. A large amount of experimental data is reported and reviewed.

The next two chapters, on "Sealed High Altitude Enclosures" and "Speed and Acceleration," give much useful information. Requirements as to temperature, pressure, humidity, ventilation, oxygen content, etc., are reviewed. The accelerations along three reference axes of an airplane during acrobatic maneuvers are given in a convenient table, along with data showing the physical effects.

The next chapter, on "Accidents," lists the Civil Aeronautics Authority's accident statistics, which show, for instance, that about half of the accidents to civil aircraft are caused by pilot errors. Captain Armstrong has for many years been a leading proponent of simplification of the work of pilots so that causes of fatigue will be lessened. Designers will have this important matter brought forcibly to their attention.

The closing chapters deal with "Psychology of Flight," "Protective Flying Equipment," and "Aerial Relief and Sanitation."

Though it is prepared primarily for the physician, the medical terminology is reduced to a minimum consistent with the scientific nature of the work. Aircraft designers, operators, and pilots will find much information that they can readily absorb and that will be invaluable to them for the further advance of the safety of aviation.

Meteorological Conditions Associated with Aircraft Lightning Discharges and Atmospherics

E. J. MINSER

Transcontinental and Western Air

ABSTRACT

From an analysis of a large number of actual cases, lightning discharges to aircraft in flight are determined to be between two oppositely charged regions in cumulo type clouds and to occur most frequently in the zone adjacent to the freezing isotherm, *i.e.*, from 26° to 34°F. The origin of the electrical charge in cumulo type clouds is explained as resulting from the selective separation of positive and negative ions in the earth's electrical field by cloud and precipitation particles, and final concentration at the freezing isotherm through disruption of rain drops, the charge in the cloud being determined by the cause of disruption. Flight procedure through cumulo type clouds to avoid lightning discharges, is given.

INTRODUCTION

WITH the increase in number of large, all metal, transport planes flying regular schedules, there has been a consistent increase in the number of lightning discharges encountered by aircraft. In 1935, with the introduction of Douglas DC-2 equipment, the first definite discharges were reported, and since that time this phenomenon has been frequently observed, not only in the United States, but in various other sections of the northern hemisphere.

The first lightning discharges were generally considered as freaks of nature, a "one in a million" event, and the possible hazard was overshadowed by the novelty of the phenomenon. When, however, the frequency of occurrence increased, a definite hazard was recognized, even though structural damage in each case was of a minor degree. Lacking any specific knowledge of this phenomenon, no means of prevention could be readily devised, except a general warning "to keep clear of thunderstorms."

This warning, wise as it appeared, did not decrease the number of discharges encountered, for an analysis of case histories soon revealed that the majority of discharges were not being encountered in thunderstorms but occurred in cumulus type clouds that produced showers. As this type of cloud is common in alll atitudes within the usual range of altitudes traversed by scheduled operations, the air transport industry was faced with a very grave problem.

During the winter of 1937–38 a detailed analysis of the meteorological conditions prevailing at the time discharges were encountered was begun. Until that time most of the research had been conducted by radio engineers, who worked on the premise that the discharges were the result of the airplane triggering a discharge between two cloud masses or, in the opinion of some, the result of a discharge between a cloud mass and the airplane. At the same time efforts were made to protect the radio equipment and other vulnerable parts of the plane and to devise means by which the electric charge could be drained off. Damaged parts of aircraft were shipped to the General Electric Company which offered to make suitable measurements in an effort to determine the nature of the discharges with respect to time duration and current magnitude.

Up to the present time over fifty case histories of discharges reported in the United States have been analyzed in this study. In many of the early cases much valuable data were lacking and while pilots could recall certain of the conditions that existed, the information was far from being as complete as an investigation of this type demanded. However, about twenty-five accurate and complete case histories are available and it is upon these that this study is based.

ANNUAL AND DIURNAL DISTRIBUTION

Early in this study the annual distribution of discharges was plotted, primarily because the date of occurrence was one element that was available in every case. This curve revealed that two definite peaks occurred during the year with a maximum frequency in early spring, with a lesser peak in late fall. Since these peak periods are during the time of least thunderstorm frequency in the United States the early observed fact that discharges infrequently occurred in thunderstorms was borne out.

The diurnal frequency of occurrence revealed a definite peak between 4 and 8 p.m., which time period coincides with the period of maximum convection over the continent.

ALTITUDE

The mean altitude at which discharges were encountered was 10,000 feet with a maximum of 18,000 feet and a minimum of 2000 feet, with no one level predominant.

TURBULENCE

In all cases some degree of turbulence was reported. Light turbulence was usually present within the cloud,

Presented at the joint meeting, I.Ae.S. and Soaring Society of America, Elmira, New York, July 1, 1939.

suddenly increasing to moderate or severe just prior to the discharge.

Precipitation

In every case precipitation was observed prior to and during the discharge. As well as could be determined by the pilots the precipitation was generally in the form of rain and/or wet snow, rarely dry snow.* When dry snow was observed the precipitation generally changed to wet snow and/or rain at the time of discharge. When snow alone was observed the discharge appeared to be vertical rather than horizontal.

Cloud Forms

It is difficult for a pilot to determine accurately, while on instruments, the type of cloud in which he is flying. Since no discharge was ever reported except when in a cloud, information necessary to establish the average cloud type could not be determined from the pilots' reports. Ground observers in the vicinity of the discharge generally reported cumulus type clouds as the predominant type, which is supported by the other meteorological data. The analysis of weather maps generally revealed modified polar air as being the prevailing air mass which likewise, because of its inherent instability, also supports this conclusion.

Electrical Phenomena

Electrical phenomena observed by the pilots are typed as aural and visual. This differentiation is necessary since static heard in the radio receivers increases with the intensity of corona discharge, which, of course, is invisible in daylight.

Static was in all cases severe. Ordinarily, it was weak until precipitation was encountered, at which time a definite increase in intensity was observed, becoming a steady roar at the time of discharge. With the discharge, the intensity decreased to a degree comparable to that present prior to encountering precipitation.

When the discharge occurred at night a corona discharge was reported in every case. The corona invariably followed a definite time sequence in all cases where observed and the degree of static varied directly as the intensity of the corona.

The corona discharge usually was observed to begin upon encountering precipitation and remain constant for a limited time, being generally restricted to extremities of the airplane having a small radius of curvature such as the nose, propeller tips, and wing tips. This static and/or corona would endure for a period of fifteen to thirty seconds, and end abruptly with the lightning discharge which was usually observed as a vivid flash. Thunder, if heard at all, generally resembled a shotgun discharge.

Temperature

The average temperature existing at flight level is 28°F. In those cases where this element was reliably reported the extremes were one case each of −5°, 10°, and 40°F. The remaining temperatures fell within the limits of 25° to 34°F. Considering the wide variation of altitudes at which discharges were encountered the concentration of temperatures to a small spread near freezing is of interest, and it was this fact that motivated a more intense study to determine, if possible, the fundamental causes of lightning discharges.

In the geographical regions where the majority of the lightning discharges were encountered it was determined from aerological data that the mean elevation of the freezing isotherm was below surface during the winter months and above three kilometers during the summer. Thus, during the spring and fall the freezing isotherm would lie between one and three kilometers. Since the maximum frequency of discharges occurs during these two seasons, the importance of temperature as a factor in the generation of electrical charges in cumulus clouds was recognized.

Physical Results of Discharges

The damage to the structure of the plane and equipment has, in all cases, been of a minor nature and in no instance has it caused the failure of any essential part. Damage has been confined to punctures of the skin or forming frames, burned off trailing antennas, fusing of radio lead-in parts, torn fabric, and damaged tail cones. In every instance the damage was restricted to those parts of the structure having small radii of curvature, but in no one case was the damage of mechanical or aerodynamic importance. The points of ingress and egress of the discharge have always been identified.

For an extended period of time the General Electric Company and other organizations have recorded the intensity of lightning discharges to the earth and have fairly well established the maxima and minima of currents, time duration of discharges, and quantities of electricity involved. A comparison of holes burned in laboratory specimens by a controlled current of known magnitude and duration with the actual damaged aircraft structure indicates that in certain instances modern all-metal aircraft have withstood safely both high current short time and low current long time discharges as great as those known to have occurred in the General Electric studies.

* Wet snow observed in cumulus clouds under these conditions appeared to consist of a conglomerate of snowflakes and water. Because of their irregular form these particles cannot be classified as soft ice pellets, neither does the term sleet truly apply. The "splashing" of these particles on striking the windshield indicates that considerable liquid water is present, and hence the term "wet snow" is used.

It is therefore believed that modern all-metal aircraft in flight is not endangered by lightning discharges and no hazard exists under such circumstances.

History of a Typical Discharge

The usual sequence of events culminating in a lightning discharge through an airplane is as follows:

Flight is being conducted at an altitude where the temperature is near freezing, on and off instruments in towering cumulus clouds from which occasional showers are observed. On entering an unusually large cloud light to moderately wet snow or rain is encountered. If the cloud is entered on the forward side where up drafts are most prominent, precipitation is usually in the form of rain and moderate tubulence is experienced. If the rear of the cloud is entered, wet snow is the usual precipitation form.

Shortly after entering the region of precipitation, static increases in the radio and at night a corona discharge (St. Elmo's Fire) is visible on the wings, propeller tips, nose, and other extremities of the airplane's structure. As flight is continued through the cloud the intensity of the static increases to a steady roar, the corona becomes more vivid, with streamers extending forward into the cloud, and turbulence becomes more pronounced. These conditions continue for ten to twenty seconds, then a flash of lightning occurs, ending abruptly the static and corona, after which turbulence steadily decreases.

This sequence of events is interpreted to indicate that the distribution of the electrical charge in a convective type cloud is roughly that shown in Fig. 1. In this

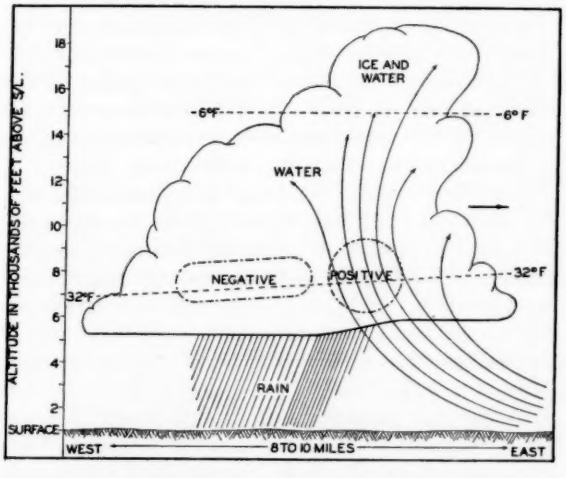

FIG. 1. Generalized diagram showing the distribution of electrical charge, hydrometeors and air currents in a shower cloud.

diagram, the cloud is shown to be moving eastward with the ascending currents entering the cloud base in the forward portion. In this part of the cloud a region of positive electricity is indicated.

In the rear of the cloud, where precipitation is in the form of wet snow, a region of negative electricity is indicated, with a neutral zone separating the opposite charges.

An airplane in flight through the regions of concentrated charge in the cloud would rapidly assume the charge of its environment and the charge would be gained faster than it would be dissipated except by brush discharge, which produces severe static and corona. On entering the neutral zone the airplane may, by virtue of its length as a conductor, initiate a discharge between the oppositely charged portions of the cloud.

Origin of the Electrical Charge

The information obtained from the case histories used in this study is believed to contribute toward the solution of the origin of the electric charge in thunderstorms. In the past, cloud masses having a high electrical charge were considered to be limited to the cumulo-nimbus type. In this study the majority of lightning discharges were found to have occurred in cumulus clouds of the shower type. Discharges occurring in thunderstorms were limited to less than 10 per cent of the cases, which is considerably less than would ordinarily be expected. This fact alone makes necessary a reconsideration of the prevailing theories of the origin of the electrical charges in thunderstorms.

That the electrical charge in thunderstorms originates in the cloud itself is generally accepted. The process whereby quantities of positive and negative electricity are produced and then separated so that two portions of the cloud are oppositely charged has been the subject of considerable theoretical and practical research, and the opposing theories proposed by C. T. R. Wilson[1] and G. C. Simpson[2] have been developed.

During this study an effort was made to explain the various observed conditions by these existing theories. While each of these theories was applicable in certain instances, it now appears probable that a combination of the two, plus the introduction of Bergeron's ice crystal theory of precipitation[3] satisfactorily explains the origin and distribution of the electrical charge in thunderstorms.

In fine weather, the electrical field of the atmosphere is positive, and the earth carries a negative charge. In such a field negative ions are driven upward while positive ions move downward toward the earth. The mobility of these ions is about 1.5 cm. per sec. in a field of gradient 1 volt per cm., but when captured by condensation or Aitken nuclei their mobility is only 0.005 to 0.0003 cm. per sec.

When, through condensation, cloud particles form in a stratum of the atmosphere, free ions are captured and the polarity of the droplet becomes opposite to the existing electrical field, that is, the lower surface of the drop will carry a positive charge with a negative charge upon its upper surface. As long as the cloud particles

have no appreciable vertical movement the electrical field in the cloud remains positive with respect to the earth.

In a cloud of convective origin (cumulo type) the cloud particles are subject to extensive vertical displacements and the normal electrical field is disturbed. Cloud particles carried upward by ascending currents readily exceed the velocity of the upward moving negative ions. Since the upper surface of the drops are negatively charged, downward moving positive ions are attracted to the drop and captured, and the droplet in this manner becomes positively charged. Eventually, the upper portions of the cloud, at least that portion subject to strong vertical convection, also becomes positively charged.

Cloud particles that have formed at the condensation level (where the temperature is above freezing) and are carried by the ascending currents to a region of subfreezing temperature remain in liquid form, and do not freeze. Water vapor in the ascending air must continue to condense as the temperature is lowered through adiabatic cooling, and will increase the size of the cloud particles. At some critical temperature condensation becomes more improbable and sublimation of water vapor takes place on sublimation nuclei present. Thereafter, above that level, only ice crystals form, and the upper portion of cumulus type clouds becomes a mixture of ice and water particles.

The ice particles, being in the form of needles and plates, have a very slow rate of fall and the direction of fall is erratic. If the cloud remains supersaturated for some time the crystals will continue to grow and form flakes. Also, because of the lower vapor pressure over ice, sublimation at the expense of adjacent water particles will occur. However, because of their erratic direction of fall, crystals must readily collide with drops, and a conglomerate of ice and water will form.

In the rear portion of the cloud the strength of the ascending currents rapidly diminishes and the velocity of fall under gravity of the ice-water particles soon exceeds the sustaining force of the airstream. Since they are now exposed to more frequent collisions with the slower falling water particles, the size of these particles rapidly increases.

During the descent the polarity of the particle is positive with respect to the earth, that is, the lower surface is charged positively. Negative ions, moving upward in the electrical field, are therefore attracted and captured by the drop and carried downward, and through this filtering process the upper positive region is protected against neutralization by ascending negative ions.

The initial disruption of the droplet immediately after reaching the 32°F. isotherm appears to be the important phase in the origin of the electric charge. As an ice-water conglomerate, these particles have a high viscosity, and being irregular in form their rate of fall is retarded. Such particles would also intercept and capture free negative ions much more rapidly than would the smaller, slow moving water particles.

Upon melting, the form of the droplet becomes more nearly streamlined, its velocity of fall rapidly increases and, on attaining its terminal velocity, the particle disrupts. In 1927 Simpson[4] applied the experiments of Lenard to the breaking of drops by an air current and concluded that a separation of electrical charge is thus produced in a thunderstorm. Through this process the negative ions are liberated and the remaining positively charged liquid drops fall free. In this manner, a region of high negative charge is established below the freezing isotherm.

In the region of strong ascending air streams, the disruption of droplets likewise occurs. However, the water particles retaining the positive charge cannot fall free but are held suspended or carried aloft in the ascending currents unless the mass of accumulated water exceeds the sustaining force of the vertical air stream. The negative ions separated during this process are carried into the upper and rear portions of the cloud where they are captured by falling precipitation forms and concentrated below the freezing isotherm by the method previously described. In this manner two oppositely electrically charged regions are established in a horizontal plane in the thunderstorm.

In Fig. 2 the history of cloud particles, free ions, and precipitation forms in a typical cumulo-nimbus type cloud is shown. This diagram differs somewhat from that presented by Simpson[2] in that a third region of activity is designated along the front of the cloud. It is through the upward movement of cloud particles in this region that the positive charge at the top of the cloud is sustained.

A lightning charge within the cloud may occur between the negatively charged region below the 32°F. isotherm and (1) the positive region at the top of the cloud, (2) the positive region in the ascending air stream, (3) the earth, and between the positive region in the ascending current and earth.

In a large cumulus cloud that will produce showers, the electrical field may never attain the potential necessary to initiate a lightning discharge and the charges will gradually dissipate through leakage and neutralization. An airplane, however, moving between the two horizontally charged zones may, by virture of its own length as a conductor, plus the short-circuiting effect of a trail of ionized gas particles (due to corona discharge from the plane) initiate a discharge. The airplane then becomes a conductor of the discharge. Data reviewed in this study verify this conclusion and account for all discharges reported.

It should be remembered that in an extensive thunderstorm the electrical generating mechanism is not limited to a single cell as illustrated in Fig. 2. Several such cells undoubtedly exist and the mechanism is duplicated in varying degrees of intensity within a single well-developed cumulo-nimbus cloud.

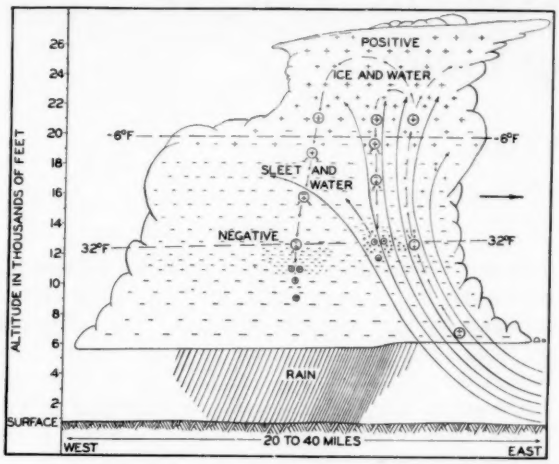

FIG. 2. Generalized diagram showing the distribution of meteorological elements and the mechanism of the separation of electrical charges in a typical thunderstorm.

FLIGHT PROCEDURE

Since the initiation of a lightning discharge through an airplane in flight requires the passage of the plane between two oppositely charged portions of the cloud, discharges may be avoided by the following flight procedure:

(1) Avoid, if possible, instrument flight through large cumulo-type clouds, especially at the level where the temperature is between 25° and 35°F.

(2) If, when on instruments, it is apparent from the temperature and degree of static and corona discharge that the airplane is in a highly charged zone, and a discharge is imminent, reduce speed and descend.

(3) If a change in altitude is not possible and reduction of speed does not materially reduce corona or static, keep eyes focused on the instrument panel, which should be brightly lighted at night. This will help to prevent temporary blindness if a discharge occurs near the cockpit.

Compliance with the above suggestions has in several instances enabled pilots to avoid lightning when all conditions indicated that a discharge was imminent. In no instance was a discharge encountered when this procedure was followed.

RAIN AND SNOW STATIC

Rain and snow static is a term applied to those radio atmospherics frequently experienced when an airplane is flown through precipitation. The fact that this type of static does not occur in all types of precipitation nor at all temperatures, requires explanation.

In flight through a charged cloud or charged precipitation, an airplane quickly assumes the charge of its environment and continues to gain the charge faster than it can be dissipated through normal leakage. When the potential of the airplane is sufficient to produce a brush discharge or corona, the steady hissing in the radio receivers is heard.

Charged precipitation cannot be easily avoided, particularly by scheduled transports. Records indicate, however, that the most severe rain static occurs when rain is encountered at temperatures near freezing or below thunderstorms. Snow static is also most severe when it is encountered at temperatures near freezing and the intensity decreases directly with the temperature.

Rain and snow static can then be attributed to the same causes as lightning, that is, regions of high electrical charge, and can be avoided or minimized by recognizing and avoiding these regions.

CONCLUSION

No effort has been made in this paper to present quantitative electrical values of the processes described. Wilson using Macky's[5] figures obtains values that are in accord with direct thunderstorm measurements. Since the charge separation effected by the difference in rate of fall of precipitation forms and cloud particles approximates Wilson's theory, application to the process described in this paper appears practical.

Further investigation of the generation of electrical charges in thunderstorms and cumulus clouds is being continued as additional data are accumulated. Although the reports of pilots received since a summary of this paper was presented last winter substantiate the theory advanced herein, the number of reports is limited and it is possible that further information may require a revision of these views.

REFERENCES

[1] Wilson, C. T. R., Journal of the Franklin Institute, Vol. 208, page 1, 1939.

[2] Simpson, G. C., Proc. Roy. Soc., Series A, No. 906, page 309, 1939.

[3] Bergeron, T., *On the Physics of Cloud and Precipitation*, Mem., U.G.G.I., Lisbon, 1933.

[4] Simpson, G. C., Proc. Roy. Soc., Series A, No. 114, page 376, 1927.

[5] Macky, Proc. Roy. Soc., Series A, No. 133, page 565, 1931.

Book Review

Dive Bomber, by ENSIGN ROBERT A. WINSTON; Holiday House, New York, 1939; 191 pages, $2.00.

This is a well written story of the training of a naval aviator from his enlistment to his emergence as a dive bombing test pilot.

The book gives an excellent picture of the work of naval pilots at Pensacola, at naval air stations, and on aircraft carriers. The author, having had experience as a newspaper writer before joining the Navy, presents the career of a naval aviator most effectively.

Dynamic Problems of the Tricycle Alighting Gear

JEAN WYLIE

Douglas Aircraft Company

ABSTRACT

After a brief review of the research program of the Douglas Aircraft Company on tricycle type alighting gear, a mathematical analysis is developed for the longitudinal stability of the plane while taxiing on the ground. From this analysis certain criteria are developed for the avoidance of porpoising. A second and extremely necessary theoretical analysis of nose-wheel shimmy discusses not only the cause but also the amounts of damping that have yielded satisfactory gears. From the equations and sample figures given, routine calculation only is necessary to compute damping requirements on any installation, provided all constants are given or can be estimated.

I. Dynamic Problems of Tricycle Alighting Gear

RESEARCH work conducted by the Douglas Aircraft Company on tricycle type alighting gear installations has been divided into three distinct phases. Preliminary test work was done with a small scale test cart towed behind a truck. This experimental cart was readily adjustable for almost all possible configurations. The results of these tests were so promising that one of the OA-4A amphibian observation planes was equipped with a nose wheel for testing on an actual airplane. Although the tests were limited because of time, the fundamental conclusion that a tricycle alighting gear is not critical was definitely confirmed. Continued test work on this installation appeared unnecessary. The third phase of research continues constantly and is designed to furnish design criteria and to investigate from a theoretical viewpoint dynamic problems such as maneuverability, porpoising, and shimmy. From the test work it was immediately apparent that the critical dynamic problem is the prevention of shimmy of the nose wheel. Indications were obtained that in certain designs porpoising of the airplane while taxiing might prove at least unpleasant; the ground maneuverability was considered to be some function of the geometry of the installation about which more should be learned.

These dynamic problems will be discussed in the reverse order of their importance. A dynamic investigation of ground maneuverability is too complicated mathematically to be of interest to the engineer. It is possible, however, to set up the equations of equilibrium for an airplane making a steady turn at constant speed, provided the following assumptions are made: the radius of the turn is large; aerodynamic drag and tail damping, restoring moments induced by rolling friction of nose wheel, and deflections in the springing system may be neglected. The principal conclusion that may be drawn from such an analysis is that the critical tipping condition occurs when the coefficient of side friction equals the cotangent of the ground angle from the center of gravity of the plane to one of the main wheels.

Presented at the West Coast Annual Meeting, I.Ae.S., Pasadena, California, June 17, 1939.

II. Longitudinal Dynamic Stability

The following study of the dynamic longitudinal stability of the tricycle type alighting gear must be presented in a simplified preliminary form, not only to minimize the mathematical complications but also to maintain consistency with the rather drastic assumptions which must be made in order to treat the problem from the theoretical point of view. The basic assumptions which are necessary in order to develop the equations of motion for the free uncontrolled motion of an airplane equipped with the tricycle alighting gear running on the ground are: (1) The tail load is considered only in calculating the equilibrium of moments about the center of gravity and is considered as negligible in the balance of the vertical forces. (2) Tail drag is negligible; variable drag and all parasite drags are considered to be concentrated at the center of gravity. (3) The forward thrust is also assumed to pass through the center of gravity (true for most modern designs) and to be sufficient to balance the drag and ground friction. (4) Ground friction is assumed to be proportional to the weight on the wheel. (5) The ground effect is accounted for in the aerodynamic coefficients and efficiencies; the ground effect on the tail-plane is of second order for tricycle gear airplanes. (6) The actual tire-oleo combination shock absorbing characteristics can be replaced by equivalent linear springs with constants K_F and K for the nose and main wheels, respectively; the damping of the shock system is negligible for the preliminary investigation. (7) The longitudinal oscillations are negligible.

The following notations are used:

μ = Rolling ground friction coefficient, usually about 0.03 for fields in good condition.
q = Dynamic air pressure.
U = Forward velocity of airplane relative to wind.
z = Vertical motion coordinate, positive downward.

Θ = Pitching motion coordinate, positive diving.
m = Mass of airplane.
a = Slope of wing lift curve.
α_W = Angle of attack of wing.
a_T = Slope of tail lift curve.
α_T = Angle of attack of tail.
η = Tail efficiency.
S = Wing area.
S_T = Tail plane area.
P_F = Vertical load on nose wheel.
$P, \dot{P}$ = Vertical load on each main wheel.
K_F = Static position equivalent linear nose gear spring constant.
K = Static position equivalent linear main gear spring constant.
K_B = Pitching radius of gyration about the center of gravity.
l_T = Tail length, from the C.G. to the C.P.$_T$.
d = Distance of C.G. forward of C.P.
h_1 = Nominal static height of C.G. above the ground.
t = Mean aerodynamic chord of the wing.
$l = l_1 + l_2$ = Wheel base, where l_1 is distance from the C.G. to the contact point of nose wheel, and l_2 is the distance from the C.G. to the main gear contact point.

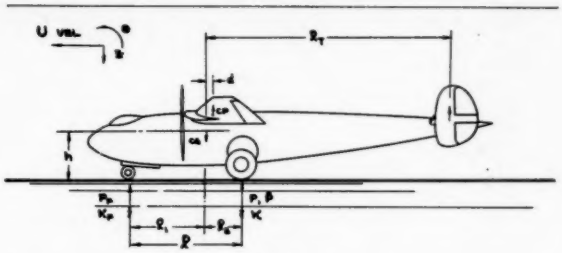

FIG. 1.

In order to develop the equations of motion one assumes a downward velocity $\dot{z}$ and a pitching rotation $\dot{\Theta}$ of the airplane. In the time interval δt the net changes in the oleo-tire reactions will be:

Nose Wheel: $\Delta P_F = -K_F(\dot{z} + l_1\dot{\Theta})\delta t$

Main Wheel: $\Delta P = \Delta\dot{P} = -K(\dot{z} - l_2\dot{\Theta})\delta t$

At the same time the angle of attack of the wing changes:

$$\Delta\alpha_W = \frac{\dot{z}}{U} - \dot{\Theta}\delta t \tag{1}$$

and the change of the angle of attack of the tail is:

$$\Delta\alpha_T = \left(\frac{\dot{z}}{U} - \dot{\Theta}\delta t\right)\left(1 - \frac{2a}{\pi AR}\right) - \frac{l_T\dot{\Theta}}{U} \tag{2}$$

Neglecting the lift of the tail surface one can summarize the balance of the vertical forces:

$$-m\ddot{z} = \left(\frac{\dot{z}}{U} - \dot{\Theta}\delta t\right)aqS + K_F(\dot{z} + l_1\dot{\Theta})\delta t + 2K(\dot{z} - l_2\dot{\Theta})\delta t \tag{3}$$

Similarly one can balance the changes in the pitching moment on the airplane (neglecting the influence of thrust and drag):

$$I_B\ddot{\Theta} = \{2l_2K(\dot{z} - l_2\dot{\Theta})\delta t + 2h_1\mu K(z - l_2\dot{\Theta})\delta t - l_1K_F(\dot{z} + l_1\dot{\Theta})\delta t + h_1\mu K(\dot{z} + l_1\dot{\Theta})\delta t\} +$$
$$\eta a_T l_T\left\{\left(\frac{\dot{z}}{U} - \dot{\Theta}\delta t\right)\left(1 - \frac{2a}{\pi AR}\right) - \frac{l_T\dot{\Theta}}{U}\right\}qS_T + \left(\frac{\dot{z}}{U} - \dot{\Theta}\delta t\right)aqSd \tag{4}$$

Eqs. (3) and (4) are the basic equations for the uncontrolled oscillations of the airplane on the ground when the magnitude of the disturbance is small.

Eq. (3) is solved formally for $\dot{\Theta}$, giving

$$\dot{\Theta} = [m\dddot{z} + (aqS/U)\ddot{z} + (K_F + 2K)\dot{z}]/[aqS - l_1K_F + 2l_2K] \tag{5}$$

It is convenient to introduce new constants formed from the airplane characteristics:

$$B_1 = l_1K_F - 2l_2K \tag{6}$$
$$B_2 = K_F + 2K \tag{7}$$
$$B_3 = \rho aS/2 \tag{8}$$
$$B_4 = \rho\eta a_T l_T S_T/2 \tag{9}$$
$$B_5 = l_1^2K_F + 2l_2^2K \tag{10}$$
$$B_6 = dB_3 + (1 - 2a/\pi AR)B_4 \tag{11}$$

Eq. (5) can now be rewritten as:

$$\dot{\Theta} = [m\dddot{z} + UB_3\ddot{z} + B_2\dot{z}]/[U^2B_3 - B_1] \tag{5'}$$

Eq. (4) may now be rewritten with new symbols and with the substitution of Eq. (5):

$$mK_B^2(m\dddot{z} + UB_3\ddot{z} + B_2\dot{z}) + UB_4l_T(m\ddot{z} + UB_3\dot{z} + B_2z) + (B_5 - \mu h_1B_1 + U^2B_6)(m\dot{z} + UB_3z + B_2\dot{z}) - U(U^2B_3 - B_1)B_6z + (U^2B_3 - B_1)(B_1 - \mu h_1B_2)\dot{z} = 0 \quad (12)$$

This linear differential equation is expanded and rearranged; at the same time it is expressed in the more concise operator form:

$$m^3K_B^2D^4 + [mK_B^2UB_3 + mUB_4l_T]D^4 + [mK_B^2B_2 + U^2B_3B_4l_T + m(B_5 - \mu h_1B_1 + U^2B_6)]D^3 + [UB_2B_4l_T + UB_3(B_5 - \mu h_1B_1 + U^2B_6) - U(U^2B_3 - B_1)B_6]D^2 + [B_2(B_5 - \mu h_1B_1 + U^2B_6) + (U^2B_3 - B_1)(B_1 - \mu h_1B_2)D]z = 0 \quad (13)$$

Eq. (13) is a fundamental form of the characteristic equation for the dynamic behavior of the airplane supported on tricycle alighting gear. From general theory of classical dynamics one can apply the theorem that the oscillatory motion will be stable or self-damped, when all the coefficients and the Routh's Discriminant of the characteristic equation are the same sign. The character of any motion can be determined therefore without a formal solution of Eq. (13). The six stability conditions obtained are summarized in the following inequalities.

$$m^2K_B^2 \geqq 0 \quad (14)$$

$$mU(K_BB_3 + l_TB_4) \geqq 0 \quad (15)$$

$$mK_B^2B_2 + U^2l_TB_3B_4 + m(B_5 - \mu h_1B_1 + U^2B_6) \geqq 0 \quad (16)$$

$$Ul_TB_2B_4 + UB_3(B_5 - \mu h_1B_1 + U^2B_6) - U(U^2B_3 - B_1)B_6 \geqq 0 \quad (17)$$

$$B_2(B_5 - \mu h_1B_1 + U^2B_6) + (U^2B_3 - B_1)(B_1 - \mu h_1B_2) \geqq 0 \quad (18)$$

$$mU^2\{K_B^2B_3 + l_TB_4\}\{K_B^2B_2 + (U^2/m)l_TB_3B_4 + B_5 - \mu h_1B_1 + U^2B_6\}\{l_TB_2B_4 + B_3(B_5 - \mu h_1B_1 + U^2B_6) - B_6(U^2B_3 - B_1)\} - \{K_B^2B_3 + l_TB_4\}^2\{B_2(B_5 - \mu h_1B_1 + U^2B_6) + (U^2B_3 - B_1)(B_1 - \mu h_1B_2)\}m^2U^2 - m^2K_B^2U^2\{l_TB_2B_4 + B_3(B_5 - \mu h_1B_1 + U^2B_6) - B_6(U^2B_3 - B_1)\}^2 \geqq 0 \quad (19)$$

Eq. (19) is the evaluation of Routh's Discriminant. These inequality conditions will be separately discussed now for possible design conditions and for the analysis of the modes of motion.

Eq. (15) is independent of the forward velocity; hence

$$K_B^2B_3 + l_TB_4 \geqq 0 \quad (15.1)$$

$$1 + \eta\frac{a_T}{a}\left(\frac{l_T}{K_B}\right)^2\frac{S_T}{S} \geqq 0 \quad (15.2)$$

This equation indicates the influence of the tail plane in causing large damping loads and moments because of its sweeping motion. For an increase in the scale of an airplane more of the weight tends to be carried in the wing, so that l_T/K_B is an increasing function of the design weight; the larger airplanes have a proportionately larger tail damping.

Eq. (16) represents a stabilizing influence of the forward speed,

$$mK_B^2B_2 + mB_5 - m\mu h_1B_1 + U^2(l_TB_3B_4 + mB_6) \geqq 0 \quad (16.1)$$

$$K_B^2B_2 + B_5 - \mu h_1B_1 \geqq 0 \quad (16.2)$$

The second form of the equation was obtained by considering the most unfavorable case of no forward velocity.

$$K_B^2(K_F + 2K) + (l_1^2K_F + 2l_2^2K) - \mu h_1(l_1K_F - 2l_2K) \geqq 0 \quad (16.2')$$

If one assumes, and this is a good approximation of the actual installation, that the static deflections of the shock strut and tire are equal for the nose wheel and main gear, then one can write

$$K_F/2K = l_2/l_1 \quad (20)$$

Substitution in (16.2′) gives

$$2K\{K_B^2(1 + l_2/l_1) + l_2^2 + l_1l_2\} \geqq 0 \quad (16.3)$$

Hence, in general, the inherent stability of the tricycle alighting gear increases as the fraction of the total load on the nose wheel increases.

Eq. (17) can be simplified to remove the internal velocity variation. Thus

$$l_T B_2 B_4 + B_3 B_5 + B_1 B_6 - \mu h_1 B_1 B_3 \geqq 0 \tag{17.1}$$

Expanding this equation,

$$\{(l_1^2 K_F + 2l_2^2 K) + d(l_1 K_F - 2l_2 K) - \mu h_1 (l_1 K_F - 2l_2 K)\} + \eta \frac{a_T S_T}{aS} \left\{ l_T^2 (K_F - 2K) + \left(1 - \frac{2a}{\pi AR}\right)(l_1 K_F - 2l_2 K) l_T \right\} \geqq 0 \tag{17.2}$$

Substitution of Eq. (20) yields

$$l_1 l_2 + l_2^2 + \eta (a_T S_T / aS) l_T^2 (1 + l_2/l_1) \geqq 0 \tag{17.3}$$

This condition also shows that the stability of the tricycle increases as the center of gravity moves forward; the tail length becomes an important factor because of the damping moment of the tail.

The fifth condition can be written

$$B_2 B_5 + U^2 [B_2 B_6 + B_1 B_3 - \mu h_1 B_2 B_3] \geqq 0 \tag{18.1}$$

The first term is always positive, so that instability can occur only if the second term be negative. If instability is to be entirely prevented the condition imposed is

$$B_2 B_6 + B_1 B_3 - \mu h_1 B_2 B_3 \geqq 0 \tag{18.2}$$

$$(K_F + 2K) \left[(d - \mu h_1) + \eta l_T \left(1 - \frac{2a}{\pi AR}\right) \frac{a_T S_T}{aS} \right] + (l_1 K_F - 2l_2 K) \geqq 0 \tag{18.3}$$

Substitution of Eq. (20) in Eq. (18.3) yields

$$\eta (a_T S_T / aS) l_T (1 - 2a/\pi AR) \geqq \mu h_1 - d \tag{18.4}$$

If the inequality (18.4) be violated then the dynamic longitudinal stability of the tricycle alighting gear decreases as the second power of the forward speed.

Routh's Discriminant for the general case of the airplane running with all wheels in contact with the ground is too complex to allow of study. The stability of the tricycle type alighting gear must be satisfactory at all speeds when the nose wheel is off the ground. This condition becomes a static requirement that the center of gravity of the airplane lie ahead of the main gear when the ship is tail heavy and the tail is pulled down until the buffer rests on the ground. Dynamically, this condition is justifiable because one of the accepted methods of take-off for a tricycle plane consists of making the ground run with the nose wheel off the ground.

The theoretical equations developed can be applied easily to this case by setting K_F to zero where it appears. The change in the arm of the main wheel reaction about the center of gravity is neglected because the magnitude of the oscillations is assumed infinitesimal. This assumption may be partially corrected by a judicious variation of the ground friction constant μ.

The third inequality (16) can be written in the form

$$2KmK_B^2 + U^2 \frac{\rho a S}{2} \frac{\eta \rho a_T S_T}{2} l_T^2 + m \left[2Kl_2^2 + 2\mu h_1 l_2 K + U^2 \frac{\rho a S}{2} d + \left(1 - \frac{2a}{\pi AR}\right) U^2 \frac{\eta \rho a_T S_T}{2} l_T \right] \geqq 0 \tag{16.4}$$

$$\left[1 + \frac{l_2^2}{K_B^2} + \frac{\mu h_1 l_2}{K_B^2} \right] + \frac{U^2}{2K} \left\{ \frac{\rho a S}{2} \frac{d}{K_B^2} + \frac{\eta \rho a_T S_T l_T}{K_B^2} \left(1 - \frac{2a}{\pi AR}\right) \frac{\rho a S}{2m} \frac{\eta \rho a_T S_T}{2} \frac{l_T^2}{K_B^2} \right\} \geqq 0 \tag{16.5}$$

for the special case when the ship is on only its main gear. Eq. (16.5) can be expressed in dimensionless form through the introduction of the wing mean aerodynamic chord, denoted by t,

$$\frac{d}{t} \geqq - \eta \frac{a_T l_T S_T}{atS} \left\{ \left(1 - \frac{2a}{\pi AR}\right) + l_T \frac{\rho a S}{2m} \right\} \tag{16.6}$$

This relation is easily recognized as the basic static longitudinal stability of the plane. Any airplane with static longitudinal stability will satisfy the stability condition.

The fifth condition is expressed in Eq. (18.3) when K_F vanishes:

$$d \frac{\rho a S}{2} + \eta \frac{\rho a_T l_T S_T}{2} \left(1 - \frac{2a}{\pi AR}\right) - l_2 \frac{\rho a S}{2} - \frac{\mu h_1 \rho a S}{2} \geqq 0 \tag{18.3'}$$

$$\eta \left(1 - \frac{2a}{\pi AR}\right) \frac{a_T l_T S_T}{atS} \geqq \left[\frac{l_2 - d}{t} + \frac{\mu h_1}{t} \right] \tag{18.5}$$

This condition is almost invariably critical for the airplane running on its main gear. Instability occurs because the center of lift of the wing is too far ahead of the main gear (point of support); the tail volume, which measures the amount of balancing moment to be expected from the tail plane, fixes the maximum aft position of the main gear.

If Eq. (18.5) is violated slightly, the design will still be stable as long as the take-off speed is reasonably less than the critical speed with all of the wheels on the ground. In this case the stability requires pilot effort to keep the nose wheel on the ground; this is a possible but very treacherous tricycle installation.

Eq. (18.5) is considered the basic design criterion for the design of a dynamically stable tricycle alighting gear. It correlates the tail volume effective in balance with relative position of the center of pressure on the wing and with the center of gravity of the airplane. Basic porpoising difficulties of flying boats are essentially a consequence of the violation of an equation analogous to (18.5), although the hump speed trim changes may appear to be initial disturbing factors.

The dynamic stability criteria of the tricycle alighting gear are summarized: (1) The fraction of the wheel load carried by the nose wheel should be as large as possible consistent with an adequate wheel base. (2) The main gear should be so positioned that the center of gravity is always forward of the wheel reaction, when the center of gravity is in its aftermost position and the tail is pulled to the ground. (3) The ship must have static longitudinal stability and hence sufficient tail volume to insure adequate available balancing moments. (4) The main gear must be located relative to the wing so that the criterion of Eq. (18.5) is satisfied.

Dynamic Stability of the Tricycle Type Alighting Gear on the Douglas DC-4

The previously developed theory for the behavior and stability of the tricycle type alighting gear is applied in this section to the Douglas DC-4 airplane. Two cases will be considered: the center of gravity in its most forward and in its most rearward design position. It will further be assumed that in each respective case the pressure in the tires and oleos are correctly adjusted. This is admittedly not satisfactory, but is an assumption which must be made in lieu of any even more arbitrary assumption. Below are listed the required dimensions, which have been obtained from the official reports of the Douglas Aircraft Company.

m = 1864 slugs
l = 370.00 in.
l_1 = 303.00 in. (C.G. fwd.)
= 345.47 in. (C.G. aft)
l_2 = 67.00 in. (C.G. fwd.)
= 24.53 in. (C.G. aft)
d = 27.61 in. (C.G. fwd.)
= −14.86 in. (C.G. aft)
ζ_F = 10.66 in. (static)
ζ = 11.93 in. (static)
l_T = 618.00 in. (C.G. fwd.)
= 575.53 in. (C.G. aft)
P_F = 10,860 lb. (C.G. fwd.)
P = 24,570 lb.
K_F = 1019 lb. per in. (C.G. fwd.)
K = 2050 lb. per in. (C.G. fwd.)

μ = 0.03 rolling friction
h_1 = 125.00 in.
K_B = 183.2 in pitching radius of gyration
S = 2150 sq.ft.
S_T = 412.28 sq.ft.
a = 4.83 per rad.
a_T = 4.49 per rad.
η_T = 0.81
t = 212.45 in. M.A.C.
P_F = 3980 (C.G. aft)
P = 28,010
= 373 lb. per in. (C.G. aft)
= 2346 lb per in. (C.G. aft)

The first equations to be evaluated numerically will be those in which the damping of the oleo springs has been neglected. A first case will be to investigate the dynamic stability of the DC-4 while running at any constant ground speed with the nose wheel off the ground. This is a critical case insofar as stability is concerned, and is of interest since one of the accepted methods of take-off involves making most of the ground run with the nose wheel off the ground. The six constants B_i are given below.

Constant	C.G. Fwd.	C.G. Aft
B_1	−274,500	−115,000
B_2	4100	4642
B_3	1.028	1.028
B_4	91.9	85.3
B_5	18,400,000	28,200,000
B_6	84.2	36.4

The characteristic equation, the roots of which determine the stability characteristics of the airplane, can be written in the form

$$\lambda(A\lambda^4 + B\lambda^3 + C\lambda^2 + D\lambda + E) = 0 \qquad (13)$$

With the above tables of dimensions the coefficients can be computed. The constants are given below, where 1168×10^{10} has been divided out

	G.G. Fwd.	G.G. Aft
A_1	1.000	1.000
B_1	$0.001458U$	$0.001336U$
C_1	$2.496 + 0.000001842U^2$	$2.54 + 0.000001014U^2$
D_1	$0.001962U$	$0.001960U$
E_1	$0.000879 + 0.000000490U^2$	$0.0000551 + 0.000000304U^2$

For dynamic stability not only must all the coefficients be positive, but also Routh's Discriminant,

$$R = B_1C_1D_1 - B_1^2E_1 - A_1D_1^2 \geqq 0$$

must be greater than zero. When the center of gravity is in its most forward position the evaluation of R yields

$$R = 10^{-6}U^2(3.29 + 0.00000423U^2)$$

and when the center of gravity is in its aftermost position the evaluation yields:

$$R = 10^{-6}U^2(2.87 + 0.000002112U^2)$$

Therefore the dynamic stability of the uncontrolled oscillation of the DC-4 with the nose wheel off the ground is satisfactory.

Critical dynamic stability occurs with the center of gravity in its aftermost design position. It is of interest to determine the influence of the tail efficiency on the dynamic stability of the alighting gear when the ship is riding on its two main wheels; for this purpose a revised calculation will be summarized in which it is assumed that the tail efficiency is only $\eta_T = 0.70$:

$B_1 = -115{,}000$	$A = 1168 \times 10^8$
$B_2 = 4692$	$B = 1.490U \times 10^8$
$B_3 = 1.028$	$C = (2996 \times 10^8 + 0.000984U^2 \times 10^8$
$B_4 = 73.7$	$D = 1.88^8U \times 10^8$
$B_5 = 2{,}820{,}000$	$E = (0.0644 \times 10^8 + 0.0000225U^2 \times 10^8)$
$B_6 = 29.4$	

One can write the reduced coefficients as:

$$A_1 = 1.000;\ B_1 = 0.001250U;\ C_1 = 2.566 + 0.000000843U^2;\ D_1 = 0.001618U;\ E_1 = 0.0000551 + 0.0000000193U^2$$

Evaluation of the Routh's Discriminant in this cases gives,

$$R = 10^{-6}U^2(2.62 + 0.00000169U^2)$$

The reduction of the tail efficiency factor is more effective (at least on the DC-4) in cutting down the stabilizing influence of speed than in reducing the basic stability, as measured by the relative magnitudes of Routh's Discriminant.

The critical case with the center of gravity aft and the high and measured tail efficiency of 0.81 will now be examined to determine the effect of velocity on the critical speeds and the damping factors. The periods for a fictitious zero velocity are

$$\lambda^4 + 2.564\,\lambda^2 + 0.00000551 = 0$$
$$\lambda^2 = -1.282 \pm \sqrt{(1.282)^2 - 0.00000551}$$
$$\lambda_{1,2}^2 = -2.56392$$
$$\lambda_{3,4}^2 = -0.00008$$
$$\lambda_{1,2} = \pm 1.601i$$
$$\lambda_{3,4} = \pm 0.00894i$$

The period for a complete mode is obtained by division into 2π,

$$T_1 = 2\pi/\lambda_1 = 3.92 \text{ secs.};\ T_2 = 2\pi/\lambda_2 = 704 \text{ secs.}$$

The effect of speed on these two modes of vibration is different, although in both cases damping is introduced; solution for a high speed during take-off follows:

$$U = 1000 \text{ in. per sec.} = 56.8 \text{ m.p.h.}$$

$$\lambda^4 + 1.336\lambda^3 + 3.578\lambda^2 + 1.960\lambda + 0.304 = 0$$

This quartic is factored by means of a division formula,

$$\lambda_{1,2} = -0.411 \pm 1.550i$$
$$\lambda_{3,4} = -0.257 \pm 0.1278i$$

The periods for these two modes of vibration are,

$$T_1 = 2\pi/1.550 = 4.06 \text{ secs.};\ T_3 = 2\pi/0.1278 = 49.2 \text{ secs.}$$

The first mode of vibration apparently has its principal source in the heaving of the ship; the damping is rather high. From the length of the period one can judge that it takes about two seconds to transfer the energy stored in the oleos into kinetic and potential energy of the ship. The second mode of motion is mainly a trim change. The length of the period relative to the damping indicates that for all practical purposes the motion is a subsidence.

III. Nose-Wheel Shimmy

Nose-wheel shimmy is the most critical dynamic problem to be solved in the design of a successful installation of tricycle alighting gear. "Shimmy" is a violent lateral and torsional oscillation to which all rubber-tired freely castering wheels are subject. It is a coupling between the lateral tire deflection under load and the lack of symmetry of the tire pattern about the support axis. Years ago the problem plagued the automobile industry and was alleviated in general by damping the lateral motion of the front axle. Some present day automobiles have a mild form of the shimmy when equipped with certain tires and traveling at high speed.

All experimental and theoretical investigations have indicated two closely related types of shimmy of a freely castering wheel: At extremely low forward speeds, when the dynamic acceleration effects may be neglected, the normal center of the tire pattern, or the load point, follows a sinusoidal path with a characteristic wave length depending on the rolling radius. This motion or kinematic shimmy is neutrally stable. A second and usually violent dynamic shimmy occurs as the speed is increased. In this case the dynamic effects cannot be neglected.

Following is a summary of the notation used in the development of a theory of shimmy:

- r = Rolling radius of the tire.
- t' = Lateral component of trail $(-2t\Theta)$.
- t = Trail, distance from intersection of axis and ground to the load point in the plane of the wheel when rolling forward.
- a = Offset of wheel axle forward of axis.
- Θ = Angle of rotation of wheel plane about axis from equilibrium.
- λ = Lateral displacement of load point on ground due to tire deflection and other causes.
- α = Axis caster angle.
- s = Distance along path of wheel.
- S = Characteristic wave length of kinematic shimmy.
- μ = Coefficient of friction of wheel on ground in lateral motion.

I_w = Moment of inertia of nose wheel, for, and rotating parts about the spindle axis.
E_λ = Tire elasticity under load.
V = Airplane forward speed.
ϵ = Non-dimensional caster angle coefficient (Fig. 13).
τ = Time variable.
δ = Increment symbol.

From an analytical point of view kinematic shimmy is easy to visualize. If the path of the load point be approximated by a circle of radius R, then, using the notation defined at the end of this section, the change in the net load point deflection per unit forward motion is the angle of axis rotation,

$$\frac{d}{ds}(\lambda - 2t\Theta) = -\Theta \tag{1}$$

If R is much greater than the rolling radius, which in turn is much greater than the effective tire deflection, the path radius can be approximated as

$$R \approx r^2/2(\lambda - 2t\Theta) \tag{2}$$

From differential geometry this equation can be rewritten as

$$d\Theta/ds = 2(\lambda - 2t\Theta)/r^2 \tag{3}$$

Combination of Eqs. (1) and (3) gives

$$d^2\Theta/ds^2 = -2\Theta/r^2 \tag{4}$$

This differential equation has a harmonic solution of the form

$$\Theta = \Theta_0 e^{i\frac{\sqrt{2}}{r}s} \tag{5}$$

with a characteristic wave length

$$S = \sqrt{2}\pi r \tag{6}$$

In this and the following theoretical investigation the restriction to small oscillation amplitudes must be maintained. Only test data can justify any extrapolation of the conclusions to the usual types of large amplitude unstable shimmy.

Dynamic shimmy arises because of unstable coupling between the tire deflection and the axis rotation. Eq. (3), which means that in the case of kinematic shimmy the moments about the axis are in equilibrium, must be modified for the inertia of the rotating parts. The moment about the axis is assumed to vary linearly as the tire dissymmetry; then

$$\frac{d^2\Theta}{d\tau^2} = C_1\left\{(\lambda - 2t\Theta) - \frac{r^2}{2}\frac{d\Theta}{ds}\right\} \tag{7}$$

$$V^2\frac{d^2\Theta}{ds^2} = C_1\left\{(\lambda - 2t\Theta) - \frac{r^2}{2}\frac{d\Theta}{ds}\right\} \tag{8}$$

The constant C_1 measures the rolling tire scrubbing moment, and can be determined:

$$C_1 = \epsilon r E_\lambda / I_w \tag{9}$$

where ϵ is a non-dimensional coefficient depending on the caster angle.

In dynamic shimmy the lateral deflection of the load point is governed by a number of factors; when the tire is deflected laterally and rolling straight its elasticity tends to diminish the displacement of the load point:

$$\delta_1\, d\lambda/ds = -C_2\lambda \tag{10}$$

This effect is assumed to be a linear function of the deflection and the constant C_2 has a theoretical value of $1/r$, which will be used in the equations. If the wheel is rolling with a non-vanishing axis angle, the tendency of the wheel to track can be expressed:

$$\delta_2 d\lambda/ds = -\Theta \tag{11}$$

If the wheel is turning about the axis at the same time it is rolling forward, the unsymmetrical ground scrubbing moment affects the lateral deflection linearly,

$$\delta_3 \frac{d\lambda}{ds} C_2 \frac{r^2}{2}\frac{d\Theta}{ds} \tag{12}$$

This component varies as the lateral elasticity of the tire, the actual tire deflection, and the curvature of the shimmy track. Addition of Eqs. (10), (11), and (12) yields a kinematic equation of motion;

$$\frac{d\lambda}{ds} = -\Theta - C_2\left\{\lambda - \frac{r^2}{2}\frac{d\Theta}{ds}\right\} \tag{13}$$

To the dynamic Eq. (8) is added a viscous damping term,

$$K\dot{\Theta} = KV\, d\Theta/ds \tag{14}$$

$$V^2\frac{d^2\Theta}{ds^2} = C_1\left\{(\lambda - 2t\Theta) - \frac{r^2}{2}\frac{d\Theta}{ds}\right\} - \frac{KV}{I_w}\frac{d\Theta}{ds} \tag{15}$$

Since the gyroscopic moments are stabilizing, especially at high speeds, it is conservative to neglect them. Eqs. (13) and (15) are combined to eliminate the variable λ;

$$\frac{d^3\Theta}{ds^3} + \frac{d^2\Theta}{ds^2}\left\{\frac{1}{r} + \frac{r^2C_1}{2V^2} + \frac{K}{VI_w}\right\} + \frac{d\Theta}{ds}\left\{2t\frac{C_1}{V^2} + \frac{K}{rVI_w}\right\} + \frac{C_1}{V^2}\left(1 + 2\frac{t}{r}\right)\Theta = 0 \tag{16}$$

Since all the coefficients of Eq. (16) are positive, Routh's Discriminant will determine the minimum amount of damping to stabilize the shimmy;

$$\frac{C_1}{V^2}\left(1+2\frac{l}{r}\right) \geqq \left\{\frac{1}{r}+\frac{r^2}{2}\frac{C_1}{V^2}+\frac{K}{VI_w}\right\}\left\{2t\frac{C_1}{V^2}+\frac{1}{r}\frac{K}{VI_w}\right\} \tag{17}$$

$$\frac{K}{I_w} = -\frac{V}{2}\left[\left(2rt+\frac{r^2}{2}\right)\frac{C_1}{V^2}+C_2\right]+\sqrt{\frac{C_1}{C_2}\left(1-tr^2\frac{C_1}{V^2}\right)+\frac{V^2}{4}\left[\left(2rt+\frac{r^2}{2}\right)\frac{C_1}{V^2}+C_2\right]^2} \tag{18}$$

In general K must be calculated as a function of the velocity V of the motion.

The frequency of the neutrally damped shimmy motion can be computed by substituting in Eq. (16):

$$\Theta = \Theta_{max.}e^{i\omega s} \tag{19}$$

$$-i\omega^3-\omega^2\left[\frac{1}{r}+\frac{r^2}{2}\frac{C_1}{V^2}+\frac{K}{VI_w}\right]+i\omega\left[2t\frac{C_1}{V^2}+\frac{1}{r}\frac{K}{VI_w}\right]+\frac{C_1}{V_2}\left(1+2\frac{l}{r}\right)=0 \tag{20}$$

The imaginary part of Eq. (20) is more convenient;

$$\omega = \sqrt{2t\frac{C_1}{V^2}+C_2\frac{K}{VI_w}} \tag{21}$$

In order to stabilize any divergent oscillation it is necessary to design a damper capable of absorbing the energy increase in the motion during a cycle. Whether a viscous damper or a friction damper is used the energy to be dissipated in each quarter cycle of the oscillation is

$$\int_0^{\Theta_{max.}} K\dot{\Theta}\,d\Theta = \int_0^{\Theta_{max.}} KV\,d\Theta/ds\,d\Theta \tag{22}$$

If Eq. (19) be substituted in the above integral, the work absorbed by the damper in each quarter cycle is

$$\int_0^{\Theta_{max.}} K\dot{\Theta}\,d\Theta = (\pi/4)\omega KV\Theta^2_{max.} \tag{23}$$

or for each complete cycle,

$$W = \pi\omega KV\Theta^2_{max.} \tag{24}$$

If a friction damping device is used to stabilize the gear with a constant friction torque T, the energy absorbed per cycle is $4T\Theta_{max.}$, so that the minimum moment is:

$$T = (\pi/4)\omega KV\Theta_{max.} \tag{25}$$

In order to determine the value of $\Theta_{max.}$ (aside from making an arbitrary limit to its value) it is assumed that for the small oscillation shimmy the critical amplitude occurs at the instant of incipient lateral skidding;

$$\mu P_F = E_\lambda\lambda \tag{26}$$

The coefficient of ground friction μ depends on the terrain. The equilibrium tire deflection is obtained by setting $d\Theta/ds$ to zero in Eq. (13) and allowing $d\lambda/ds$ to vanish. Hence

$$C_2\lambda = -\Theta \tag{27}$$

$$|\Theta_{max.}| = \frac{C_2\mu P_F}{E_\lambda} \tag{28}$$

A hydraulic damper to control shimmy must have an effective resisting moment of

$$C_{max.} = -\omega KV\Theta_{max.} \tag{29}$$

when the maximum angular velocity is

$$\dot{\Theta} = -\omega V\Theta_{max.} \tag{30}$$

The value of the maximum hydraulic damping moment is 1.273 times the friction torque required. If the stability of the nose wheel be judged by the amount of damping required to prevent shimmy, the stability varies as the second power of the reciprocal of the load on the wheel.

The analytical treatment developed can be extended to determine the effect of change in the design parameters. The effect of an offset, which alters the effective trail, can be calculated by partial differentiation of Eq. (18);

$$\frac{\partial}{\partial t}\left(\frac{K}{I_w}\right) = -\frac{rC_1}{V} + \frac{\frac{V^2}{4}\left[2rt\,\frac{C_1}{V^2} + C_2 + \frac{r^2}{2}\,\frac{C_1}{V^2}\right]\left(2r\,\frac{C_1}{V^2}\right) - \frac{C_1 r^2}{2C_2 V^2}}{\frac{K}{I_w} + \frac{V}{2}\left[\frac{C_1}{V^2}\left(2rt + \frac{r^2}{2}\right) + C_2\right]} \tag{31}$$

Eq. (21) also contains t, hence it must also be partially differentiated;

$$\partial\omega/\partial t = C_1/\omega V^2 \tag{32}$$

The effect of trail on the fricton damping torque required is computed by differentiating Eq. (25);

$$\frac{\partial T}{\partial t} = \frac{\pi}{4} V\Theta_{max.}\left\{\omega\,\frac{\partial K}{\partial t} + K\,\frac{\partial \omega}{\partial t}\right\} \tag{33}$$

$$\frac{\partial T}{T} = \frac{1}{K\omega}\left\{\omega\,\frac{\partial K}{\partial t} + K\,\frac{\partial \omega}{\partial t}\right\} dt \tag{34}$$

$$\frac{\partial T}{T} = \frac{1}{K}\,\frac{\partial K}{\partial t}\,dt + \frac{C_1}{\omega^2 V^2}\,dt \tag{35}$$

$$T(t) = T_0\left\{1 + \delta t\left[\frac{1}{K}\,\frac{\partial K}{\partial t} + \frac{C_1}{\omega^2 V^2}\right]\right\} \tag{36}$$

Since a forward offset of the axle increases the effective trail, the shimmy stability of the nose wheel decreases. Similar methods may be used to determine the relative influence of the other parameters.

If the nose wheel has a centering device with a moment $-f\Theta$, then Eqs. (18) and (21) become, respectively,

$$\frac{K}{I_w} = -\frac{V}{2}\left\{\frac{C_1}{V^2}\left(2rt + \frac{r^2}{2}\right) + C_2 + \frac{rf}{V^2 I_w}\right\} + \sqrt{\frac{C_1}{C_2}\left(1 - tr^2\,\frac{C_1}{V^2} - \frac{rf}{2V^2 I_w}\right) + \frac{V^2}{4}\left\{\frac{C_1}{V^2}\left(2rt + \frac{r^2}{2}\right) + C_2 + \frac{rf}{V^2 I_w}\right\}^2} \tag{37}$$

$$\omega = \sqrt{2t\,\frac{C_1}{C_2} + C_2\,\frac{K}{VI_w} + \frac{f}{V^2 I_w}} \tag{38}$$

Although small amounts of centering tend to destabilize shimmy slightly, the effect is so small that it may be neglected in all computations.

One of the most important initial assumptions made was to neglect the gyroscopic moments which stabilize the wheel at high speed. The angular momentum about the axle is $(V/r)I \approx 2I_w V/r$ so that the gyroscopic couple resisting rotation about the spindle axis is

$$-2I_w\,\frac{V}{r}\,\dot{\Theta} = -\frac{2I_w}{r}\,V^2\,\frac{d\Theta}{ds}$$

This term is added to the right side of Eq. (15):

$$V^2\,\frac{d^2\Theta}{ds^2} = C_1\left\{(\lambda - 2t\Theta) - \frac{r^2}{2}\,\frac{d\Theta}{ds}\right\} - \left\{\frac{KV}{I_w} + \frac{2}{r}V^2\right\}\frac{d\Theta}{ds} \tag{39}$$

Eq. (13) is unaffected; the system of simultaneous differential equations formed may be solved in the previously used manner.

Considerable numerical investigation has been done on the basis of the theory in order not only to justify it but also to apply it in design. Fig. 2, which is a graph of the K function for the OA-4A, indicates the rapid development of shimmy instability once the critical range is entered. The small region of stability at very low velocities is the régime of kinematic shimmy. Figs. 3 and 4 are the damping torque requirements (friction damper) for the OA-4A and the DC-4, respectively. The scale effect will be discussed later. The effect of speed on the shimmy frequency of the DC-4 installation is shown in Fig. 5. The frequency tends to assume a constant value, from which it drops rapidly only as the speed drops very low. As would be expected, the damper decreases the frequency only slightly. Fig. 6 is a similar figure calculated for the OA-4A; an observed frequency of from 3.5 to 4.0 cycles per second is considered a satisfactory check on

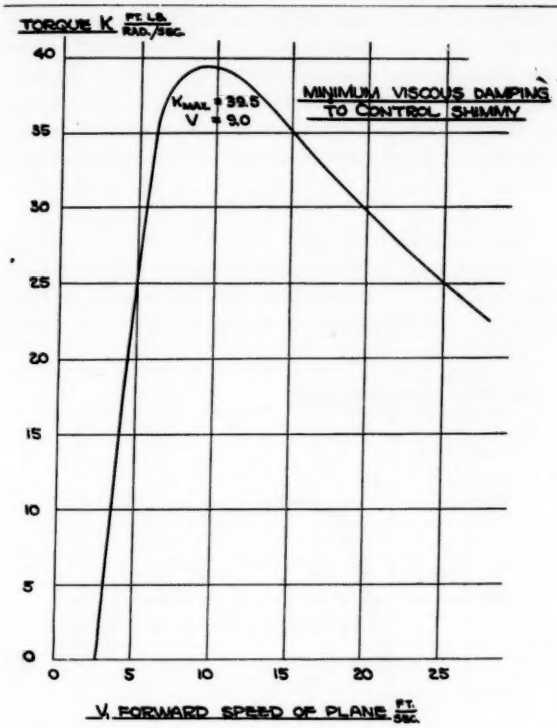

FIG. 2.

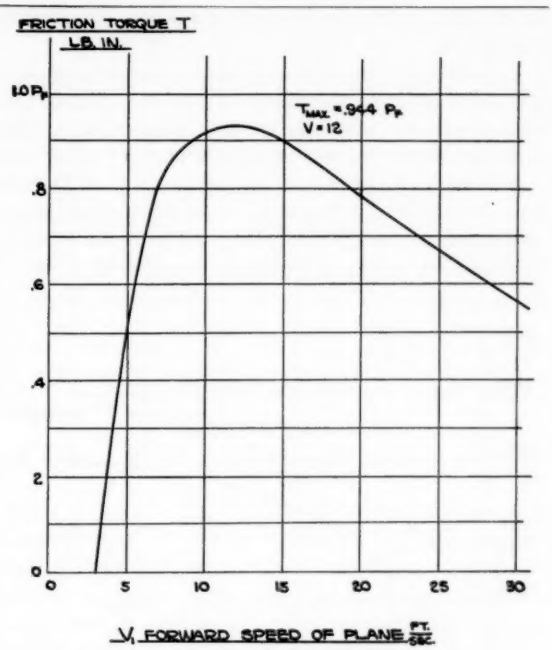

FIG. 3. Minimum friction damping torque.

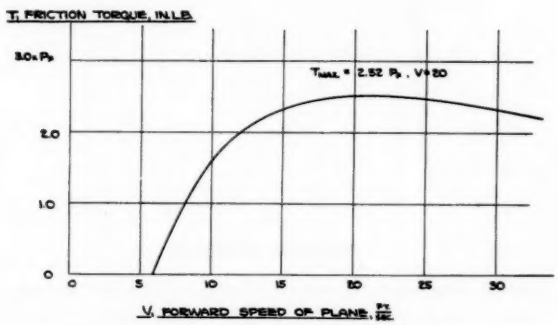

FIG. 4. Minimum friction damping to control shimmy.

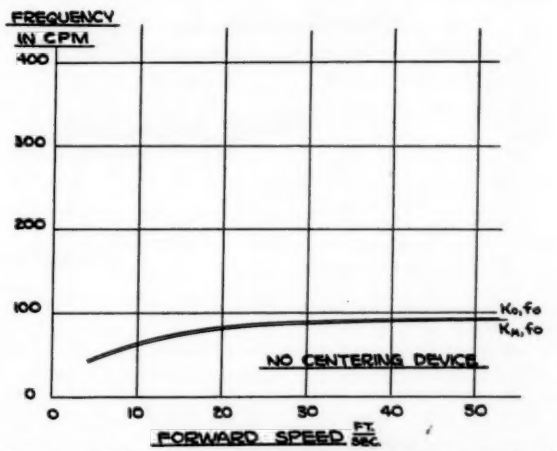

FIG. 5. Influence of speed on frequency of typical nose-wheel installation types.

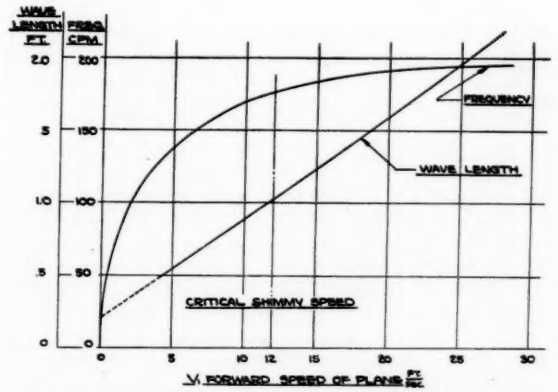

FIG. 6. Shimmy characteristics—minimum damping.

the computations. Fig. 7 shows the increase in the lag of the spindle axis displacement behind the tire deflection laterally as the speed is increased. The upper dashed curve shows that the effect of a damper designed to balance the critical shimmy condition is to increase the lag about 30° almost uniformly over the entire speed range. Fig. 8 indicates that with increasing speed the axis rotation tends to diminish relative to the unit tire deflection. The damper decreases the unit tire deflection per unit axis displacement. Fig. 9 shows design curves for the DC-4 with combined friction and hydraulic damping devices. Fig. 10 proves that a small centering device on the DC-4

nose wheel cannot appreciably alter the damping requirements.

Calculations have also indicated that tire pressure has slight effect on the damping required, although increased pressure raises the speed for maximum damping and diminishes the maximum non-skidding amplitude.

Summary of the results of calculations on Douglas and Northrop (El Segundo) nose-wheel installations has indicated a scale effect that may most conveniently be based on the gross weight of the aircraft. Fig. 11 is a logarithmic graph of the friction damping moment coefficient. The slope of the curve is one-half; since the load on the wheel varies as the weight for geometrically similar airplanes the damping moment varies as the three-halves power of the gross weight, or the nine-halves power of a characteristic linear dimension.

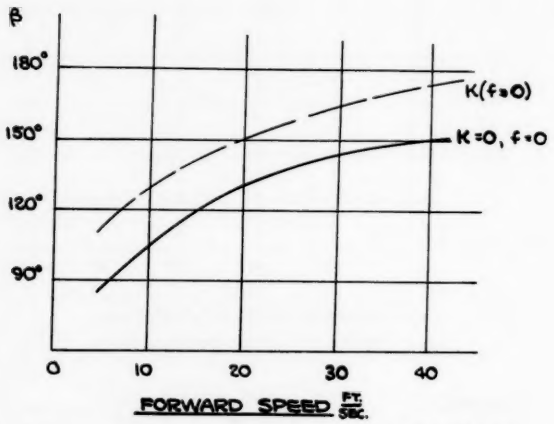

FIG. 7. Lag of spindle rotation behind tire deflection.

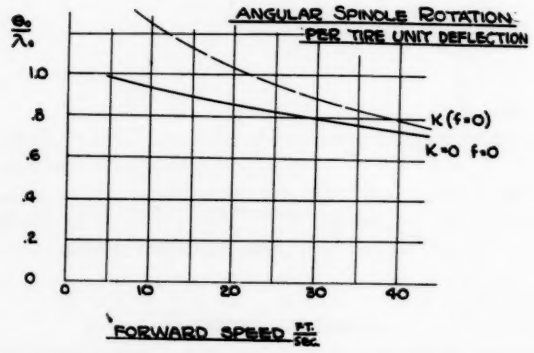

FIG. 8. Angular spindle rotation per tire unit deflection.

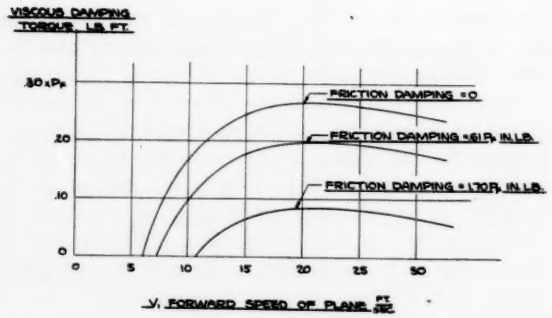

FIG. 9. Influence of friction torque on minimum required viscous damping.

APPENDIX

The Lockheed Aircraft Corporation very kindly furnished some of the results of their test cart experiments for study in checking the theoretical analysis. The results of calculations using the data are drawn

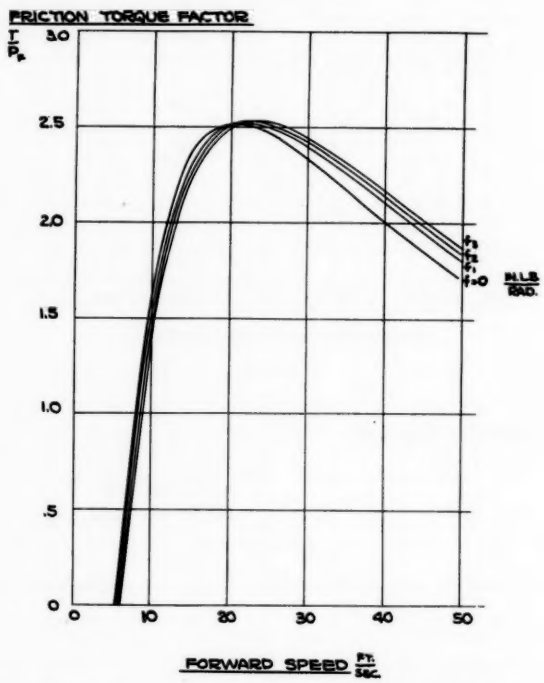

FIG. 10. Influence of centering device on friction damping requirements.

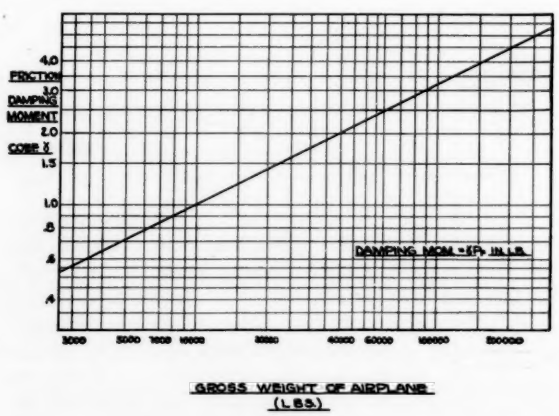

FIG. 11. Minimum friction damping to control nose-wheel shimmy ($\mu = 0.55$).

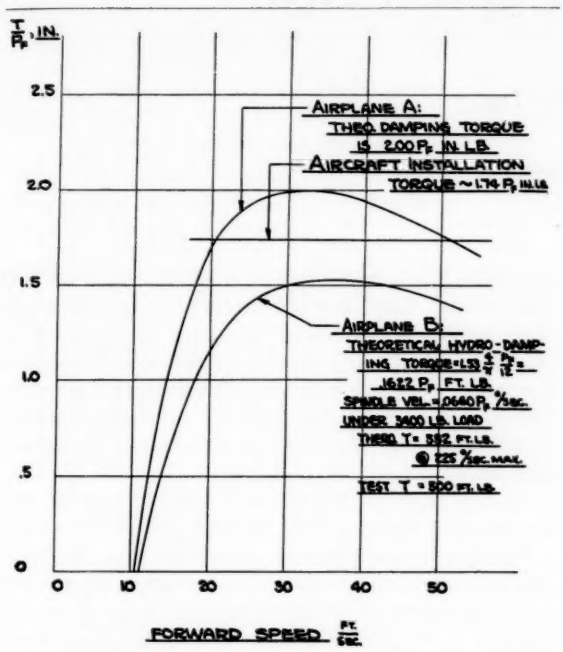

FIG. 12. Theoretical and experimental shimmy damping requirements.

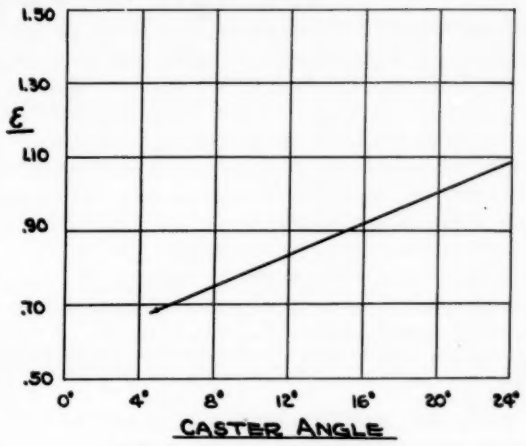

FIG. 13. Caster angle coefficient.

in Fig. 12. In connection with this comparison it should be noted that comparable Lockheed nose-wheel installations are equipped with larger wheels than similar Douglas designs were. Airplane A had a nose wheel with fairing attached so that its moment of inertia was relatively high. The calculated amount of friction damping moment is 2.00 P in. lb. The installation actually had 1.74 P in. lb. The check within 13 percent is conservative and satisfactory. Friction torque was so high as to affect seriously the ground handling characteristics. Airplane B was equipped with a hydraulic damping device with a moment on test conditions of 500 ft. lb. The minimum theoretical torque at 225° per sec. axis velocity is 552 ft. lb. Agreement is conservative and within 10 percent. A comparison of figures indicates that for the relatively larger wheels used the critical speed is considerably higher.

Letter to the Editor

November 27, 1939

Dear Sir:

In December, 1936, a short report was made of the development of strain-sensitive materials as applied to strain measurements in airplane propellers. Since that time a great deal of progress has been made in improving the resistance element in the direction of making it suitable both for static and dynamic use.

The previous resistor elements were composed of aggregates of carbon or graphite in which the strain sensitivity depends on contact areas of the carbon aggregate. While suitable for dynamic strains, an undesirable hysteresis between strain and electric resistance appeared under static conditions which, together with a considerable temperature coefficient of resistance, made the previous strips uncertain for static work.

Since that time a large amount of work has been done by Prof. A. C. Ruge and the writer at the Massachusetts Institute of Technology using metallic conductors as the strained element and it has been found possible to reduce both the temperature difficulty and the hysteresis so that strain may be dependably measured to better than one millionth of an inch on a one-inch gage length.

The difficulty of cementing the strained conductor to a metal surface has been overcome to a point where the gage is sufficiently free of creep so that measurements can be made over a period of months. Tests of the change of resistance at frequencies up to 40,000 cycles per second have not indicated any upper limit to the response and we believe that the resistance change occurs as rapidly as a change of strain can occur in the metal to which the wire is bonded. While the strain sensitivity is somewhat less than that of the carbon elements, it is well within the limits of portable galvanometers for static use and no difficulty has been encountered in utilizing present-day high-fidelity amplifiers and oscillographs for dynamic conditions.

The change in electrical resistance of wire has previously been described by Dr. Carlson who has long made use of it in his strain gages. An important modification of this method is due to Dr. D. S. Clark and his associates of the California Institute of Technology, who described a wire-wound dynamometer in connection with his impact machine in a paper for the American Society for Testing Materials entitled, "Stress-Strain Relations under Tension Impact Loading" (by D. S. Clark and G. Dätwyler, A.S.T.M. Proceedings, Vol. 38, Part II, 1938). The problem of temperature compensation and a possible method of forming the gage, together with performance tests, is to be published as a report of the N.A.C.A. It is hoped that this development will contribute to the growing knowledge of stress distribution in such complicated structures as modern airplanes.

A. V. DE FOREST
Massachusetts Institute of Technology

Design of High Speed Gears

KLAAS KNIBBE

Continental Motors Corporation

ABSTRACT

The surface stresses on gear teeth are calculated in terms of radius of curvature of the tooth flank.

Upon this is based a method to determine the maximum energy that can be safely transmitted from one gear to another during one revolution.

This quantity of energy, divided by the square of the diameter of the pinion and a constant is called "power-function of the gear" and is a dimensionless quantity. It can be easily determined by a tooth form layout to any enlarged scale.

This power function is calculated with various pressure angles, addenda, and gear ratios.

DESIGNING a successful reduction gear to handle power outputs of modern aircraft engines in excess of 1000 hp. has proven to be a very difficult problem.

Fortunately, considerable work has been done to guide the design; that of Buckingham* is outstanding. A formula by which the loading of gear teeth due to the impact of the teeth can be calculated, allowing both for speed and tooth errors, is given in this reference. The Lewis formula gives a measure of the strength of the tooth. In the average high speed application, however, the conventional tooth strength is not the controlling factor. The final step is in the so-called "Wear Factor." This is a function of the surface stresses on the tooth flank. The purpose of the present paper is to supplement this last and most important phase of the gear problem.

It has been observed that high speed gears have a tendency to show wear at or near the base circle of the teeth. As a result, the use of short addendum and dedendum teeth has been introduced with considerable success, such as 10/12 pitch; this means the pitch itself is 10 P., but the addendum and dedendum correspond to 12 P. As shown later in this paper, this is a move in the right direction, but better results can be expected in any individual case by the method suggested below.

The stress on the tooth surface depends upon the radii of curvature as worked out by Hertz. With an involute gear these radii are determined by the instantaneous position of the point contact. It will be shown that, for a given stress, the load-carrying capacity is a maximum at the pitch point with 2 equal gears. This load carrying capacity decreases along the line of contact, and is equal to zero at both base circles. Later it is proven that one definite length of tooth contact allows a maximum of energy to be transmitted per tooth contact. This maximum times the number of teeth is the energy transmitted per revolution of the gear. By reducing the latter quantity to a dimensionless function a so-called power function is introduced.

In this paper no limitations regarding cutters, etc., are taken as criteria; only involute curves are used.

First, two equal gears are considered and the power function calculated with various pressure angles and tooth numbers. Due consideration is given to the number of teeth in contact. In a graph it is shown that a 30° pressure angle is much better than 20°; also large tooth numbers give better results; in other words with a certain pitch diameter, a finer pitch is better.

Next, the other extreme, a pinion with a rack, again varying the pressure angle and number of teeth, is investigated. Here it is shown that a small pressure angle is superior. Large tooth numbers are only slightly better.

Other gear ratios, including internal gearing, are dealt with graphically and the results are shown for one particular number of teeth in the pinion and 3 pressure angles.

The capacity of internal gearing is very large. When two cylinders are in contact as shown in Fig. 1 the well known equation of Hertz applies:

$$P = k\, r_1 r_2/(r_1 + r_2) \qquad (1)$$

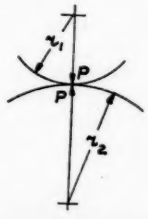

FIG. 1. Two cylinders pressed against each other are stressed according to Hertz equation

where P = load carrying capacity per 1 in. width;
r_1 = radius of cylinder 1, 1 in. wide;
r_2 = radius of cylinder 2, 1 in. wide;
k = constant dependent upon the material only;

Received January 26, 1939.

* Buckingham, Earl, *Dynamic Loads on Gear Teeth*, A.S.M.E. Research Publication, 1932.

= compressive strength in lbs. per square inch.

In Fig. 2 a set of involute gears are shown in contact. In this figure,

R_0 = base radius of both gears;
α = the pressure angle;
N = number of teeth of both gears;
C = center distance.

The point of contact travels along the line of action GF from B to D (see Fig. 2). At point B the radius

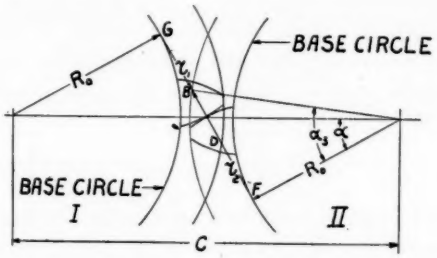

FIG. 2. Two gears are shown in contact, with their base circles and radius of curvature of the tooth flank.

of curvature of gear I is GB and the one of gear II is BF: r_1 = GB; r_2 = BF; $r_1 + r_2$ = GF. $r_1 + r_2$ does not change when the point of contact travels from B to D.

In Fig. 3 the line of action GF is shown and the load carrying capacity (Eq. (1)) is plotted perpendicular to it; this curve has a maximum in the center and becomes zero at both ends.

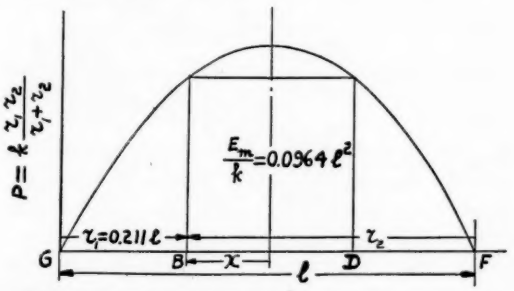

FIG. 3. Load carrying capacity of the gear teeth plotted against position of the point of contact along the line of action.

The amount of energy E that can be safely transmitted during one tooth contact is $E = P \times$ BD, or $E =$ BD $\times\ kr_1r_2/(r_1 + r_2)$. For a given travel BD, E will be a maximum when BD is located symetrically as shown. If BD = 1 then $r_1r_2 = 0$. For the other extreme, BD = 0 and $E = 0$. Between these two values of BD there is one at which E is a maximum. This is the most favorable condition. Substituting for r_1 and r_2 in terms of x and l, and setting $dE/dx = 0$, it can be shown that

$$E_m = 0.0964kl^2 \tag{2}$$

$$r_1 = 0.211l \tag{3}$$

where E_m is the maximum value of E. When the two base circles and pressure angle are given as shown in Fig. 2, the points B and D on the line of action can be determined for a maximum value of E; B and D determine the outside radii of the gears and the angle α_3.

This process of applying the proper amount of addendum can be used successfully provided the tooth does not become pointed at a smaller outside diameter than B or D call for. In this case BD must be made shorter accordingly, and the most favorable E is obtained with pointed teeth. Two equal gears will be examined first, *viz.*, 1–1 ratio and later a pinion and rack combination or 1–infinite ratio. Fig. 2 shows the 1–1 ratio gears.

Without the pointed teeth limitation from Eq. (2) $E_m/kC^2 = 0.0964 \sin^2 \alpha$. If A is the energy transmitted per revolution, and N is the number of teeth in the pinion, $A = N \times E_m$, and

$$A/kC^2 = 0.0964\,N \sin^2 \alpha \tag{4}$$

The function A/kC^2 is dimensionless and depends upon the number of teeth and pressure angle only. For purpose of identification this function is called "power function."

The power a set of gears of given pitch diameter can transmit is proportional to the square of this pitch diameter, the r.p.m., a material constant, and the power function. The latter accounts for the tooth profile, pressure angle, and number of teeth.

$$\text{Power function} = \frac{A}{kC^2} = F_p = \frac{Nr_1r_2\text{BD}}{(r_1 + r_2)C^2}$$

This power function is calculated for $\alpha = 20°$, 25°, and 30° and plotted against N in Fig. 5. Curves for the number of teeth in contact Y, as determined by the equation (see Fig. 2),

$$Y = \frac{\text{BD}}{(2\pi/N)R_0} = \frac{0.578 \tan \alpha}{\pi/N} \tag{5}$$

for $Y = 1$, 1.5, and 2.0 are also plotted in Fig. 5.

The teeth become pointed when (see Fig. 2) $\tan \alpha_3 =$ BF$/R_0$. This can be reduced to

$$\tan \alpha_3 = 1.578 \tan \alpha$$
$$\text{inv}\ \alpha_3 = \text{inv}\ \alpha + \pi/2N$$

When the pressure angle α is given, α_3 and N can be calculated for pointed teeth. This "pointed teeth" line is a boundary; above this line the teeth are pointed. It is shown in the Appendix that with pointed teeth the power function A/kC^2 is a function of N and α; the values of which are shown in Fig. 5 in the upper portion of the 1–1 ratio bundle.

It is apparent that in this case a gear can be considerably improved for wear properties by changing the pressure angle from the standard 20° to 30°.

Also the number of teeth in contact improves with this change. The next case to investigate is the other

extreme of gear ratios, *i.e.*, 1–∞, *viz.*, a pinion engaged with a rack. For the rack, $r_1 = \infty$ and Eq. (1) becomes $P = kr_2$. Hence $E = P \times \text{BD} = k\text{BF} \times \text{BD}$. Since $r_2 = \text{BF}$ with a given DF this is a maximum when $\text{BF} = {}^1/_2\text{DF}$. Using this value

$$E_m = k\text{DF}^2/4$$

Since

$$\text{DF} = R_0 \tan \alpha_3 = (C/2) \cos \alpha \tan \alpha_3$$
$$E_m = {}^1/_{16}\, kC^2 \cos^2 \alpha \tan \alpha_3$$

With a given α, E is a maximum when α_3 is a maximum. The largest value of α_3 occurs when the teeth of the pinion are pointed as shown in Fig. 4.

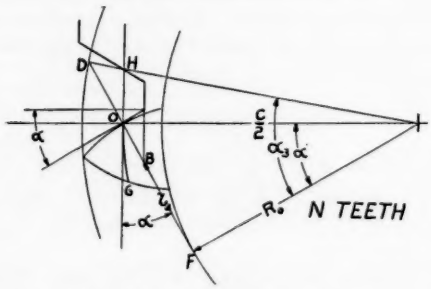

FIG. 4. A gear in contact with a rack; equal tooth thickness at the pitch line.

First it is assumed that the teeth thickness of pinion and rack are equal on the pitch line Fig. 4, $\text{OH} = \text{OG} \times \pi C/2N$, where N = number of teeth in the pinion. Then

$$F_p = A/kC^2 = {}^1/_{16}\, N \cos^2 \alpha \tan^2 \alpha_3$$

$$\text{inv } \alpha_3 = \text{inv } \alpha + \pi/2N$$

With α and N given, α_3 and the power function F_p have been calculated and plotted in Fig. 5 (see the bundle marked 1–∞ ratio; equal teeth thickness).

The number of teeth in contact is given by (see Fig. 4),

$$Y = \text{DB}/(2\pi/N)R_0 = N \tan \alpha_3/4\pi \qquad (6)$$

Y has been calculated and plotted in Fig. 5 for the various pressure angles. The limitation of the pointed rack condition for $\alpha = 30°$ occurs at N approximately 31 and for $\alpha = 25°$ and 20° the number of teeth is very large.

This rack and pinion can be improved considerably by disregarding the condition of equal tooth thickness of pinion and rack at the pitch line. If GO in Fig. 4 is made thicker, this will increase α_3 and E, and decrease OH. The maximum α_3 is reached when the rack also becomes pointed.

As in the previous case (see Fig. 6),

$$\text{E} = {}^1/_{16}\, kC^2 \cos^2 \alpha \tan^2 \alpha_3$$
$$\text{GH} = C\pi/N$$
$$\text{OD} = \text{OF} \sin \alpha$$
$$\text{OF} = \text{OB}' \tan \alpha$$
$$\text{OD} = \text{OB}' \sin \alpha \tan \alpha$$
$$\text{OB}' = R_0 \tan \alpha - {}^1/_2 R_0 \tan \alpha_3$$

Point B′ is again half-way between E and Q. As in the previous case, using the geometrical relationships shown in Fig. 6,

$$A/kC^2 = (N/16)\cos^2 \alpha \tan^2 \alpha_3 \qquad (7)$$

$$\text{inv } \alpha_3 = \text{inv } \alpha + \pi/N - (\tan \alpha - {}^1/_2 \tan \alpha_3)\sin^2 \alpha \qquad (8)$$

From these two equations α_3 and A/kC^2 have been calculated and A/kC^2 is plotted in Fig. 5 (see the bundle 1–∞ ratio; rack and pinion pointed). For the number of teeth in contact, see Eq. (6). These are also plotted in Fig. 5.

USE OF CHARTS

Fig. 5 considers only two gear ratios 1–1 and 1–∞. The power function $F_p = A/kC^2$ for any intermediate ratio must have a value between those indicated by the upper and lower bundle of Fig. 5. Also, it must be kept in mind that ideal values are shown by the graph. The purpose of the chart is merely to indicate tendencies particularly with respect to pressure angles. For instance, a 20 tooth gear meshed with another 20 tooth gear may be improved almost 100 percent by

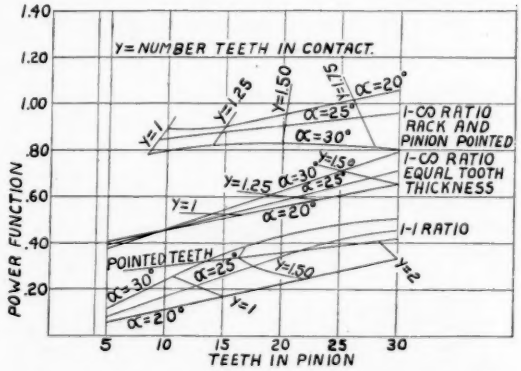

FIG. 5. The power function of two equal gears and a pinion and rack shown for various pressure angles and teeth numbers.

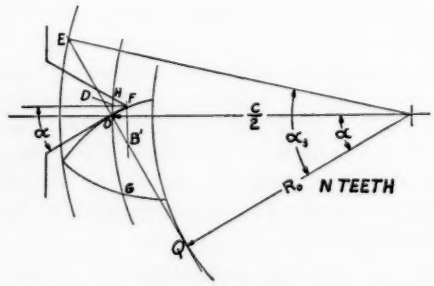

FIG. 6. A gear in contact with a rack; both are pointed.

changing from 20° to 30° pressure angle, while the number of teeth in contact is increased. On the other hand if this gear is meshed with a rack, the lower pressure angle is more desirable. Furthermore, any given gear design may be quickly checked on this chart to see how closely it approaches the ideal. Since the power function is non-dimensional it will be sufficient to lay out the gear set to any scale and then measure r_1, r_2, and C, from which (see Fig. 2),

$$F_p = A/kC^2 = Nr_1r_2\mathrm{BD}/(r_1 + r_2)C^2 \qquad (9)$$

is readily calculated so that comparison with the chart can be made.

Fig. 7 gives the information of chart 5 in a different form by plotting the power function against gear ratio.

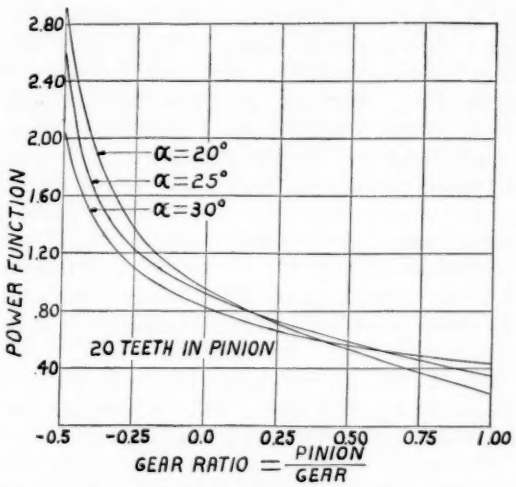

FIG. 7. The power function for various gear ratios and pressure angles is shown.

The gear ratio is the number of teeth in the pinion divided by the number of teeth in the gear. Negative values refer to internal gearing. The great capacity of internal gearing is at once apparent while the contrary requirements with respect to pressure angle for different ratios is clearly shown.

The above has been applied to actual gears built, and it was found that whenever the power function was increased, the wear qualities also improved. There was no opportunity to test it quantitatively.

No consideration has been given in this paper to specific sliding, which is important in certain applications. As far as methods of manufacture are concerned, it is possible to use standard cutters and apply a certain amount of tooth correction on one of the gears, usually the smaller one. By this process the power function can be greatly improved. In this paper it is assumed that the load upon the gear tooth is constant. Unfortunately, this is not the case, particularly for the impact loading due to tooth errors. This tooth load will reach a maximum somewhere upon the tooth profile and is most likely to occur when the load is transferred from one tooth to another. The location and magnitude of this maximum load is also vitally effected by the mass effects and flexibility of the gears. This is an extensive subject by itself, and merits further study. The principal aim of this paper is to introduce a quantity which enables the designer to compare the capacity of a given gear application with the tooth profiles as the only variable.

APPENDIX

In general for two equal gears the following applies (see Fig. 2):

$$E = k(\mathrm{GB} \times \mathrm{BF/GF})\mathrm{BD}$$

E = Energy per tooth contact
BF = $R_0 \tan \alpha_3$
GF = $C \sin \alpha$
GB = $C \sin \alpha - R_0 \tan \alpha_3$
BD = $2R_0 \tan \alpha_3 - C \sin \alpha$
R_0 = $\frac{1}{2}C \cos \alpha$

Substituting these values and introducing A, the energy per revolution and N the number of teeth ($E = A/N$),

$$\frac{A}{kC^2} = N\left[\frac{3}{4}\cos^2\alpha \tan^2\alpha_3 - \frac{1}{2}\sin\alpha\cos\alpha\tan\alpha_3 - \frac{\cos^3\alpha}{4\sin\alpha}\tan^2\alpha_3\right]$$

And if the teeth are pointed

$$\mathrm{inv}\ \alpha_3 = \mathrm{inv}\ \alpha + \pi/2N$$

With α and N given, α_3 and A have been calculated and A/kC^2 is plotted in Fig. 5, against a number of teeth for various pressure angles.

The number of teeth in contact (see Fig. 2),

$$Y = \mathrm{BD}/(2\pi/N)R_0 = (\tan\alpha_3 - \tan\alpha)/(\pi/N)$$

Since BD = $C \cos \alpha_3 \tan \alpha_3 - C \sin \alpha$. Y has been calculated according to this equation and is plotted in Fig. 5.

Book Review

Private Pilot's Handbook, by W. C. CHAMBLISS and W. F. MACDONALD; Aerotex Publishing Company, New York, 1939; 130 pages, $2.50.

This manual is intended to prepare students for the Private Pilots certificate of the Civil Aeronautics Authority. It gives in simple language the fundamentals of navigation, meteorology, and the Civil Air Regulations as they relate to contact flight operations ordinarily performed by private pilots.

It is not intended to be an exhaustive treatise but rather to give a clear understanding of the elementary phases of the subjects, so that a pilot may safely operate his plane in accordance with the rules he must know to qualify for a private pilot rating.

The text is supplemented with questions to check the care with which the student has read each chapter. It will provide the student pilot with much useful information and should help him to qualify as a private pilot.

A Fixture for Obtaining Pin-End Conditions in Column Testing

HOWARD W. BARLOW

*New York University**

ABSTRACT

Difficulties attending the use of rollers, knife-edges and other devices used for obtaining ideal hinged-end conditions for tests of columns are discussed briefly. A new testing fixture is described which incorporates ball-bearing assemblies and gives hinged-end results for specimens having flat, parallel ends. Corrections for effective free-length are unnecessary. Results of tests on columns fabricated from thin stainless steel sheets are given to indicate the quality of the results. Possibilities for improvements and further application to tests of elastically restrained columns, eccentrically loaded columns, and sheet-stringer combinations are suggested.

INTRODUCTION

A BASIC problem in the experimental determination of allowable loads on hinged-end columns is the selection of a suitable fixture for mounting the ends of the specimen to be tested. Numerous devices have been developed from time to time with varying degrees of success. Some of the difficulties associated with the more common of these have been discussed by Wagner.[1]

At the present time the knife-edged testing fixture[2] is probably used more than any other type. Particularly is this true in the testing of sheet-stringer combinations. In general, knife-edged fixtures have one degree of freedom, although in some instances[3] additional degrees of freedom have been incorporated. The use of a knife-edged jig requires the determination of the effective free-length of the column, and presents the problem of accurately centering the ends. These difficulties have been overcome with reasonable success and results of knife-edged tests of columns are considered to be satisfactory.

In the testing of very large columns, testing fixtures with greased ball-and-socket joints are generally used. A jig with this type of joint has been modified for use in testing small sections by means of using a layer of small ball bearings between the ball and the socket. The major drawback of this particular fixture is the difficulty of accurately machining the ball and socket in order to obtain a true and smooth setting for the steel balls. Any inaccuracies greatly increase the friction in the arrangement and invalidate the results.

Little need be said about the use of single rollers in obtaining pin-end conditions since they are generally unsatisfactory as compared with knife-edged fixtures. Unless conditions are carefully controlled, single rollers will give results which are extremely inaccurate.[1]

A multiple roller fixture[4] was developed for the testing of large structural steel columns. This consisted essentially of a semi-cylindrical loading bar and a concave, semi-cylindrical base. The annular space between the two was filled with a single layer of steel rollers. The rollers were $1^1/_2$ inches in diameter and had their centers located on a circle of 6 inch radius whose center was located at the midpoint of the face of the loading block. A friction test indicated a coefficient of moving rolling friction of 0.002. The device performed very satisfactorily. Additional tests of carefully ground steel rollers between flat plates, and tests of steel ball bearings between semi-circular grooved races both indicated coefficients of starting rolling friction in the neighborhood of 0.0006. The indication is then that the use of carefully ground ball bearings or roller bearings should result in a coefficient of starting friction much less than 0.002.

In the testing of light columns, such as are used in airplane structures, it is highly desirable that the type of fixture used be one which will give an absolute minimum of friction and permit rapid and accurate alignment. Since it is reasonably easy to prepare test specimens in such a way that their ends are flat and parallel, a satisfactory testing jig also should permit the use of flat-end test specimens.

DEVELOPMENT OF A NEW TYPE OF FIXTURE

During the course of some recent structural investigations at New York University,[5] a new type of column testing fixture was developed which seems to possess these desirable qualities. It also eliminates the undesirable features of the ball-and-socket, knife-edged, and single roller arrangements. The original jig is shown in Fig. 1. It consists essentially of a hardened and

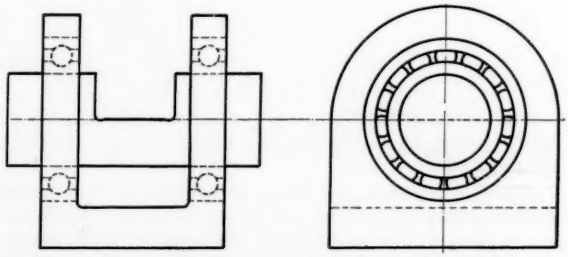

FIG. 1. Original model of new type of hinged-end column testing jig.

Received August 7, 1939.

* On leave from University of Minnesota, 1938–39.

ground steel loading bar mounted between two ball bearings which are held in a cast-iron base. The loading bar is notched to a depth equal to exactly one-half the diameter of the bar. A flat, hardened surface is thus provided upon which to rest the end of the column being tested and the arrangement permits the end of the specimen to rotate about the axis of rotation of the bar. If the specimen is located so that its neutral axis coincides with the center-line of rotation of the loading bar, then the specimen will deflect exactly as would a column ideally attached at its neutral axis. On the other hand, any desired amount of eccentricity can be readily obtained. This particular device has only one degree of freedom.

It is necessary that the entire fixture be accurately machined, but this is by no means difficult and does not require the services of an expert machinist. Fixtures are prepared in pairs, one for each end of the column. The upper one is bolted in the top head of the testing machine and the lower is clamped to the base of the machine in order to prevent slippage during the test. The pair of fixtures must be aligned carefully when setting up. This can be done by using the cylindrical loading bars as reference points.

A minimum of friction is developed in the device through the use of commercially procurable ball bearings. The extreme accuracy and high quality of machining obtained on commercial ball bearings make them ideally suited for this particular type of device. They are much more satisfactory than any custom-built device requiring hand work. It is possible to use commercial roller bearings, but the probability of increased friction in the event of slight misalignment is greater than for ball bearings; consequently, the latter type is believed to be preferable.

Since the effective free-length of the column is equal to the distance between flat loading surfaces, no calculations for determining effective free-length are needed. Further, the amount of friction is extremely small and probably much less than that experienced in any other type of testing fixture.

Experiments Conducted

In order to determine the value of the end-fixity coefficient c for this jig, two straight, solid rods of cold-rolled steel, one-half inch in diameter and 24 inches long, were tested. Each specimen had an area of 0.1962 sq. in., a moment of inertia of 0.00307, a slenderness ratio of 192, and was definitely in the Euler range. The ends were ground flat and parallel within limits of 0.0005 inches. The specimens were carefully centered in the testing jig and failed at compressive loads of 1523 and 1524 pounds, respectively.

The modulus of elasticity in tension, E, was found by test to be 29,100,000 pounds per square inch. From the Euler relationship in which $c = PL^2/\pi^2EI$, c was found to have a value of 0.996. This deviation from unity can be attributed to experimental error. Further calibration tests are contemplated.

In order to examine further the usefulness of this new type of fixture, a number of hollow specimens fabricated from thin stainless steel sheet were tested. The results for different gages of a typical cross-section are shown in Fig. 2. All of the specimens were carefully centered

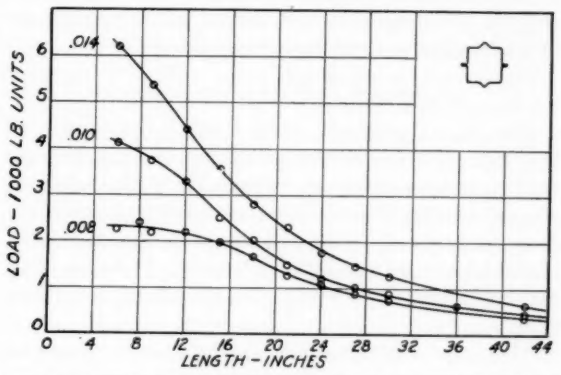

Fig. 2. Results of hinged-end column tests on typical hollow stainless steel section.

and were tested in a hand-operated Olsen testing machine. It may be seen that the test points lie on reasonably smooth curves. This fact may be regarded as proof that the specimens were centered accurately and that small initial curvatures had no effect on the results.[6]

Improvements Contemplated

The use of a hinged-end column testing jig having but one degree of freedom has been criticized. This particular type of fixture, however, is useful in certain special cases and is much easier to construct and use than one having more than one degree of freedom. In many instances the axis of failure of test specimens is obvious from a consideration of the sectional properties, and the specimen can be so mounted in the jig as to fail about the proper axis. In this case the simpler jig is the best to use. When it is desired to duplicate conditions found in structures in which the member is free to rotate about one axis, but restrained from rotation in any other plane because of the action of gussets or other members, a test fixture having a single degree of freedom may be used to good advantage.

In the experimental determination of critical loads for sections where the axis of failure is in doubt, it is desirable to have a fixture with two degrees of freedom. Accordingly a new machine was designed and is now being constructed. The basic principles are identical to those of the first model, but two degrees of freedom are provided so that the column being tested may deflect about any axis in the plane of its cross-section.

Furthermore, it is seen from Fig. 1 that the shortest column that can be tested in the original jig is approximately five inches, since the top portions of the bearings

and castings do not permit the loading faces of the bars to be brought close together. The new fixture eliminates this difficulty by a method which is, in effect, the same as cutting through the entire jig along the horizontal plane through the center of the loading bars, and making use of half-bearings and semi-cylindrical load bars. This new design will permit the testing of columns of one-half inch minimum length. It is also possible to incorporate this feature in the original device which had a single degree of freedom.

Additional Applications Possible

The use of semi-cylindrical loading bars and half-bearings gives rise to the possibility of extending the use of this type of fixture to the investigation of sheet-stringer combinations. The base casting could be sufficiently long to provide mountings for as many intermediate bearings as might be desired. The type of jig for this investigation would have a single degree of freedom.

This type of fixture might also be used to advantage in the investigation of elastically restrained columns.[6] It would eliminate the problem of determining the effective free-length and the ends of the loading bars would, at the same time, provide adequate attachment for the elastic restraining device.

Conclusions

The following conclusions may be drawn regarding the advantages of this new type of fixture in tests of columns: (1) No corrections for effective free-length are required. (2) Any desired amount of eccentricity may be provided without difficulty. (3) The amount of friction is a minimum. (4) Two degrees of freedom may be obtained readily. (5) The bearings are commercially procurable and are extremely accurate.

References

[1] Wagner, Herbert, *Remarks on Airplane Struts and Girders under Compressive and Bending Stresses. Index Values*, N.A.C.A. Technical Memorandum No. 500, Washington, D. C., February, 1929.

[2] Timoshenko, S., *Theory of Elastic Stability*, page 172, McGraw-Hill Book Company, Inc., New York, 1936.

[3] Bridget and others, *Some New Experiments on Buckling of Thin-Walled Construction*, A.S.M.E., Vol. 56, page 569, 1934.

[4] *Steel Column Research. Second Progress Report of the Special Committee*, Transactions A.S.C.E., Vol. 95, page 1152, 1931.

[5] Propper, Edouard M., *The Column Strength of Certain Thin-Walled Stainless Steel Sections. A Thesis*, New York University, June, 1939.

[6] Osgood, William R., *Column Strength of Tubes Elastically Restrained against Rotation at the Ends*, N.A.C.A. Technical Report No. 615, Washington, D. C., 1938.

Book Reviews

Why the Weather, by Charles Franklin Brooks; Harcourt, Brace and Company, New York, 1938 (second printing of 1935 edition); 295 pages, $2.50.

This extremely interesting and instructive book is based on lectures by Prof. Brooks to Meteorology classes at Clark University. It is "written primarily for the general reader who likes to know the why of that much talked about but little understood, topic—the weather."

Divided into four parts, devoted respectively to spring, summer, autumn, and winter weather, both the unusual and prosaic manifestations of the forces at work in the atmosphere are described.

While the subject matter is directed primarily toward explaining the weather in the United States many comparisons are made between the various features of this country's weather and that of other parts of the world. A chapter entitled "Aviation" gives a clear general description of those features of the weather which directly affect flying.

The Drama of the Weather, by Sir Napier Shaw; Cambridge University Press, London and New York, 1939; 307 pages, $3.50.

To those familiar with the other works on meteorology by Sir Napier Shaw the present volume needs no further recommendation. The first edition, appearing in 1933, has been revised and brought up to date.

The central idea is that "weather is the work of an accomplished artist; and, for its display, pictures are more potent than formulae." Many excellent photographs and diagrams form the skeleton around which the subject matter is built.

The chapter headings give an idea of the unique manner of presentation: "Pageantry in the Sky," "Ideas of the Drama, Ancient and Modern," "The Watchers: What They See and What They Say," "The Score," "The Chorus. Rhythmic Aspects of the Records," "The Weather-Map Presents the Play," "Where Our Rain Comes From," and "Chapter and Verse for Weather in Relation to Agriculture."

The author's clear, concise, and thoroughly entertaining treatment of the weather and its underlying causes in a style understandable to the general reader recommends *The Drama of the Weather* most highly.

Atoms in Action, by George Russell Harrison; William Morrow and Company, New York, 1939; 370 pages, $3.50.

Many books have been written popularizing the abstruse concepts of relativity, atomic theory, etc.—in short, the more or less academic aspects of modern physics. Prof. Harrison's book deals rather with the applications of physics to our everyday life and, as such, should enjoy a much wider appeal than the former type.

Beautifully written and easily understood explanations are given of recent triumphs of applied physics in the fields of farming, telephony, glass, lighting, vacuum tubes, radio, television, medicine, optics, photography, sound recording, air conditioning, aviation, and allied topics.

The material on aviation, though brief, is an authoritative discussion of the physical principles involved in flight, an account of the performance of present-day aircraft, and the trends which will determine future types. While directed primarily toward the general reader the aeronautical specialist will likewise find it fascinating reading.

A Simple Method of Measuring Landing and Take-Off Speed

CLARENCE L. JOHNSON

Lockheed Aircraft Corporation

TWO of the most difficult performance characteristics of aircraft to measure are the true landing and take-off speeds. The airplane airspeed indicator is not suited for obtaining these velocities because of the difficulty in calibrating the pitot-static head for position error at angles near the stall, particularly where the angle changes rapidly and also because the presence of the ground generally modifies any free flight calibration. At the present time, many photographic methods involving the use of high speed cameras taking up to 100 photographs per second are used to take pictures of the airplane as it lands on a runway marked off in known distances. The space-time curve is derived knowing the actual camera speed. The velocity of the airplane added to the measured wind velocity gives the landing speed. For accurate work, only electrically driven cameras are satisfactory as spring driven cameras almost always vary too greatly in speed, requiring involved calibration. This method naturally cannot be used with seaplanes. It is generally unsatisfactory because the piloting technique is very difficult, inasmuch as the pilot must make a minimum speed spot-landing fairly close to the cameras. In some cases, the camera is mounted inside the airplane, taking pictures of the lines through a cabin window as the ship lands. The exact point of contact must be noted by a ground observer.

The above are only two of a large number of camera methods of measuring speeds. All involve the use of a fairly large ground crew and none of the camera methods can be more accurate than the measurement of the wind velocity and the atmospheric pressure and temperature, which are used to correct the speeds to sea level air density. The air temperature must be carefully obtained outside the airplane at wing height in a shaded location away from ground radiation and direct sunlight. Computing the results of a camera test is a tedious task and the results are not immediately obtainable. The cost of such testing is very high.

In order to obtain greater accuracy, simplicity, and ease of testing, the writer devised a very simple method of measuring velocities near the ground which eliminates all the objections to the camera system. A swiveling pitot-static head is located on the airplane away from slipstream effects and the boundary layer of any part of the ship. The head swivels about the spanwise axis of the airplane, and it may be located on the fuselage nose, above or beneath the wing or any such place regardless of position error due to local flow velocities. The pitot or total pressure lead only is used while the aircraft is in motion. It is directly connected by a fairly large line ($^1/_8$ in. inside diameter) to a very sensitive total pressure gage capable of measuring from 1.7 to 5.0 inches of water pressure above static pressure with the desired accuracy. At the instant of landing or taking off (as indicated by a signal light connected to each landing gear shock strut), the total pressure is read on the gage. When the airplane comes to a stop after landing, it is taxied back to the approximate landing or take-off point, headed into the wind and the gage switched over to a line connected with the static openings in the swiveling pitot-static head or opened to cockpit pressure. A second reading is taken on the pressure gage. If the runway has no slope, the second reading may be taken any place on the field. The difference between the pressure on landing and when stopped gives the true impact pressure at landing speed or

$P_1 - P_2 = {}^1/_2\rho V^2$ where V is the landing speed.

Referring to Fig. 1, the following considerations apply:

P_O = True static pressure away from airplane.
V_O = True landing speed.
P_A = Local static pressure at swiveling pitot-static head on landing. This is influenced by the pressure distribution around the airplane.
V_A = Local velocity at swiveling head.

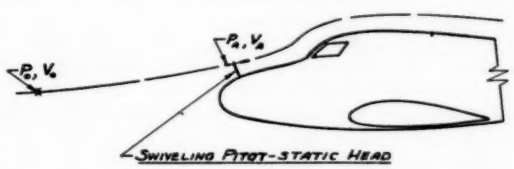

FIG. 1.

No energy has been gained or lost from point O to point A, the swiveling pitot-static head is always parallel to the streamlines, so Bernoulli's equation applies:

$$P_O + {}^1/_2\,\rho_O V^2{}_O = P_A + {}^1/_2\,\rho_A V_A{}^2 = K =$$

total pressure

Since $\rho_O = \rho_A$ for the relatively low velocities involved, the value of K is obtained from the instrument reading on landing or take-off and P_O is obtained with

Received August 21, 1939.

the airplane stopped as described above. If the wind velocity is appreciable it is, of course, necessary to obtain the static pressure reading at a point away from the airplane out of the influence of the potential flow over it.

Then:

$$V_O = \sqrt{2(K - P_O)/\rho_O}$$

Care should be taken to obtain an instrument sufficiently sensitive to give large deflections for accurate readings. A shut-off valve is used to protect the unit from excessive pressures at high speed.

Fig. 2 shows a swiveling pitot-static head located on the nose of a Lockheed Model 14 airplane on which the test method was developed. Excellent results were obtained using this device.

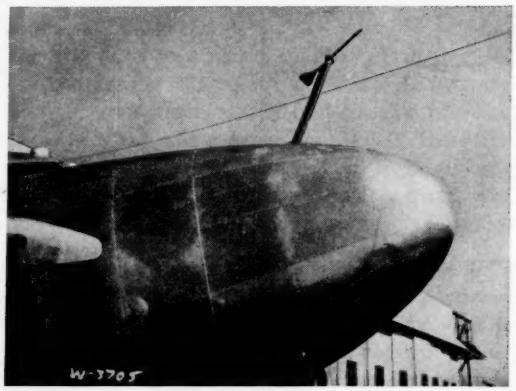

FIG. 2.

By taking total pressure readings at known time intervals on the take-off, many interesting data on acceleration may be obtained as an aid in computing excess propeller thrust available. The test method is not subject to dynamic flow errors such as influence static pressure instruments (altimeter and rate of climb indicators) on take-off.

Book Reviews

Aero Engineering, a collected work; The Steiger Company, New York, 1939; three volumes, 1 chart case, 2000 pages, $35.00.

This work represents a series of monographs by 40 contributors. It takes up the principles, production, construction, operations, maintenance, inspection, testing, and repair of British airplanes, engines, and their components, accessories and instruments in addition to some subjects of general interest, *e.g.*, principles of flight, engine developments, materials of construction, wind tunnels, etc.

The material in the first category is encyclopedic in scope, though the fact that it deals practically exclusively with products manufactured in Great Britain effectively limits its usefulness. The articles of general interest are of a semi-technical nature and are designed for the mechanic or engineer with no aeronautical background.

A detailed review of the work is practically impossible in a limited space because of the wealth of material and the lack of continuity which is more or less unavoidable in a collection of monographs by different authors.

Volume I is devoted to "Principles and Construction." In addition to material on the general subjects listed above many chapters describe airplane instruments and accessories. Each instrument or part is described by an expert and is illustrated by large drawings and photographs.

Volume II treats of airplane production. The most recent British practices in the entire field are covered in detail. Each step in the production of airplanes and power plants is treated from a practical standpoint, so that the work may not only provide a comprehensive view of the British airplane factory but will serve as a reference work for the particular fields.

Volume III has chapters on the general subjects of maintenance and overhaul but is concerned mainly with the servicing of the better known types of British aircraft, engines, parts, and accessories.

A supplementary volume is a collection of pictures and charts of characteristics of fifty British airplanes.

The 2000 pages and 2000 illustrations, plans, and photographs make this work in effect an encyclopedia of the aeronautical industry as it exists in England in 1939.

Star Altitude Curves; Weems System of Navigation, Annapolis, Maryland, 1939; Seven Volumes, covering Latitudes 0° to 70°N., size $8\frac{1}{2} \times 14$ inches, $5.00 per 10° band of latitude.

Each page of these books is a "grid" made of the altitude curves of three stars, each in a different color. Along the right and left edges of the grid are scales of latitude, while Local Sidereal Time scales in hours and minutes run across the top and bottom. A correction is given for the annual change in altitude of each star.

For a position by the *Star Altitude Curves*, only two observed altitudes, one observed time and one subtraction of time are required, with the result that a position may be obtained in about two minutes, with a saving of 80 per cent of the work ordinarily required.

The use of the Almanac, refraction correction, right ascension, declination, hour angle, azimuth, and the usual plotting of the line of position are all eliminated by this new and fast method.

The *Star Altitude Curves* fill a long-felt need for a quick, accurate, and simple method of position-finding by stars and should be in the working library of every practical navigator.

Aerodynamik und ihre Praktische Anwendung am Flugzeug, by OTTO LEIB; Dr. M. Mattheisen & Co., Berlin, 1939; 147 pages; R.M. 3.75.

Most of the English books on simple aerodynamics treat the subject from the standpoint of the engineer. Instead, this book approaches it from the standpoint of elementary physics and is an excellent introduction to the field. The author is an instructor in a school for pilots in Germany and the material is intended as a ground school text. The mathematics used are of high school level in this country.

About 60 percent of the text is devoted to aerodynamics. Sections on mechanics of flight and performance and short chapters on engines, propellers, load factors, and icing make up the remainder.

Unfortunately, the text is in the old German style. For this reason it makes difficult reading for one accustomed to the Roman type.

Institute Notes

Donald W. Douglas to Receive Daniel Guggenheim Medal

The Daniel Guggenheim Medal for 1939 has been awarded to Donald Wills Douglas, President of the Douglas Aircraft Company of Santa Monica, California. The medal, which is to be presented at the Honors Night Banquet of the Institute on January 26, 1940, is given to Mr. Douglas "for outstanding contributions to the design and construction of transport airplanes."

Mr. Douglas is an Honorary Fellow and past-president of the Institute. He received the Collier Trophy for 1935, in recognition of his development of twin-engined commercial transport airplanes. The same year he delivered the Wilbur Wright Memorial Lecture, in London, of the Royal Aeronautical Society.

At the meeting which confirmed the award for this year, Dr. J. C. Hunsaker was elected Chairman of the Board of Award to succeed Dr. George W. Lewis. Major Lester D. Gardner was elected Vice-Chairman and Elmer A. Sperry, Jr., Secretary.

The Daniel Guggenheim Medal Fund was established in 1928 to provide a gold medal and certificate to be presented annually in recognition of notable achievements in the advance of aeronautics, in commemoration of the support given by Daniel Guggenheim to the advancement of aeronautics through donations to universities and for the encouragement of civil aviation. The Fund is administered by nine directors designated by the American Society of Mechanical Engineers, the Society of Automotive Engineers, and the Institute of the Aeronautical Sciences. The recipient of the award is chosen by the directors and foreign representatives from England, France, Germany, Holland, Italy, and Japan.

The recipients of the Award have been: 1929, Orville Wright; 1930, Dr. Ludwig Prandtl of Germany; 1931, Dr. F. W. Lanchester of England; 1932, Juan de la Cierva of Spain; 1933, Dr. Jerome Clarke Hunsaker; 1934, William E. Boeing; 1935, Dr. William Frederick Durand; 1936, Dr. George William Lewis; 1937, Dr. Hugo Eckener of Germany; 1938, A. H. R. Fedden of England.

Personnel Opportunities

The Personnel Bureau serves individual members, as well as organizations seeking to employ aeronautical specialists. Any member or organization may have notices listed without charge.

Available

A seasoned executive, available January 1, 1940. Age 47, basically trained in engineering and law. Twelve years commissioned service in U.S. Army, former member of the executive staff of an aeronautical trade organization. Sound experience in production, training, service, public and personnel relations, promotion and sales. Address Box 95, Institute of the Aeronautical Sciences.

Rotating Wing Aircraft Meeting

The Second Annual Rotating Wing Aircraft Meeting, sponsored by the Philadelphia Branch of the Institute, was held on November 30th and December 1st at The Franklin Institute in Philadelphia. The meeting was very successful both from the standpoint of attendance and the high standards of the papers presented. A running account of the meeting with short digests of the papers presented will appear in the January issue of the Journal.

Eighth Annual Meeting Honors Night Dinner

Tentative programs of the Eighth Annual Meeting of the Institute on January 24, 25, and 26, 1940, in New York, will be in the hands of Institute Members by December 26th.

About forty technical papers in Aerodynamics, Aircraft Design, Air Transport, Aviation Medicine, Meteorology, Power Plants, Propellers, Radio, Instruments, and Structures, will be presented.

The Honors Night Dinner will be held on the evening of January 26th at the Biltmore Hotel. Mr. Donald W. Douglas will be presented with the Daniel Guggenheim Medal for 1939, and the Sylvanus Albert Reed, Lawrence Sperry, and Octave Chanute Awards will be presented. The newly elected Fellows and the American Honorary Fellow will receive their certificates and the next President of the Institute will be inaugurated. The guest speaker will be Hon. Robert Hinckley, Chairman of The Civil Aeronautics Authority.

Branches

Polytechnic Institute of Brooklyn. The first meeting of the school year was held on October 5th. Angelo Veterito spoke on "Pressurized Cabins," using as a basis the Institute branch lecture. Robert Kidder spoke on the difficulties encountered in construction and his experiences flying a six-foot gas model. At the second meeting, on October 26th, Stanley Jarosh gave a lecture on "Blind Flying." Fifty members attended the two meetings.

Carnegie Institute of Technology. The first meeting of the school year was held on October 3rd, at which those present were acquainted with the history, purpose, and activities of the Institute. At the second meeting, on October 20th, Andrew Virostek delivered the branch lecture, "Instrument Flight Training." After a general discussion, Prof. George B. Thorp showed a series of color slides which he took at the Tenth Annual Soaring Contest at Elmira. Twenty members attended each of the two meetings.

University of Cincinnati. At a meeting on October 28th Hans Belitz read the branch lecture, "Instrument Flight Training," which was followed by an interesting discussion. On October 14th, W. R. Owens spoke to the Student Branch on "Aircraft in Warfare." The importance, duties, tactics, and organization of air warfare were discussed.

Los Angeles. The meeting of the Branch on November 3rd was devoted to the subject, "Cooling and Cowling." The program was divided into two parts: (1) a paper entitled "The Fundamentals of the Cooling Problem" by C. C. Wood of Douglas Aircraft Company; (2) a series of discussions on "Practical Problems of Cooling and Cowling" by Messrs. Cutting, Kendrick, Lombard, Reiser, Rockefeller, Shogren, Young, and Youngs, representing Pratt and Whitney, Vega, California Institute of Technology, Consolidated, Vultee, Douglas, North American, and Wright, respectively. A dinner preceded the technical program. The meeting was attended by 175 persons.

University of Michigan. Mr. Cass Hough of the King Manufacturing Company spoke to 125 students on the subject of "Instrument Flying" at the October 12th meeting of the Student Branch. On October 19th, 250 students attended a meeting at

which the film "The American Way," presented by Mr. Frank M. Burg of American Airlines, was shown. After the showing Mr. Burg led a discussion of air transportation. At a meeting on November 9th Edward Kurzawa was elected Vice-Chairman for the remainder of the school year. The film, "Rio Cruise," furnished by Mr. Warren A. Pine of Pan American Airways, was shown to a group of 75 students and friends.

University of Minnesota. On November 1st Prof. Brush spoke to the Student Branch on his trip to Europe last summer. His visits to most of the European countries enabled him to obtain first-hand information on their aircraft. One of the interesting features of their construction was the cast engine mounts. About 80 members attended the meeting.

University of Notre Dame. At the meeting on November 9th, the following officers were elected: Edward A. Pratt, Chairman; Mario Potetti, Vice-Chairman; William S. Thomas, Secretary-Treasurer; Prof. F. N. M. Brown, Honorary Chairman. After a short talk by Burt J. Hall on the aims and objectives of the Branch, Mr. J. A. MacLean gave a lecture on "Shock Struts," in which he described the problems encountered in their design, as well as a short history of landing gear design.

Seattle. On October 25th Mr. E. G. Emery, Jr., of the Boeing Aircraft Company, presented a paper on "Submerged Engines," and Mr. C. W. Morris of the same company spoke on "Turbo Superchargers." An interesting discussion followed the presentations. About 165 members, affiliates, and friends attended the meeting.

Stanford University. At a meeting on October 17th, Mr. Richard deH. Williams presented the branch lecture on "Instrument Flight Training," supplemented by descriptions of some of his own experiences. Following the presentation, Prof. E. G. Reid demonstrated by use of a revolving chair and enclosed Bank and Turn Indicator, the false indications of the human equilibrium system. Following this, Prof. Reid demonstrated the effects of vertigo.

Books and Clippings

The library of the Institute has been acquired through gifts of books, pamphlets, and clippings. It is serving a useful purpose in providing information to many engineers, writers, and companies who use the library for reference.

Almost every member of the Institute has aeronautical books and papers which he no longer uses and which would make valuable additions to the library. They are requested to send these Parcel Post collect to the Institute. Their receipt will be promptly acknowledged.

Old newspaper clippings are especially wanted, as the Institute's files on aeronautical subjects and biographies are becoming more and more complete. Clippings regarding members' activities should be sent to the Biographical files, where they will supplement a permanent running record of members' achievements.

The Institute has received duplicates of many books. Companies and individuals who are acquiring books for libraries may be able to secure these rare books by inquiring at the Institute.

Gifts to the Archives

The British Air Ministry has sent several books on airworthiness.

Mr. Harry Guggenheim has sent a copy of "The Seven Skies."

Mr. Richard C. Molloy has given a valuable collection of newspaper clippings.

General Umberto Savoja has added two Fiat airplanes to the Institute's collection of models.

Mr. Arthur Nutt has sent some early aeronautical magazines.

Changes in Membership

The following changes in the membership of the Institute have occurred since the publication of the previous issue of the Journal:

Elected to Member Grade

Bauer, George Carl, M.E.; M.I.Ae.S.; Chief Draftsman, Curtiss-Wright Technical Inst.

Boehnlein, Charles Thompson, M.E.; M.I.Ae.S.; Asst. Prof., Aerodynamics, Mathematics & Mechanics, Univ. Minnesota.

Cook, William Hough, M.S.; M.I.Ae.S.; Vibration Engineer, Boeing Aircraft Co.

Cozzone, Frank Paul, M.E.; M.I.Ae.S.; Chief of Structures, Curtiss-Wright Technical Inst.

Ebel, William Kenneth, B.S. in M.E.; M.I.Ae.S.; Chief Engineer, The Glenn L. Martin Co.

Fuller, Ernest Willie, B.S. in Ae.E.; M.I.Ae.S.; Chief Engineer, Aero. Div., The Acrotorque Co.

Harris, Thomas Aubrey, B.S.; M.I.Ae.S.; Asst. Physicist, N.A.C.A.

Hodgman, Frederick Southworth, M.I.Ae.S.; Gyropilot Engineer (Aircraft), Sperry Gyroscope Co.

Lancor, Joseph H., Jr., B.S. in E.E.; M.I.Ae.S.; Research Engineer, Sperry Gyroscope Co.

McCullough, Arthur Lee, C.E.; M.I.Ae.S.; Airplane Pilot, Pan American Airways Co.

Maxfield, William, M.I.Ae.S.; System Supt. of Maintenance, Transcontinental & Western Air, Inc.

Minser, Edward John, M.I.Ae.S., Chief Meteorologist, Transcontinental & Western Air, Inc.

Elected to Technical Member Grade

Anderson, Morris Clement, Lab. Mechanician & Flight Training Instructor, Rensselaer Polytechnic Inst.

Bowser, James Warren, B.S. in Ae.E.; Senior Detailer, Engineering Dept., Lockheed Aircraft Corp.

Frost, Verne Clayton, S.B. in Ae.E.; Stress Analyst, Consolidated Aircraft Corp.

Klenke, William Henry, Jr., Asst. Export Manager, Aviation Mfg. Corp.

Laule, Gerald, Design Draftsman, Lockheed Aircraft Corp.

Meirs, John, C.E.; Stress Analyst, Grumman Aircraft Engineering Corp.

Spaulding, Edward Hastings, B.S. in Ae.E.; Stress Analyst, Lockheed Aircraft Corp.

Walton, Arthur Lee, B.S. in M.E.; Layout Draftsman, Douglas Aircraft Co.

Wright, Kenneth Earle, B.S. in M.E.; Ensign, U.S. Naval Reserve.

Transferred from Member to Associate Fellow Grade

Comdr. Lloyd Harrison, Assembly & Repair Officer, U.S. Naval Air Station, Pensacola; Elgin L. Shaw, Research & Development Engineer, Goodyear-Zeppelin Corp.

Transferred from Technical Member to Member Grade

Robert R. Dexter, Aero. Engineer; O. T. Larson, Genl. Supt., Trans-Canada Airlines Ltd.; E. Robert Reff, Sr. Stress Analyst, The Glenn L. Martin Co.

Transferred from Student Member to Technical Member Grade

Frank T. Abbott, Jr., Engineering Draftsman, U.S. Naval Gun Factory; Alfred E. Ades, Draftsman, Trans-Canada Air

Lines, Ltd., Canada; J. L. Adrian, Jr. Aero. Engineer, U.S. Army Air Corps; Floyd G. Alden; A. W. Allsop, Jr. Detail Draftsman, Lockheed Aircraft Corp.; George Armbruster, Exp. Test Engineer, Pratt & Whitney Aircraft, United Aircraft Corp.; Irving Ashkenas, Aero. Engineer, North American Aviation, Inc.; Welcome W. Bender, Jr., Jr. Stress Analyst, Glenn L. Martin Co.; Paul F. Bikle, Engineer, Taylorcraft Aviation Corp.; Allen E. Bjerke, Asst. Meteorologist, Eastern Air Lines; Aaron Bloom; Edward Borek, Aero. Engineer, Douglas Aircraft Co.; Edmund J. Borowski, Detailer-Layout Man, Lockheed Aircraft Corp.; F. T. Brooks, Jr. Detailer, Lockheed Aircraft Corp.; Louis Lee Burke, Stress Analyst, Vultee Aircraft Div., Aviation Mfg. Corp.; L. H. Campbell, Draftsman, Beech Aircraft Co.; Alfred Jean Carah, Static Test Engineer, El Segundo Div., Douglas Aircraft Co.; A. Raymond Carchia; Russell M. Carlson, Engineer, Vought-Sikorsky Aircraft, United Aircraft Corp.; John A. Carran, State Engineering Exp. Sta., Georgia School of Technology; Fred Chang; Stephen Chris, Engineer, Douglas Aircraft Co.; D. M. Conner, Checking Dept., El Segundo Div., Douglas Aircraft Co.; L. W. Cook, Engineer, Hastings Mfg. Co.; Albert F. Crannage, Instructor in Aeronautics, Rensselaer Polytechnic Institute; Walter J. Crichlow, Stress Analyst, El Segundo Div., Douglas Aircraft Co.; Chester G. Davis, Meteorologist, American Airlines; Thos. C. Delker, Jr. Aero. Engineer, Bendix Products Div., Bendix Aviation Corp.; Edward C. Denzin, Stress Analyst, El Segundo Div., Douglas Aircraft Co.; P. A. DiNoto, Aero Engineer, Curtiss Aeroplane Div., Curtiss-Wright Corp.; John A. Dodge, Sr. Detail Draftsman, Lockheed Aircraft Corp.; Daniel D. Champlain, Flying Cadet, U.S. Army Air Corps.; Charles Donovan, Draftsman, Douglas Aircraft Co.; S. W. Doolittle, Draftsman, Douglas Aircraft Co.; Frederick P. Eade, Aero. Custodian, Aero. Engineering Dept., Purdue Univ.; H. H. Epstein; William J. Gander, Jr. Engineer, Grumman Aircraft Eng. Corp.; Gordon W. Graff, Aero. Engineer, Stinson Aircraft Div., Aviation Mfg. Corp.; Richard De Grey, Detail Draftsman, Lockheed Aircraft Corp.; Marvin J. Gordon, Project Engineer, Du Bois Martin Aircraft Co.; Karl H. Guttmann, Aero. Engineer, Ranger Engineering Corp.; Carl E. Hall, Jr. Detail Draftsman, Lockheed Aircraft Corp.; P. Colton Halstead, Flying Cadet, U.S. Army Air Corps; Leo A. Hidde, Final Assembler, Lockheed Aircraft Corp.; Marion S. Israel, Aero. Engineer, El Segundo Div., Douglas Aircraft Co.; J. E. Jean, Jr. Stress Analyst, Lockheed Aircraft Co.; Robert W. Jenny, Engine Tester, Wright Aeronautical Corp.; Philip O. Johnson, Aero. Engineer, North American Aviation, Inc.; Ernest L. Joiner, Jr., Senior Detailer, Lockheed Aircraft Corp.; E. S. Kavanaugh, Engineer, Braniff Airways, Inc.; Walter R. Krajewski, Steel Inspector, Inland Steel Corp.; John W. Krug, University Fellow, Yale Univ.; Orion C. Lamb, Jr. Detailer, Lockheed Aircraft Corp.; R. T. Lamson, Flying Cadet; U.S. Army Air Corps; Tom A. Lee, Engineer, North American Aviation, Inc.; Lindsay J. Lina, Jr. Aero. Engineer, Hydrodynamics Div., N.A.C.A.; Richard Marvin Lord, Jr., Draftsman, Bendix Limited; Cameron N. Lusty, Jr. Engineer, Barkley-Grow Aircraft Corp.; Paul W. Lynahan, Draftsman, Fleetwings, Inc.; George F. MacDougall, Jr.; Bruno P. Marchi; Philip W. McLane, Aero. Engineer, Lockheed Aircraft Corp.; Lt. W. B. Mechling, Naval Aviator, U.S. Navy; Richard H. Myers, Draftsman, Stewart-Rogers, Inc.; N. M. Nojima; V. J. Norris Instructor, Curtiss-Wright Technical Institute; Vincent North, Jr. Aero. Engineer, U.S. Army Air Corps; H. C. Nystrom, Layout Draftsman, Glenn L. Martin Co.; V. J. Park, Jr., Engineer, Ryan Aeronautical Co.; T. F. Peterson; Clark N. Piper, U.S. Army Air Corps; Raymond W. Pyle, Engineer, Ryan Aeronautical Co.; Boyd E. Quate, Meteorologist, United Air Lines Transport Corp.; Frank Rambaldini, Stress Analyst, Ryan Aeronautical Co.; Julius Raven, Aviation Cadet, U.S. Navy; Donald E. Rialson, Stress Engineer, Lockheed Aircraft Corp.; Austin L. Sea; L. E. Settergren, U.S. Army; T. Shimazaki, Teaching Assistant, Univ. of California; J. C. Siltanen; Ted Smith, Student Engineer, Douglas Aircraft Co.; Louis H. Stephen; Philip S. Thorjusen, Jr. Draftsman, Lockheed Aircraft Corp.; R. Stanton Thornley, Draftsman, Glenn L. Martin Co.; Edward W. Thrall, Jr., Stress Analyst, El Segundo Div., Douglas Aircraft Co.; C. C. Tsao, Engineer, Central Aircraft Co., China; H. C. Tsien, Engineer, N.R.C. Machine Works, China; G. Y. Tsubota, Design Engineer Guggenheim Aero. Lab., Calif. Inst. of Technology; A. S. Turner, Loftsman, Douglas Aircraft Co.; Octavian Urdea; J. L. Velazquez, Stress Analyst, El Segundo Div., Douglas Aircraft Co.; Gilbert Weiss, Jr. Aero. Engineer, U.S. Naval Aircraft Factory; E. A. Zeitlin, Stress Analyst, Interstate Aircraft & Engineering Corp.

Book Reviews

I'll Take the High Road, by WOLFGANG LANGEWIESCHE; Harcourt, Brace and Company, New York, 1939; 254 pages, $2.50.

The student who is taking flying lessons wants to talk of little else. He spends as much time as he can at the airports and discusses every phase of aeronautics with anyone who will talk with him. Mr. Langewiesche has written a book that will be a substitute for much such airport talk. It contains exactly the kind of information that the new pilot wants. It tells him of the emotional experiences of a young college instructor who is so determined to become a pilot that he makes personal financial sacrifices which are only understandable to those who are under the magic spell of the air. As the chapters proceed the student pilot will learn of means to extend his flying time by cooperative methods used by fixed base operators. The author even mastered parachute jumping to add to his flying time and experience.

As might be expected from an author who has recently written such an excellent book on *Lightplane Flying* he concludes with his experiences in flying small sport aircraft cross-country.

He writes easily and uses the vocabulary of flying with good taste. The book will find eager readers among the thousands of students who are taking flying instruction. It will save them asking many questions, foolish or otherwise, and give them much useful information.

Aircraft Drafting Room Manual, by JAMES G. THOMPSON; Aviation Press, San Francisco, 1939; 286 pages, $3.50.

The function of this handbook is the establishment of definite drafting practices for the preparation of engineering drawings for the aeronautical industry.

It is not intended to give instruction on how to prepare a drawing; such training is a pre-requisite to its use. It is intended rather to serve as a manual for small aircraft companies where the size of the engineering staff does not justify the preparation of a company handbook. It will serve as a reference manual for the qualified engineering draftsman and as a complete text of aviation drafting room practices.

Included in the manual is a brief but comprehensive survey of the material, processes, and finishes used in the manufacture of metal airplanes.

It has been compiled by the author from practical experience and therefore is presented in a form well adapted to its practical use.

Aeronautical Reviews

These brief reviews of recent articles on aviation subjects are published by the Army Air Corps for the information of its officers, and are printed here each month by permission of the Chief of the Air Corps

Aerodynamics

The Wind Tunnel of the Institute of Mechanical Sciences of the University of Pisa. R. Giovannozzi. Construction, arrangement, and equipment of the wind tunnel, particularly means taken to eliminate vibration and to ensure regularity of flow, are described. Results of preliminary experiments completed in the tunnel to determine distribution of velocity, the effect of the counter propeller, the variation of the static pressure in the free jet, and the turbulence of the flow are discussed.

Wind tunnel is of the classical Goettingen type having simple return and free jet, guide vanes at the angles, and development in a vertical direction. The tunnel consists of four parts, two horizontal (the higher one of which contains the free jet) and two vertical. Diameter 1.10 meters. Maximum velocity 51.2 meters/sec. (114.5 m.p.h.). Oscillation of the velocity ±0.65 percent. Critical value of the Reynolds Number (for which *cr* of the sphere has the value of 0.3) 219,500. Normal useful power of the motor 40 kw. Long description. *L'Aerotecnica*, July, 1939, pages 737–759, 20 illus., many equations.

Aircraft Design

Engineering Experimental Aircraft. W. A. Hite. Engineering management in regard to rapid development work necessary, shop engineering, handling experimental drawings, and scheduling the work is described. Principal features of the Vultee Trainer airplane, now under contract to the U.S. Army Air Corps, are presented to illustrate what is meant by "designing experimental airplanes for manufacturing economy." Wing, control surfaces, and fuselage of the Trainer are discussed. *S.A.E. Preprint for National Aircraft Production Meeting*, October 5–7, 1939, 10 pages, 7 illus.

The High, the Middle or the Low? Undoubtedly the high-wing tricycle layout which is now emerging will serve—with some modifications particularly in high-lift devices—up to cruising speeds very much greater than anything now contemplated. At speeds of much above 450 m.p.h. the remedies to the compressibility stall are thin wing sections and smooth surfaces with no sudden changes of form. The high-wing monoplane with a very thin wing would probably be the best solution. Possibly designers will be driven to the cantilever biplane at least in moderate sizes in an effort to make a wing stiff as well as thin. In the smallest and in the very large sizes, there seems hope of really high speeds in the future—600 m.p.h. and more. Military machines with increasing speeds will most certainly follow the high-wing phase. The return to the high-wing, as shown by the DeHavilland Flamingo, high-wing advantages, fin area *versus* dihedral, future prospects, and the all-wing ideal are discussed. *Aeroplane*, October 5, 1939, pages 424–426, 5 illus.

Performance Estimation. C. F. Toms. Formulas and methods presented have been found useful in routine performance estimation and in design, and refer to the effects on steady level flight speed of induced drag and changes in parasite drag and weight. Expressions are given, in convenient "constant" form, for minimum drag and power required with the associated speeds. Two applications of the formulas developed are shown but no attempt is made to deal with actual estimation of parasite drag, attention being confined to use of the appropriate constant when it has been estimated. *Flight, Aircraft Engr. Sup.*, October 5, 1939, pages 39–42, 294, 5 illus., 2 tables, 15 equations.

A Simplified Method for Development of Prototype Airplanes as Applied to Consolidated Model 31 Long Range Patrol Boat. B. W. Sheahan. Description of the Model 31 52-passenger high-wing monoplane flying boat which made its initial test flight ten months after construction was authorzed. Saving in time possible through the building of a stripped airplane to determine the basic flying characteristics prior to completing the article in all its details is discussed. All items of equipment not necessary for flight were taken care of in the flight model by providing equivalent ballast. It is recommended that contracts for experimental airplanes be written to permit the construction and testing of a full-scale flying model in which all equipment non-essential to primary flight testing is omitted, the second stage of the contract providing for installation of the equipment items. Drawing system used at Consolidated in speeding up the transfer of information from the engineering department to the manufacturing divisions is described. *S.A.E. Preprint for National Aircraft Production Meeting*, October 5–7, 1939, 7 pages.

Two Motors or Four? Arguments on the respective merits of two-engine and four-engine transport airplanes in relation to modern designs of medium size. "At present, for motors of up to about 3000 h.p. and aeroplanes of up to about 80,000 lb. (35 tons) loaded weight, two motors seem to be just as safe and more efficient economically and aerodynamically than are four motors of the same total horse power. . . . On this basis the two-motor aeroplane will be cheaper to build, easier to fly and maintain, and more economical to operate." *Aeroplane*, September 28, 1939, pages 401–402, 4 illus.

Stress Analysis and Structures

Analysis of Spherical Shells of Variable Wall Thickness. M. F. Spotts. Solution to the problem of finding the forces and moments which occur in a spherical shell which is axisymmetrically loaded, when variation in wall thickness is taken as a quadratic function of the coordinate of latitude. Love-Meissner differential equations for the case of non-uniform wall thickness are derived and, by appropriate substitutions, are reduced to one linear equation of the fourth order having constant coefficients. Solution to this equation, when taken in the homogeneous form, is the general solution for all problems where shell surface is free from external force, and the only loads on the shell consist of forces and moments applied at the boundaries. When the shell surface itself is loaded, a particular integral, which will depend upon type of loading, must also be obtained for the non-homogeneous equations. Solution is illustrated by a numerical example for a shell of one boundary when acted upon by deadload forces, and results are plotted. *Jour. Applied Mechanics*, September, 1939, pages A-97–A-102, 7 illus., 75 equations.

Clamped Rectangular Plates with a Central Concentrated Load. D. Young. Results of calculations, with the use of Timoshenko's method, for maximum deflection, moment, and edge shears for rectangular plates of various proportions with all four edges clamped and loaded by a single concentrated load at the center. *Jour. Applied Mechanics*, September, 1939, pages A-114–A-116, 3 illus., 4 tables, 17 equations.

Designs for Spot Welding. C. F. Marschner. Phases of shop practice which affect design. Reduced costs are pointed out and it is shown that cost per weld would be from one-eighth to one-tenth the cost per rivet for any given design. Aerodynamic advantages of spot welding and the improved appearance obtained are considered. Weight savings through the elimination of rivet heads are listed. A method of cold working spot welds to increase their yield strength to that of the parent metal is described. To be concluded. *Aero Digest*, October, 1939, pages 57–58, 156, 4 illus., 1 table.

A Theory of Flexure for Beams with Nonparallel Extreme Fibers. W. R. Osgood. Theory presented is shown to reduce to the ordinary theory of flexure as the angle between the extreme fibers approaches zero. Maximum fiber stresses computed by the theory and by the ordinary theory for a plate girder with non-parallel flanges show that for angles between the flanges up to 20° the ordinary theory can never be in error more than about 5 percent, but for larger angles the error in general increases rapidly with the angle. Theory is applied in an example as an approximation to a beam with curved extreme fibers, and is confirmed by test results. *Jour. Applied Mechanics*, September, 1939, pages A-122–A-126, 6illus., 21 equations.

Vibration Problems. J. Ormondroyd. Major part of any vibration analysis lies in the calculation of the dynamic specifications of the simplified system which represents the machine or structure being studied. Dynamic specifications of a system are the numerical values of the masses, moments of inertia, spring constants, and damping constants which determine its dynamic behavior. These quantities are the coefficients which appear in the differential equations of motion of the system. Mass, moments of inertia, spring constants, damping constants, Coulomb friction, internal friction in solids, and impactive damping are discussed. *Jour. Applied Mechanics*, September, 1939, pages A-127–A-130, 1 illus.

What Will It Weigh? G. H. Tweney. The method presented for arriving at preliminary weights for airplane structures has been shown to be accurate within 1 to 3 percent. Use of the chart will enable the builder to arrive at a fairly accurate weight value for his design before he has started construction. In the chart, the ratio of weight empty to gross weight is plotted against disposable load in pounds. Data for the chart were obtained by computing all values for about 150 different types of airplanes whose weights were already known and then combining them into one chart. Total weight empty is computed and weights of the fuselage structure, landing gear, tail surfaces, power unit, and wing structure are estimated. *Western Flying*, October, 1939, pages 19–21, 1 illus.

Aircraft Alighting Gear

Airplane Brake Installation and Control Consideration. H. H. Kerr and F. C. Frank. Problems of adapting the brake to the airplane are discussed and a method of selecting adequate brakes is described. Factors in landing-gear and axle design affecting brake efficiency are outlined with suggestions. Design of the brake-operating mechanisms both for power and manual brakes is considered. Suggestions are presented on ways of designing control systems. Care in design of operating linkage to eliminate friction and flexibility, selection of a master cylinder of proper proportions and capacity for manual operation, and method of mounting the cylinder are explained. *S.A.E. Preprint for National Aircraft Production Meeting*, October 5–7, 1939, 11 pages, 4 illus., 1 table, 5 equations.

Aircraft Maintenance

You Can't Beat the Dutch. Overhaul and service shops of K.L.M. at Schiphol, and methods of maintenance employed for aircraft, power plants, propellers, and instruments are described with illustrations of equipment. *Aviation*, October, 1939, pages 22–29, 30 illus.

Aircraft Manufacture

Job-Lot Aircraft Stampings. F. J. Oliver. Drawbacks of the rope drop hammer, drop hammer technique, combination lead-zinc dies, and deep drawing in stages are discussed. To be continued. *Iron Age*, October 19, 1939, pages 50–55, 11 illus.

Aircraft Performance Testing

The Testing of Large Aircraft. E. T. Allen. Paper previously abstracted from preprint. *S.A.E. Jour. (Trans.)*, October, 1939, pages 444–448, 456, 1 table.

Aircraft

CZECHOSLOVAKIA

Aero A.300 Two-Engine Airplane for Bombardment and Long-Distance Reconnaissance. Aero A.300 (two Bristol Mercury IX engines of 830 hp., top speed 470 km./hr. at 5500 meters) of mixed construction is described in great detail with tables showing characteristics, performances, and bomb and other loads for each of its five missions. Descriptions are also given for other Czechoslovakian aircraft including: the Aero A.304 two-engine airplane for reconnaissance, training, day and night bombardment, and photogrammetry; Avia 158 two-engine bomber and long-distance reconnaissance airplane; Avia 534 single-seater pursuit; Avia 35 and 135 single-seater pursuits; Letov S 50 three-seater two-engine observation airplane; Letov S.231.2 single-seater pursuit; and Letov S.528 two-seater Army-Cooperation airplane. *Rev. de l'Armée de l'Air*, July–August, 1939, pages 447–476, 32 illus., many tables.

GERMANY

Fighters of the Luftwaffe. Heinkel and Messerschmidt fighters are described and facts are given about the record breakers. The Messerschmidt Me. 109R in which F. Wendel reached 469.225 m.p.h. had much less wing area than the standard fighter, a wing of different section and plan form, a redesigned fuselage, a new cockpit enclosure, and a striking cruciform tail reminiscent of those on the old Macchi racing seaplane. It was powered with a very much boosted Daimler-Benz D.B. 601A engine said to deliver 1800 hp. at 3500 r.p.m. The Messerschmidt Me. 110 two-seater twin-engined fighter and multi-purpose machine has two fixed 20- or 23-mm. shell guns and four machine guns. Prototype (two D.B. 601 engines with two-speed superchargers, each engine delivering 1360 hp. maximum) has a top speed of 379 m.p.h. at 16,400 ft.

Only a few details and photographs of the Me.110 are given but the various versions of the Me.109Bf and the Heinkel 112 single-seater fighters are described in detail and illustrated. Cutaway drawing of a typical Heinkel He 112 shows two 20-mm. shell guns mounted in the wings and a pair of synchronized machine guns. Manufacturer's figures are listed for characteristics of the Heinkel He 112 when powered by Jumo 210G and D.B. 601A engines, respectively (top speeds 317 m.p.h. and 354 m.p.h.).

Heinkel 112U record-breaker fighter has a different fuselage and tail from the standard model, and cockpit enclosure is built into the fuselage rather than being installed as a unit on top, sacrificing rearward vision. Undercarriage is of wider track and retracts inwardly. A short description of this version included. *Flight*, October 5, 1939, pages 286a–286d, 287, 10 illus., 1 table.

Germany's Dive Bombers. H. F. King. Specialized types of dive bombers, diving brakes, and bomb displacement gear, as well as German dive-bombing tactics are discussed. The Junkers Ju.87 two-seater dive bomber is described and illustrated in some detail (Junkers Jumo 211 gasoline-injection engine giving 1200 hp. for take-off, maximum speed 240 m.p.h. at altitude, T.V. speed without diving brakes 430 m.p.h., ceiling 24,500 ft., all-up weight 9350 lb.). Cutaway drawing reveals equipment, armament, and structure of the latest type. Method of lowering the main bomb on arms so that it clears the propeller disk after a diving release is indicated and leading edges of the wings are cut away to show diving brakes in down position. The Ju.87 is the most widely employed and effective dive bomber in service in the Luftwaffe.

The Henschel Hs.123 single-seater biplane (B.M.W.132 600-hp. radial engine, estimated top speed 220 m.p.h.) is also described and details are given for the Heinkel He.270 two-seater (D.B. 600G inverted 910-hp. engine, top speed 267 m.p.h., range 1550 miles with disposable load of 4180 lb.); Blohm and Voss Ha.137 single-seater (Jumo 210 650-hp. engine, top speed 211 m.p.h., cruising speed 185 m.p.h., ceiling 23,500 ft., range 370 miles); and Arado AR.95 2–3-seater biplane (B.M.W. 132 radial engine). *Flight*, September 28, 1939, pages 270a–270f, 16 illus.

The Junkers Bombers. H. F. King. The new Junkers Ju.88 bomber (two Jumo 211 direct-injection engines giving 1200 hp. for take-off) now going into service in the Luftwaffe is similar to the Junkers Ju.85S which made the F.A.I. record for speed (321 m.p.h.) over 1000 km. with a useful load of 2000 kg. Nacelles of the Ju.88 hang beneath the low cantilever wing. Typical bomb load would be about 2500 lb.

The Ju.86K bomber (two B.M.W. 132 DC engines developing 945 hp. at 6560 ft.) has three standard 7.9-mm. machine guns, one in a spherical manually operated turret in the nose, one on top of the fuselage, and one in a semi-retractable dustbin. Bombs are stowed vertically according to German practice (although some of the new prototypes are believed to carry horizontally stowed bombs). Final series of the 86K have a completely redesigned shorter nose provided with more transparent panels. Production of the Ju.86K is believed to have been stopped. Span 73 ft. 9 in. Disposable load 6460 lb. Top speed little more than 225 m.p.h. Ju.89 large bombers (four Jumo 211 or D.B. 600 engines) are probably also used as transport machines and for dropping of parachute troops. Bomber is similar to the Ju.90 transport which reached 23,760 ft. carrying a load of 22,046 lb. (take-off weight from 50,800 lb. to 57,300 lb. and top speed 280 m.p.h.). Disposable load of the Ju.89 is considerably more than 17,000 lb. Ju.52/3m bomber (two B.M.W. 132A engines, top speed 160 m.p.h., ceiling 20,000 ft. and range 540 miles) is now used for training, transport, and dropping of parachute troops.

Design, construction, and performance (estimated in some cases) are described for these airplanes with photographs, cutaway drawing of the 86K, and drawings of the Ju.88 installation of the Jumo 211 engine. *Flight*, October 12, 1939, pages 300a–300e, 7 illus.

Seaplanes of the Luftwaffe. Nine types of military float and boat seaplane are in service of the Luftwaffe under the Command of the Air Defense at Sea, and since the start of the war two types of civil seaplane have been pressed into service for reconnaissance duties.

Design, armament, and performance are briefly described for the following: Dornier Do.18 flying boat (two Jumo Diesel engines, top speed 150 m.p.h., range with 1100-lb. payload 3600 miles at 115 m.p.h.); Dornier Do.24 four-seater flying boat designed for operation from rough seas (three 880-hp. B.M.W. radial engines, top speed 208 m.p.h., maximum range 2000 miles); Dornier Do.22 three-seater torpedo-spotter-reconnaissance float seaplane (B.M.W. VI liquid-cooled engine, top speed 190 m.p.h., range 970 miles at 124 m.p.h.); Dornier Do.26 long-range mail carrier now converted for military duties (four Jumo Diesel engines mounted in tandem, top speed 208 m.p.h., absolute range 5600 miles at 130 m.p.h.); Blohm and Voss Ha.138 flying boat having a peculiar layout to afford a wide field of fire from gun turrets in the nose, behind the middle motor, and in the stern of the hull (three Jumo Diesel engines, top speed 171 m.p.h., range with maximum overload 3100 miles); Blohm and Voss Ha.140 torpedo-reconnaissance bomber float seaplane (two B.M.W. 132 Dc. 880-hp. radial engines, top speed 199 m.p.h., range at 160 m.p.h. 715 miles with 1760 lb. military load); Blohm and Voss Ha.139, and 139B float seaplanes (four Jumo 205 Diesel engines, maximum speed for the former 191 m.p.h., range 3100 miles at 160 m.p.h., and for the latter top speed 202 m.p.h., range 3230 miles at 167 m.p.h.); Heinkel He.115 long-range open-sea reconnaissance seaplane record breaker (two engines, top speed 204 m.p.h.); Heinkel He.59 reconnaissance bomber seaplane (two B.M.W. VI 750-hp. engines, cruising speed 120 m.p.h.); Heinkel He.60 two-seater fighter-reconnaissance biplane seaplane for catapult launching from cruisers and battleships (B.M.W. VI 750-hp. engine, maximum speed 180 m.p.h.); and the Heinkel He.114 two-seater twin-float reconnaissance biplane (B.M.W. 880-hp. engine). *Aeroplane*, September 28, 1939, pages 393–396, 10 illus.

The Speeds of German Aeroplanes. Maximum speed of the Dornier Do.17 is 292 m.p.h., not 392 m.p.h. as mentioned in the previous issue, and maximum speed of the Messerschmidt Me.110 is, according to best information available, 385 m.p.h. at 15,000 ft., not 285 m.p.h. Bf. ref. *Aeroplane*, September 28, 1939, page 408.

GREAT BRITAIN

Conversion I. An experimental batch of amateur pilots has recently been taught to fly military aircraft so that they can ferry them, thus leaving more experienced Service pilots to do the work for which they are better suited. Advice is offered to the amateur pilot on flying the Lockheed Hudsons and the Blenheim bomber. *Flight*, October 12, 1939, page 300.

Identities in Outline. Silhouettes of British military airplanes are illustrated including: the Hawker Hurricane and Supermarine Spitfire single-seater fighters; the Armstrong-Siddeley Whitley, Bristol Blenheim, Fairey Battle, Handley-Page Hampden, Avro Anson, and Vickers-Armstrong Wellington bombers; and the Westland Lysander Army-Cooperation airplanes. Characteristic features of each are pointed out.

A second short article entitled "Aircraft Signature Tunes" discusses aural as well as visual means by which British aircraft can be identified. "Again American motors have their own characteristic sound. For instance, there is the Harvard—once heard never to be forgotten—whilst the Lockheed Hudson has the typical American motor rumble, a curious hollow sort of roar." *Aeroplane*, September 28, 1939, pages 387–389, 392, 9 illus.

U.S.A.

Nearly Half of Planes in U.S. Are Over Five Years Old, CAA Reports. Nearly 10 percent of these airplanes are more than ten years old. More airplanes were built in 1937 than in any other year, 1938 being second and 1929 third. Largest proportion of certified airplanes in use, 42.5 percent, are pleasure craft, 41.6 percent are commercial, 11.7 percent are used in connection with business, transports total 3.16 percent, and those in Government service account for 1.1 percent. Of all the commercial airplanes 59 percent are used for instruction. List of certified aircraft of various types 1926–1938. Brief note. *Western Flying*, October, 1939, page 40, 1 table.

Taylorcraft for 1940. Most noticeable change in the new models is the streamlined cowling available on the Lycoming and Continental powered ships. Cowl completely covers the engine and is so designed that exhaust of air is directed under the fuselage. Engines available are the 50-, 55-, or 65-hp. Lycoming, the 50- or 65-hp. Continental, and the 50- or 60-hp. Franklin. Wing span 36 ft. Wing area 167 sq. ft. Gross weight 1150 lb. Maximum speed 105 m.p.h. Cruising range 250 miles. Description. *Aero Digest*, October, 1939, page 114, 3 illus. *Aviation*, October, 1939, page 40, 3 illus., 1 table.

Aircraft Accidents

117 Crackups in Safety Report. Five airline accidents of minor nature and 112 non-airline accidents, eight of which were fatal, were reported by the Air Safety Board to the C.A.A. during the month of August. Causes are listed in a brief review. *Western Flying*, October, 1939, page 40.

Aircraft Assisted Take-Off

Shortening Take-Off Run. F. R. Shanley and F. P. Cozzone. Problems to be considered in connection with assisted take-off for aircraft. Assumption would be justified that a horizontal acceleration of 1 g. would be reasonable if proper seating arrangements were provided and if accelerations were not applied or relieved too suddenly. Little is gained by sudden application of accelerating force at beginning of the take-off run, and a great deal of power will be required if the assistance for the take-off is to be efficiently applied. A system based on use of the attraction of gravity and employing a falling weight as a means of applying the load is considered for assisting take-off. Computations given for an airplane similar to the Douglas DC-4, indicate that a relatively small counterweight has an appreciable effect in shortening the take-off run. *Aero Digest*, October, 1939, pages 113, 156, 3 illus.

Air Transportation

Directory of Scheduled Airline Operators. Directories of scheduled airline operators and of sources of supply of airport and airline equipment. *Aero Digest*, October, 1939, pages 121–139 (alternate pages).

Greece. Potentially Greece offers an excellent field for development of passenger and mail air services. Foreign airlines serving Athens and Salonika, airports in Greece, and the Greek air transport company are described. *Aero Digest*, October, 1939, pages 61, 156, 3 illus.

K.L.M.'s First 20 Years. A. A. B. Hartsinck. Development of the Dutch airline during the past twenty years is traced. *Aviation*, October, 1939, pages 18–21, 8 illus., 1 table.

Two Atlantic Months. More than 50,000 miles at an average ground speed of 145 m.p.h. were flown on the 16 weekly trips by the Imperial Airways' Caribou and Cabot Short "C" class flying boats (Bristol Perseus sleeve-valve engines) without a single item of mechanical difficulty. Freight and mails carried amounted to about 13,000 lb. Fuel consumption per complete return trip averaged 5500 gal. Refueling from the air was regarded as generally satisfactory, although not used on all occasions, the operation taking about 10 min. Scheduled and actual times of arrival for the 16 trips are listed. *Flight*, October 12, 1939, page 301, 1 table.

Propellers

Control Valve for Feathering Props. Acrotorque full-feathering control valve for use on Hamilton Standard Hydromatic propellers of the modified hydraulic-system type, weighs less than 3 lb. It is installed in the cockpit in the hydraulic feathering system between accumulator tank and feathering pressure line to the governor. Description. *Aero Digest*, October, 1939, page 149, 1 illus.

Study of Propellers for High-Speed Airplanes. L. Lazzarino. Analysis of how the parameters for optimum efficiency and the highest possible value of the efficiency of the propeller are diminished with increase of speed and altitude of flight. Efficiency of a system of two oppositely rotating propellers with diverse angular velocities, and the variation of efficiency with the change of ratio between the angular velocities of the two propellers are determined. Methods developed permit an approximate numerical evaluation of the efficiency, utilizing the actual experimental results available. *L'Aerotecnica*, July, 1939, pages 760–780, 5 illus., 5 tables, 43 equations.

Miscellaneous

Review of the National Air Races. Cy Caldwell. Results of the last Air Race are compared with those of previous National Air Races. *Aero Digest*, October, 1939, pages 34–35, 153, 6 illus., 1 table.

Tethering the Airplane. W. C. Clayton. Problem of preventing aircraft from being blown away in a wind storm, as the result of not being adequately tethered, and from damage by the wind while tethered is discussed from a non-technical standpoint and recommendations are made. Best procedure would be to place the airplane in an approximately horizontal position facing into prevailing winds, properly tethered down and with wheel chocks in front and back of each wheel, with parking brake on, with tail wheel locked in fore-and-aft position, and with controls locked. Two ways in which the airplane may be placed in the horizontal position are described. To be continued. *Aviation*, October, 1939, pages 34–35, 72, 4 illus.

A Permanent Industry. Glenn L. Martin. Reasons for believing in the permanent supremacy of the American aircraft industry and why the author is committed to the policy of building permanently for large-scale production. References are made to tremendous developments in materials, including a new aluminum-alloy sheet stronger than any other sheet now available, a new stainless steel having better strength-weight ratio and lending itself more readily to fabrication, a glass plastic using threads of glass having a tensile strength of one million pounds per square inch woven into a warp of another composition, and stronger than any steel which is really workable. *Western Flying*, October, 1939, pages 14–15, 21, 2 illus.

The Motion of Cylindrical Particles in Viscous Flow. R. C. Binder. Results of experiments made on the orientation of cylindrical particles in viscous flow show two different final orientations, namely: a position perpendicular to the plane of undisturbed flow, and a position parallel to velocity direction. Relation between final orientation and length-diameter ratio of the particle was found for different speeds. Comparison is made between experimental results and theoretical predictions. *Jour. Applied Physics*, October, 1939, pages 711–713, 1 illus., 1 table.

Acoustics

The Filtration of Sound. R. B. Lindsay. Acoustic filtration in solids and loaded rods; solid filters and high-pass compressional wave filters; filtration of torsional waves in solid rods; filtration of compressional waves in stratified media; and acoustic filtration in dissipative structures. *Jour. Applied Physics*, October, 1939, pages 680–687, 9 illus., 30 equations.

Acoustic Condition Factors. M. Rettinger. Term "acoustic condition factor" is used as a general term descriptive of the acoustic environs of a point in an enclosure. Relationships are expressed as ratios for several quantities, such as "useful" and "harmful" sound, direct, and generally reflected sound energy, and sound intensity. Curves indicate the loci for partial antinodes produced by interference between direct and first as well as second reflections in a rectangular room in which the sound source is located symmetrically. Equations are given expressing the minimal distance between source of sound and microphone for probably avoiding the recording of absolute nodes. *Soc. Motion Picture Engrs., Jour.*, October. 1939, pages 410–420, 8 illus., 6 equations.

Aircraft Instruments and Navigation

Instrument Corrosion. Corrosion of instruments may possibly be due to the welding of the static line connections to the instruments with an acid flux so that some of the acid is left inside the tubes and eventually carried to the instruments; or corrosion may be due to the vapor or fumes which may cover an asphalt airport pavement during warm moist weather. These explanations are offered as the causes of an exceptional amount of corrosion found on brass and aluminum parts of instruments which a chemical analysis indicated was due to an acid. Brief note only. *Western Flying*, October, 1939, page 18.

Librascope Power Computor. Instrument automatically calculates engine performance for any possible operating condition. Four dials mounted on a small case are calibrated in r.p.m., manifold pressure (in Hg), pressure altitude (1000 ft.), and carburetor air temperature (degrees F. or C.). Pointers on three scales indicate b.hp., fuel consumption per hour, and b.m.e.p. A change of value set on any of the four knobs instantly and automatically solves the complicated mathematical relations and changes the pointer readings to indicate the three new values. A fifth knob for fuel ratio is available on a computor to be used with engines employing automatic mixture control. Description. *Aero Digest*, October, 1939, page 149, 2 illus.

Pilots and Machines for Blind Flight. Lt. Pilot P. Magini. Fundamental aspects and principal meteorological conditions under which flight can be carried out without visibility are examined. Navigation and landing phases are considered, and the psychological qualifications for personnel for blind flying are pointed out. Characteristics preferable in the airplane for blind flying are dealt with and requirements in deicing equipment, other accessories, engines, propellers, radio apparatus, and instruments are discussed. *Rivista Aeronautica*, June, 1939, pages 482–510.

Navigation

Easy Cross-Country Calculations. E. Ward. The method described is said to make it easy for pilots to work out a course and drift allowance without recourse to the protractor and the course-and-distance calculator. After the necessary degrees have been added for local compass variation, the figure arrived at without instruments is quite near enough for starting the trip. Actually one can ascertain the compass course within two or three degrees. The reciprocal course for the return journey with wind from the same quarter is also shown. *Aeroplane*, September 28, 1939, page 406, 3 illus.

Patrol Plane Navigation. Lt. E. M. Block. System of navigation for a squadron of 6 to 12 airplanes which has been used constantly in Patrol Squadron 10 for over a year with complete success. Celestial navigation, dead reckoning, and single-plane navigation are discussed. *U.S. Naval Inst. Proc.*, October, 1939, pages 1468–1472.

Airports and Equipment

Electrifying Newfoundland Airport—Largest in the Americas. W. A. Pennow. Since no commercial power was available at the site of the Newfoundland Airport, all power had to be provided locally, mostly by direct Diesel engines. Power house and its equipment; control room; beacon and wind tee; contact lighting system developed by Westinghouse for use under low visibility conditions, including both green and yellow-sodium lights for runways; method of laying the cable network underground; and provision of power to a radio marker beacon. Detailed description. *Aero Digest*, October, 1939, pages 70, 73, 154, 2 illus.

Hangar Door Design. J. I. Byrns. Difficulties with the slide door of hangers, mechanical problem in power operation for a multileaf slide door, support of canopy doors, and cold-climate precautions in the design of a canopy door are considered. *Aero Digest*, October, 1939, pages 49–50, 3 illus.

Santos Dumont Airport, Rio de Janeiro, Brazil. G. F. McLaughlin. South America's largest airport is already provided with seaplane and land facilities adequate to its present needs, but a program of improvement and expansion is under way which will soon make it one of the most up-to-date air terminals in the world. General layout, three unique hangars of the full cantilever type now under construction and each capable of housing 16 Douglas DC-3 airplanes, the central administration building, and the seaplane base are briefly described. *Aero Digest*, October, 1939, pages 62, 65, 4 illus.

Electrical Equipment

Optimum Voltage for Airplanes. V. H. Grant and M. F. Peters. Equations developed for the standardization of electrical equipment for single-engine airplanes indicates that the voltage for a large number of airplanes with d.c. systems using storage batteries to carry peak loads can be standardized advantageously at 24 volts. For large airplanes where auxiliary power plants are used, it may be desirable to supplement the standard 24-volt generator-battery system with an a.c. or d.c. system of higher voltage without battery. *Electrical Engineering*, October, 1939, pages 428–431, 2 illus., 2 tables, 14 equations.

Aerial Photography and Mapping

Aerial Triangulation and Colonial Maps. Pilot Capt. M. Giovannozzi. Photogrammetric campaign on the coast of Somalia. Technical discussion of the problems involved, preparations for the mission, and methods of carrying out the survey. *Rivista Aeronautica*, June, 1939, pages 511–524, 5 illus.

Testing Apparatus

A 120,000-Exposure-per-Second Camera. D. C. Prince and W. K. Rankin. Development of a high-speed apparatus in which a thousand pinhole cameras were arranged in ten rows of 100 holes each on a drum. By rotation of the drum at 7200 r.p.m., a rate of exposures of 120,000 frames per second could be obtained. Preliminary tests of two pinhole cameras, design features of the camera developed, and application to circuit-breaker arc studies are described. *General Electric Rev.*, September, 1939, pages 391–393, 6 illus.

Harmonic Analysis of the Pressure Fluctuations in a Fluid. M. F. Treer. When large oscillations are produced, the frequencies of the resulting harmonics is not always the same as those of the applied pressure, but may be some multiple of them. A simple method for obtaining the frequency and amplitude of the harmonics that are produced is based on the slightly damped resonance effect of an oscillator. Amplitudes of an oscillator are proportional to the impressed pulsations and are increased by the natural frequency of the oscillator. On variation of this natural frequency, the amplitudes become large at several frequencies, and this enables the determination of the frequency and amplitude of the most important harmonics. In the case of a simple fluid pressure gage, oscillations are produced by inertia of the liquid inside it and degree of damping depends upon the viscosity.

Points plotted were obtained by experiments on a $^1/_4$-in. diameter pipe with a mercury gage. Tests were made at different impressed frequencies, and it was found that the length of the liquid column does not affect the value of the amplitude ratio. Method of investigation is useful where there is not room to accommodate an indicator, or where the fluctuations are too small to be measured with an ordinary type of gage. *Engineering*, September 22, 1939, pages 321–322, 4 illus.

An Impulse Measuring Set. A. S. Grant. Instrument designed to measure the crest amplitude of an electrical impulse and at the same time the decay of that impulse to a specified level below the initial peak. Instrument was intended primarily for measurement of the microphonic noise experienced in tubes, but could be equally well applied to the measurement of the crest and decrement of any similar wave form. *Jour. Scientific Instruments*, September, 1939, pages 290–297, 6 illus., 2 tables.

A Valve Wattmeter. D. M. Myers and W. K. Clothier. Instrument developed for the measurement of power, voltage, and current, within a wide range of frequencies, depends on the differential action of four triodes which operate on non-linear portions of their characteristics. Instrument is applicable to a.c. or d.c. measurements, or to a combination of the two. Simple means of adjustment and calibration is provided, for use when a triode, or other circuit component, is changed. Voltage and current range switches are included, together with a sensitivity control, which allows a reasonable reading to be obtained at low power factor. All readings are made on a d.c. milliammeter. *Jour. Scientific Instruments*, September, 1939, pages 302–309, 8 illus., 13 equations.

Materials

New Developments in Automotive Materials. Die castings on 1940 cars; DuPont "Moly-Black" molybdenum-nickel electroplating process; advantages of the new aluminum alloy automotive bearing developed by Aluminum Company of America; and developments in wood plastics reported by the Forest Products Laboratory. Descriptions. *Automotive Industries*, October 15, 1939, pages 426–427, 440, 5 illus.

Metals

Heat Treatment

Flame Hardening Small Parts. T. A. Frischman. Application of flame hardening to the cam track of a clutch actuator cam and to a cast malleable shifter fork. *Heat Treating and Forging*, September, 1939, pages 445–446, 458, 4 illus.

Heating and Liquid Quenching Massive Sections. J. A. Duma. Heating up, holding, and cooling down in the heat treatment cycle. Effect on holding time of nature or emissivity of flame, ratio of interior furnace surface to exposed steel surface, completeness of exposure, or conversely, the degree of obstruction in the path of radiation to the fired ware, and heat properties of the steel itself are discussed. *Heat Treating and Forging*, September, 1939, pages 447–450, 6 illus., 1 table.

Iron and Steel

Phosphorus in Steel. C. H. Lorig and D. E. Krause. Benefits secured by the addition of phosphorus alone or in combination with other alloying elements. In all 77 steels were prepared in the metallurgical laboratories, upon which were determined the mechanical properties of rolled bar and sheet stock and the resistance to atmospheric corrosion of the sheet. In atmospheric corrosion tests the addition of molybdenum retarded the rate of corrosion as compared with that of mild steel, while the addition of phosphorus to the molybdenum steels decreased the rate still further.

First issue—Comprehensive data for the effect of phosphorus additions on the corrosion and physical properties of a number of mild steel and for Fe-P-Cu, Fe-P-Sn, Fe-P-Cr, Fe-P-Ni, and Fe-P-Mo alloys.

Second issue—Similar data for low-alloy steels, including Fe-P-V, Fe-P-Cu-Si, Fe-P-Cu-Cr-Si, Fe-P-Cu-Ni-Mo, Fe-P-Cu-Ni, Fe-P-Si-Cu-Sn, Fe-P-Cu-Cr, and Fe-P-Cu-Mo. Results of study sponsored at Battelle Memorial Institute by the Monsanto Chemical Company. *Iron Age*, October 19 and 26, 1939, pages 33–37, 88, and 28–31, 4 illus., 4 tables.

Polishing Technique for Stainless Steels. W. M. Mitchell. First issue—Various types of stainless-steel alloys, range of commercial finishes, types of grits, and preparation of wheels are reviewed, and the proper sequence of grinding and polishing operations is stressed.

Second issue—Detailed data on polishing to various finishes and the etching and protection of stainless-steel surfaces. *Iron Age*, October 19 and 26, 1939, pages 56–59, 92–94, and 32–35 and 92, 5 illus.

Porosity of Electrodeposited Silver on Steel. F. C. Mathers and L. I. Gilbertson. Porosity of electrodeposited silver on steel as it is affected by the thickness of the plate, the roughness of the basis metal, and the method of applying the silver plate. Electrochemical Society paper. Experiments and results obtained. *Metal Industry*, September 29, 1939, pages 295–296, 4 tables.

The Working of S.A.E. Nickel Alloy Steels. Effect of alloying elements, kinds of S.A.E. nickel steels, recommended heat treatment, characteristics and applications, machining and welding. Long article. *American Machinist*, October 18, 1939, pages 865–876, 15 illus., 16 tables.

Some Observations on the Yield Point of Low-Carbon Steel. J. Winlock and R. W. E. Leiter. A study of the yield-point phenomena in low-carbon steel to determine the mechanism of transition of the metal from the elastic to the plastic state. Unlike copper and aluminum, low-carbon steel does not yield in tension until an excessively high elastic resistance has been built up, this high elastic resistance being the upper yield point. Upper yield point is believed to be of fundamental importance in the Lueders' line phenomena, and experimental evidence is given which supports this view. *A.S.M.E. Trans.*, October, 1939, pages 581–585 and (disc.) 585–587, 7 illus., 1 table.

Metal Working

Modern Methods of Die-Casting. H. L. Harvill. Advantages of the use of die-cast parts in aircraft, die-casting the control pedestal of the Douglas DC-4, injection improvements made on die-casting machines, tolerances possible on magnesium, aluminum, brass, and zinc die-cast parts, and the dies used are discussed. *Western Flying*, October, 1939, pages 16–18, 5 illus.

Superfinish. D. A. Wallace. Superfinishing technique, developed by Chrysler Corporation, is said to refine a surface to the closest approach to a geometrically true and unworked crystalline surface that has ever been commercially produced. Ways in which Superfinishing accomplishes this, method for measuring the resulting surfaces, metallurgy of the surface finish, and the lubrication of bearing surfaces are discussed in great detail. *S.A.E. Preprint for National Tractor Meeting*, September 28–29, 1939, 52 pages, 1 table.

Tools for Deep-Drawing and Pressing. J. D. Jevons. Use of graphitic steel, chromium-plated steel, cast iron, both unalloyed and alloyed, and inoculated cast iron for tools. Continued. *Metal Industry*, October 6, 1939, pages 309–313, 3 illus., 1 table.

Non-Ferrous Alloys

Electrolytic Polishing. W. C. Elmore. Investigation of electrolytic polishing of copper by the Jacquet method, which has thrown new light on the mechanism responsible for the polishing action. From a study of the voltage-current curves it is concluded that, when conditions are right for polishing, the concentration of dissolved copper at the anode is the highest possible. Accordingly the concentration gradient which exists at the anode limits the rate at which copper can dissolve, that is, diffuse into the bulk of the electrolyte (orthophosphoric acid). Since there is greater diffusion from raised areas of the anode because of steeper concentration gradients near them, the surface will become progressively more nearly level. Surface does not etch, for the concentration gradient alone controls the rate of solution. Details are given for the electrolytic polishing of iron with an orthophosphoric acid electrolyte. A convenient form of cell for electrolytic polishing is described. *Jour. Applied Physics*, October, 1939, pages 724–727, 3 illus.

Testing of Metals

Avery-Schenck Push-Pull Fatigue-Testing Machine. In the "Pulsator" push-pull fatigue-testing machine with resonance drive, specimen is gripped in a pair of sockets. One socket is attached to a ring dynamometer consisting of a thick oval tube having a flat on each side, one flat carrying the socket and the other being bolted to an adjustable bridge.

Pulsations given to the test piece are reflected in movement of the dynamometer, amplitude of the movements being read off by the microscope by aid of a slotted diaphragm. Flat spring to which the other socket is attached is oscillated by a small vertical motor. Number of cycles can be varied between 2600 and 3000/min., and the stress between 1543 and 22,046 lb., while the machine is running. Fatigue tests can be carried out under the influence of water, acids, etc., producing the effects of corrosion, and also at high temperatures. Long description. *Engineering*, October 6, 1939, page 379, 4 illus. on Plate XIV.

Classifying Steels by Spark Testing. G. E. Gordon and E. A. Reid. Spark testing is a rapid method for identifying elements found in the various types of steel, and for evaluating the approximate quantities in which they are present. Sparks produced as a rapidly revolving abrasive wheel is pressed against the steel are observed. Color, shape, and size of the sparks are greatly affected by the type and the quantity of the chemical elements contained in a steel being tested. Equipment used at the Bethlehem Steel plants and identification of the various elements are described. It is pointed out that characteristic spark produced by an electric furnace chromium steel is different from that of an open-hearth chromium steel of identical analysis. The spot test for nickel and equipment used are also described. *Iron Age*, October 19, 1939, pages 38–42, 7 illus.

Three-Dimension Photos Record Metal Defects. R. C. Gibbons. Stereoscopic methods are being used at the International Harvester Company plant for studying metal defects to determine their cause. Method has been applied to the study of surface defects, pits, and inclusions in castings and is being expanded to include examination of other materials and fatigue fractures in small metal parts, especially in springs. Process in applying the principles and precautions necessary for best results are described. *American Machinist*, October 18, 1939, pages 852–853, 4 illus.

Bearings

Boundary Friction in Bearings at Low Loads. L. M. Tichvinsky and E. G. Fischer. Bearing tests performed in the region of semifluid or boundary lubrication. Bearings $2^1/_2$ in. in diameter mounted in a rigid housing were loaded lightly and their performance studied in an attempt to correlate it with various physical properties of bearing and journal materials. Special consideration was given to journal surface finish and its measurement.

Various journal materials, similarly machined and ground, performed differently in a babbitt shell. A higher value of the coefficient of friction was associated with a relatively rougher journal finish having grinding scratches of the order of 100 micro-inches. Such finish in turn was associated with soft journal materials (180 Brinell). Boundary oil film, formed between several grades of bearing materials and a chromium-plated journal, offered different frictional resistance to motion. In the combinations of different bearing materials and the same chromium-plated journal, babbitt proved to be superior to bronze or silver. *Jour. Applied Mechanics*, September, 1939, pages A-109–A-113, 16 illus., 4 tables.

Studies in Boundary Lubrication. W. E. Campbell. Variables influencing the coefficient of static friction between clean and lubricated metal surfaces, including load, vibration, and cleanliness of the surfaces. From the survey of literature on static-friction measurement, it is shown that large discrepancies among the results of different investigators are largely due to lack of control of experimental technique. In the experimental study described, an inclined-plane and a horizontal-plate apparatus are used. Method of cleaning the surfaces is believed to be the factor having greatest influence upon results. It is concluded that invisible films which may be deposited upon the surfaces during the cleaning process can exert large effects upon static-friction measurements. Method of cleaning described involves polishing the surfaces with moist abrasive. It is shown that sulphide and oxide films on steel, copper, and brass produce a lowering in static friction depending on thickness of the film.

Static and kinetic values obtained on several bearing metals lubricated with typical oils are compared, static values being considerably higher. Differences observed are considered due in large part to viscosity effects in kinetic measurements. Analysis of static-friction measurements on typical lubricating oils leads to the conclusion that moisture and corrosion effects are responsible for many of the phenomena observed. Static-friction measurements do not lend themselves to routine testing of oils, but can be used to considerable advantage for studying single variables influencing boundary lubrication. *A.S.M.E. Trans.*, October, 1939, pages 633–641, 5 illus., 8 tables.

The Thick-Film Lubrication of Full Journal Bearings of Finite Width. M. Muskat and F. Morgan. Reynolds differential equation is solved by a successive approximation method for flooded full journal bearings, full journal bearings with central circumferential grooves, and full journal bearings provided with point sources of lubricant. Calculations are made on the variation of journal eccentricity, load-carrying capacity, and friction coefficients with the Sommerfeld dimensionless variable for the three cases and for different bearing widths. Direct experimental tests described confirm the theoretical predictions for bearings fed with lubricant at point sources. *Jour. Applied Mechanics*, September, 1939, pages A-117–A-121, 6 illus., 7 equations.

Engine Design and Research

Bore Wear from the Viewpoint of Materials. P. S. Lane. Paper previously abstracted from preprint. *S.A.E. Jour. (Trans.)*, October, 1939, pages 413–420, 16 illus., 6 tables.

Engine Flame Researches. T. A. Boyd. Paper previously abstracted from preprint. *S.A.E. Jour. (Trans.)*, October, 1939, pages 421–432, 30 illus.

Fuels and Engines. F. R. Banks. First issue—Present and future development in regard to the fuel position, plain and fancy fuels, direct fuel injection and valves.

Second issue—Spark plugs, direct injection, reduced fire risks, the Diesel engine, future engine development, that "buried" engine, cylinder size and form, general design, question of wet or dry cylinder barrel, and engines for the single-seater single-engine short-range fighter are discussed. Society of Automotive Engineers paper. *Flight*, September 28 and October 5, 1939, pages 269–270 and 291–294.

Ignition Lag in Compression-Ignition Engines. S. G. Bauer. The theory that the ignition lag, in the first approximation, is a function of $T \log p$, or peT, for a given fuel is at variance with Semenoff's theory which states that ignition lag should be a function of peA/T. The latter theory has been developed for pure gas reactions involving quite a different range of concentrations and delay time. Experimental work carried out at Cambridge University, and showing the effect of compression ratio, intake pressure, cooling-water temperature, load, injection advance, engine speed, and combustion-engine design on the ignition lag in an oil engine burning a given fuel. *Engineering*, September 29, 1939, pages 368–369, 6 illus., 1 table.

Phenomena of the Exhaust of Internal-Combustion Engines. J. B. Henderson. The slow-moving phenomena of the generation of a wave of translation in a canal by a sudden emptying of a lock are used to give a clear conception of the invisible phenomena which take place in both the cylinder and exhaust pipe of an engine when the exhaust valve is opened and which are all over in a few thousandths of a second. *Engineering*, October 6, 1939, page 378.

Progress in the Development of In-Line, Air-Cooled Engines. A. T. Gregory. Progress which has been made in the development of one particular inline air-cooled engine (the Ranger six-cylinder engine) is presented as typical of that shown by other models with commercial ratings up to 500 hp., indicating a 50 percent step-up in performance in the last five years. Operation of the ramming type of manifold is analyzed showing that, for the inline type of engine, it is possible to tune the manifold to obtain any desired b.m.e.p. curve. Resonance is shown to occur at a frequency equal to twice the frequency of the valve opening giving volumetric efficiencies as high as 97 percent on an unsupercharged engine using a single intake valve per cylinder and a single-barrel carburetor for a bank of six cylinders. Intake manifold diameter, cylinder displacement, and compression ratio are shown to affect not only ramming capacity of manifolds but also speed at which maximum ram is obtained.

Desired shape of b.m.e.p. curve for engines having either fixed-pitch or controllable-pitch propellers is discussed. Improvement in distribution by the ramming-type manifolds, methods of priming inline engines, a priming system which makes this engine comparatively easy to start under severe cold-starting conditions, and valve gear of comparatively small number of parts which may be used by the inline engine are described. Vibrating characteristics of the cam-shaft system is analyzed and a simple method is presented for determination of the required flywheel inertia or backlash in the system in order to obtain desired vibrating characteristics. *S.A.E. Preprint for National Aircraft Production Meeting*, October 5–7, 1939, 26 pages, 20 illus., 2 equations.

Suggested Modifications in Gear Teeth Formula. P. M. Heldt. Errors of the Lewis formula for calculating the strength of gear teeth are discussed and modifications are recommended. Whereas the Lewis formula involves only a slight error when applied to gears with a minimum number of teeth, the error is much greater in the case of gears with large numbers of teeth and of gear and rack combinations. Experimental results prove that the method of calculating beam strength of gear teeth by the assumption that one tooth takes the full load only when the next-following gear comes into action, gives more rational results than the method which assumes the entire tooth load to be taken at the top of the tooth.

Modifications should be applied also to the tooth-form factor to take account of the change in the stress in the weakest section of the tooth due to the perpendicular component of the tooth pressure, and so that stress in the weakest section can be based on the tangential load on the pitch circle instead of on the tangential force at the point of contact. It is shown that the value of the tooth-form factor increases with number of teeth in the gear under consideration and, more slowly, with number of teeth in the mating gear. *Automotive Industries*, October 15, 1939, pages 428–431, 4 illus., equations.

Engine, Fuel and Lubricant Testing

Exhaust Gas Analysis and Air/Fuel Ratio. R. G. Bellamy. Analysis indicating that a greater error is permissible in the determination of the oxygen content of the exhaust gas, than of the CO_2 content, to give the same standard of accuracy in the air determination. This fact, along with the simple relationship existing between oxygen content and the excess-air ratio for all gasolines and fuel oils, justifies the employment of the oxygen value for air determination in internal-combustion engines. The method is applied to both gasoline and Diesel engines. *Engineer*, September 29, 1939, pages 322–323, 1 illus., 7 equations.

Injection Research. K. J. de Juhasz. Optical indicator for measuring valve lift, optical indicator for measuring small motions, an improved form of optical indicator with stationary light source, pressure cell for measuring line pressure, impact element for measuring the momentum of the spray, mirror elements of the optical indicator, and momentum of fuel spray as recorded with the optical indicator are discussed and illustrated in drawings. Development of an optical indicator used in injection research at the Engineering Experiment Station of Pennsylvania State College. *Automobile Engineer*, September, 1939, pages 317–319, 8 illus.

Lap Gage Examination Reveals Importance of Piston-Ring Accuracy. P. E. Friend. Device for checking light-tightness, flexible-band device for measurement of circularity, and determination of radial pressure by means of the roller gage, as well as their disadvantages in piston-ring inspection, are discussed. The lap gage described is used by the Wilkening Manufacturing Company, and consists of a cast-iron cylinder and a closely fitting piston with connecting rod. Inside surface of the cylinder is converted into a lap. Rings to be studied are snapped into the piston grooves and are given from one to four strokes in the cylinder. Exact nature of the ring contact with the cylinder wall can be observed visually.

Gage offers a means of determining the uniformity of the twist and seating of a "dished" ring. It is of use in studying taper-face and straight-face compression rings and is a practical check on the accuracy with which the actual ring production consummates the theoretical design. *Automotive Industries*, October 15, 1939, pages 442–443, 453–454, 6 illus.

The Precision of Knock Rating—1936–1938. D. B. Brooks and R. B. Cleaton. Analysis is based on results of 6386 tests on 136 fuels, and shows a general improvement in precision, averaging 20 percent on all types of fuels, since the 1936 analysis. Although improvement in precision has been large for fuels of 70 octane number, it has been nil for those of over 80 octane number, emphasizing the need for more research on knock rating in this region. The 1939 C.F.R. Research Method is definitely more precise than the 1932 Research Method. The L-3 Method shows only slightly larger error than the A.S.T.M. Method. The Sunbury indicator is one-third less precise than the bouncing-pin, although it is probable that this showing would improve with use. More attention should be given to correction of compression ratio for barometric pressure. Not more than 100 hr. should elapse between overhauls, less if rating cracked fuels. Precision of rating, particularly for cracked and leaded cracked fuels, would be improved if humidity were controlled. Precision of rating, variation with octane number, relation of precision to fuel type, maximum obtainable precision, comparison of various methods, factors affecting precision, and relation of compression ratio to octane number are discussed. *S.A.E. Jour.* (*Trans.*), October, 1939, pages 449–456, 11 illus., 6 tables.

Engines

American Methods and Modes. J. I. Waddington. Comments on American engine development (Lycoming, Wright and Pratt-Whitney engines), compared with British, and an account of visits to the aviation exhibits at the New York World's Fair and to the Wright Aeronautical and Pratt-Whitney plants. Author considers that in military aircraft there is little to choose in workmanship and finish but if there is any balance it is in favor of the American product; and that Britain has a long way to go to equal American progress both in air-cooled engines and in commercial and private aircraft. *Flight*, September 28, 1939, pages 270g–270h, 271, 4 illus.

Diesel Developments. Bristol Aeroplane Company is said to be developing the Bristol Phoenix 9-cylinder radial Diesel engine. When produced experimentally four years ago the Phoenix was rated at 470 hp. This has now been increased to 635 hp. for take-off. There seems likelihood that a new Bristol Diesel will be produced with sleeve valves and a two-speed supercharger. Brief reference. *Aeroplane*, September 28, 1939, page 408.

Lanova Aircraft Diesel. K. Lohner. Results of experiments with the Lanova aircraft Diesel engine. Fuel is injected horizontally across the main combustion chamber and enters the throat of a subsidiary combustion chamber, which is only cooled indirectly and under load reaches a high temperature (600°C.). Ignition starts in the subsidiary chamber and the resultant explosion causes a pressure difference and discharge into the main chamber where combustion is completed.

Difficulties are experienced in adapting the Lanova principle to aircraft use since the engine is sensitive to the temperature of the subsidiary chamber and temperature rises very markedly under supercharged conditions. Initial ignition in the main cylinder must be avoided as otherwise very hard running results. This difficulty was overcome by adopting a form of pilot injection, by which the main fuel is sprayed into the flame issuing from the subsidiary chamber after a prior injection of a small quantity of fuel. This procedure is said to overcome starting difficulties also. Brief abstract from Yearbook of German Aeronautical Research. *Automobile Engineer*, September, 1939, page 329.

Pumpless Injection. P. L'Orange. L'Orange small high-speed Diesel engine developed in Germany employs the pressure differential between the main combustion space in the working cylinder and an antechamber. Fuel is not admitted directly but rather to a delivery channel provided with small exit channels communicating on either side of the restricted throat which establishes communication between the main combustion space and antechamber. Pressure difference between the two exit channels carries the fuel from the delivery channel to the antechamber and to the main combustion space at different stages of the working cycle. Description of engine. Paper presented at the Technische Hochschule, Karlsruhe. *Automobile Engineer*, September, 1939, page 331, 3 illus.

Wright Double-Row Cyclone 14. The Cyclone 14, 14-cylinder radial engine, now available for export sale, has a diameter of 55 in., is rated at 1600 hp. for take-off, and delivers 1350 hp. for normal operation. Bore 6.125 in. Stroke 6.312 in. Displacement 2603 cu.in. Long detailed description, including cylinder construction, crankcase sections, vibration dampers, accessories, pistons, supercharger, and lubrication. *Aero Digest*, October, 1939, pages 117–118, 3 illus. *Aviation*, October, 1939, pages 36–37, 5 illus.

Meteorology

Aerology for the Airlines. E. J. Minser. Methods employed in the Meteorology Department of Transcontinental and Western Air to interpret weather forecasts in terms of flight. Twenty-two full-time aerologists, working in shifts to keep a 24-hour schedule, review and analyze more than 20,000 weather observations each month. *Aero Digest*, October, 1939, pages 66, 69, 3 illus.

High Altitude Investigations. Meteorographs have reached a height of nearly 20 miles from time to time in the balloons sent up to high altitudes by the Meteorological Department of India. Few details only. *Flight*, September 28, 1939, page 270.

Aircraft Radio

Bendix Round Up. D. Fink. Several new pieces of Bendix equipment, and other apparatus previously announced are described in detail, including: the TA-6 transmitter having a 20-watt output, using two channels, and weighing 24 lb.; RA-10 receiver (8-tube 4-band remotely controlled) intended for short-line transport operations, for private planes, and as an auxiliary receiver for long-haul transport use; anti-rain-static equipment developed jointly by United Airlines and Bendix; TA-2 transmitter, a 100-watter with eight fixed channels, which was used by Howard Hughes on his round-the-world flight; Type MN-26 radio compass having automatic operation and a gear system used on the loop rotation indicator to introduce compensation for quadrantal error; SMRA type simultaneous radio-range beacons and 1000-watt ground-station transmitter with as many as ten independent channels; and a frequency decade generator intended to produce a crystal-controlled signal at any frequency from 0.1 kc. to 10,000 kc. in steps of 0.1 kc. *Aviation*, October, 1939, pages 32–33, 45–47, 6 illus.

CAA Demonstrates Blind Landings. D. Fink. Indianapolis blind-landing installation, put in by the International Telephone and Telegraph Corporation to C.A.A. specifications, has sixteen transmitters so that each runway is covered in both directions. Localizer antenna system is entirely free from vertically polarized waves, and hence free from multiple courses, bent courses, and the tendency of the landing aircraft to "push" the beam. Equipment was designed to operate properly throughout the range from −40° to 60°C. Receiving antenna on the plane, which, like the transmitting system, is receptive to horizontally polarized waves only, displays equal sensitivity in all directions and receives both the 109.9 Mc. localizer signals and the 93.9 Mc. glide-path signals simultaneously, separating them in a newly designed filter structure. Quasi-straight-line glide path, which is straight from an altitude of 600 ft. down to the airport surface, but which displays a bend above 600 ft., distinguishes this equipment from all its predecessors. Four basic transmitters, marker transmitters, localizer transmitter, glide-path transmitters, and receiving equipment are described in detail. *Aviation*, October, 1939, pages 30–31, 76, 5 illus.

The Importance of the Technical Equipment of Commercial Airports on the Safety of Flight. R. W. Pretzel. Auxiliary ground installations for aerial navigation over the area of commercial airports are discussed in regard to: installations in the airport buildings; installations of radio services; radio direction-finding station on the ground, and on the runways for blind landing; the illumination and signalling equipment; and the central radio transmitters. Translation in Italian from "Flughafen," No. 1, 1939. *Rivista Aeronautica*, June, 1939, pages 620–626, 8 illus.

Instrument Landing. H. W. Roberts. The experimental instrument-landing installation at Indianapolis, just completed by the International Telephone Development Company for C.A.A. is described in detail. Glide-path antenna array is so arranged that a straight-line glide path is obtained from a point 600 ft. above the outer marker down to a few feet above the inner marker at the airport boundary, permitting a constant rate of approach throughout this portion of the glide path without resetting the throttle adjustment on the airplane. *Aero Digest*, October, 1939, pages 74, 77, 7 illus.

Lear's Localizer. Combination of two ADF-6 automatic direction-finding radio compasses which produces a simple airport guidance system. Methods of operation of airplane and ground equipment are described. *Aviation*, October, 1939, page 47, 1 illus.

The Screened Loop Aerial. R. E. Burgess. Theoretical and experimental investigation of the screened-loop type of receiving aerial used in direction-finding and field-strength measurements. Theory of the screened loop is analyzed. Simplifying assumptions made are shown to lead to a good first approximation for the value of pickup for the screened loop. Pickup is computed for the special cases of the screen gap short circuited, capacitively loaded, and tuned. It is shown that enhanced pickup may be obtained by the suitable capacitive loading of the gap in preference to an increase of the number of loop turns. Practical aspect of this system is discussed, confirmatory experiments are described, and suggestions for continuation of the investigation are indicated. Research carried out as part of the program of the British Radio Research Board. *Wireless Engr.*, October, 1939, pages 492–499, 4 illus., 2 tables, 11 equations.

Personnel

The Changes of the Organism in Tests of Short Duration at High Altitudes in Low-Pressure Test Chambers. F. v. Tavel. Experimental results obtained in the low-pressure test chamber at Zurich on the effects of lack of oxygen on pilots. Translation in Italian from "Flug-Wehr und Technik," No. 4, 1939. *Rivista Aeronautica*, June, 1939, pages 633–637.

Dealing with the Problem of Personnel. C. S. Mattoon. Regulations governing the apprenticeship plan which has been functioning at the Buffalo plant of the Curtiss-Wright Corporation for several years are explained, and three separate apprentice courses which are offered by Curtiss are outlined. *Aero Digest*, October, 1939, pages 40–41, 154, 2 illus.